Identifying British Columbia's Strategically Important Wave Energy Sites

by

Xinxin Xu
B.Sc., Capital Normal University, 2013

A Thesis Submitted in Partial Fulfillment
of the Requirements for the Degree of

MASTER OF APPLIED SCIENCE

in the Department of Mechanical Engineering

© Xinxin Xu, 2018
University of Victoria

All rights reserved. This thesis may not be reproduced in whole or in part, by photocopy or other means, without the permission of the author.

Supervisory Committee

Identifying British Columbia's Strategically Important Wave Energy Sites

by

Xinxin Xu
B.Sc., Capital Normal University, 2013

Supervisory Committee

Dr. Brad Buckham, Department of Mechanical Engineering
Co-Supervisor

Dr. Bryson Robertson, Department of Mechanical Engineering
Co-Supervisor

Dr. Rosaline Canessa, Department of Geography
Outside Member

Abstract

Supervisory Committee

Dr. Brad Buckham, Department of Mechanical Engineering
Co-Supervisor

Dr. Bryson Robertson, Department of Mechanical Engineering
Co-Supervisor

Dr. Rosaline Canessa, Department of Geography
Outside Member

The West Coast of Vancouver Island (WCVI), with an average gross wave energy flux of 40-50 kW/m at the continental shelf, possesses one of the most energetic wave climates in the world and has the potential to meet the electric demands of the utility grid on Vancouver Island and numerous coastal remote communities. However, the development of wave energy sites has the potential to interrupt other existing marine activities and wave energy operations could damage the sensitive marine ecosystems.

The objective of this thesis is to identify strategically important sites for wave energy – sites that have great economic potential in an energy generation context yet have minimal impacts on existing economic uses and minimal ecological impacts. Wave energy technology agnostic frequency and directional filters were developed based on a unionized representation of Wave Energy Converter (WEC) performance generated by combining four types of WEC performance characteristics. These two filters improved the quantification of extractable wave resources by accounting for the technological limits of wave frequencies and directions.

Subsequently, a detailed economic evaluation was developed to estimate the influence of the distance to the coastline and transmission network, electricity market sizes, and a technology agnostic description of WEC farm physical layout on the selection of wave energy sites. The technology agnostic description of WEC farm physical layouts was designed based on the cable properties, cable termination/distribution, and cable protection

used in real-world projects. The WEC farm capacities are constrained by the transmission cable to minimize the cost for developing wave energy sites.

Lastly, a multi-criteria analysis, which includes four stakeholder perspective scenarios, was developed to identify the strategically important sites for future wave energy development along the WCVI. A total of 16 regions, covering an area of 392 km^2 and having an average of 35.68 kW/m wave energy flux, were identified as strategically important sites for wave farms. These regions show the potential to meet the electric demand of Vancouver Island, and they are worth further investigated when selecting a location for future wave energy development.

Table of Contents

List of Tables

List of Figures

Acknowledgments

I would like to thank everyone who help me along this long and interesting journey of my master's program. I am grateful to have experienced and accomplished all that I have with the help of the supervisors, colleagues, and friends. First and foremost thank you to my supervisors Dr. Brad Buckham and Dr. Bryson Robertson for their knowledge and expertise in ocean engineering, their patient answers to my continuous stream of questions, their encouragement when I felt frustrated, and finally for inspiring me to pursue such interesting research. Thank you to Dr. Rosaline Canessa for her knowledge and expertise in marine conservation and spatial analysis. Thank you to Dr. Helen Bailey for her knowledge and expertise in hydrodynamics. And thank you to Ewelina Luczko, Bryce Bocking, Eric Thacher, McKenzie Flower, Markus Sommerfeld and many others for always helping and supporting at both school life and personal life.

Thank all of you again, without all your help, encourage, and support, this thesis would not have been possible.

Dedication

For my parents.

Chapter 1 Introduction

Renewable energy technologies are critical to meet the electrification goals in an ecologically responsible way. The West Coast of Vancouver Island (WCVI), with an average gross wave energy flux of 40-50 kW/m at the continental shelf [1], possesses one of the most energetic wave climates in the world and has the potential to meet the electric demands of the utility grid on Vancouver Island and numerous coastal remote communities.

However, coastal areas have been utilized for centuries for many activities such as fisheries, shipping, recreation, and industry. In addition, coastal areas possess sensitive marine ecosystems that have high conservation value. Therefore, selecting future wave energy sites that combine great energy conversion potential and thus high economic development potential with minimal conflict with pre-existing activities and marine ecosystems becomes a challenge. A novel methodology to assess the wave resource, an economic evaluation on potential wave sites, and a multi-criteria Geographic Information System (GIS) analysis to identify strategically important wave sites for the southern-central British Columbia (BC) coastline will be presented in this thesis.

1.1 Background

Globally, todays energy production is dominated by non-renewable sources. Fossil fuels account for approximately 86% of global primary energy consumption, with oil representing a 33% share, coal representing a 29% share, and natural gas representing a 24% share (See Figure 1.1) [2], [3]. Similarly, global electricity production relies greatly on fossil fuel. Coal is the largest single source and holds a 41% share of the worlds' electricity generation, and natural gas, the second largest source, accounts for 22% [2], [3].

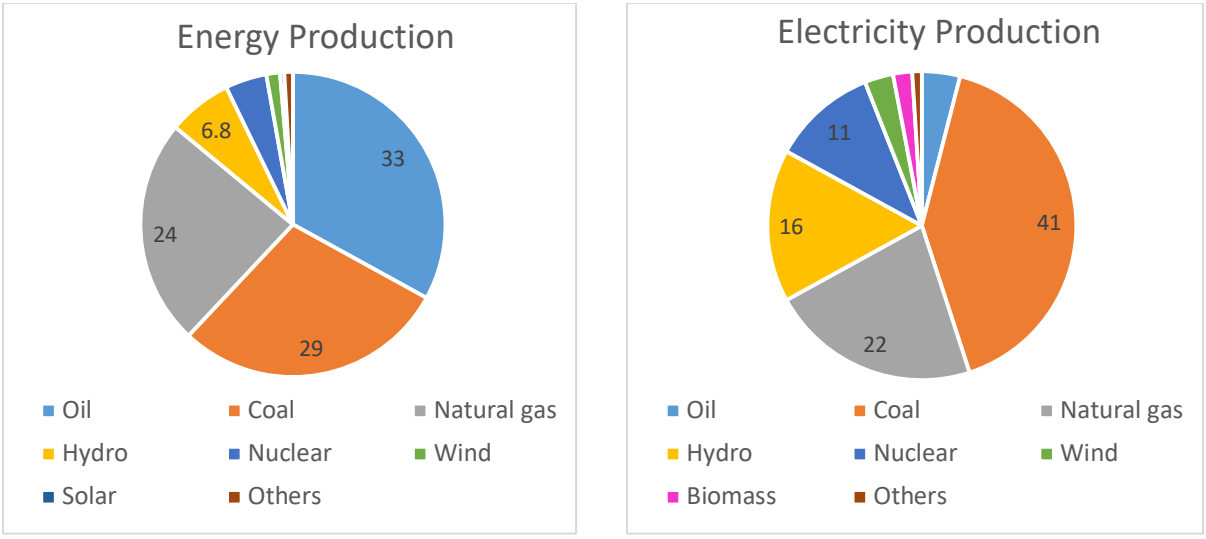

Figure 1.1 Primary sources of the world's energy and electricity production.

However, fossil fuel electricity production is contributing to serious environmental and energy security problems; consequences include environmental degradation, climate change, and external energy dependency and security of supply [4]–[8]. Environmentally, the emissions from fossil fuel combustion and transportation contain particulate matter, sulphur oxides, nitrogen oxides, volatile organic compounds, carbon monoxide and other pollutants; all of which are major contributors to urban air pollution. In addition, those pollutants are precursors of acid deposition and acidification, which can cause significant damage to ecosystems, crops and human-made infrastructure. On the climate change front, the process of generating power via fossil fuels emits large quantities of greenhouse gases; these gases accelerate climate change which is a serious threat to the prosperity of human civilization. Finally, fossil fuel reserves are distributed unevenly across the world acute dependence on particular jurisdictions such as the Middle East to maintain supply chains. With traditional fossil fuel reserves diminishing, energy portfolios that are underpinned by fossil fuels, especially imported fossil fuels, are not sustainable.

Compounding these problems, the world energy consumption is estimated to increase considerably over the next few decades due to the rapid growth in population coupled with industrialization and urbanization [7]. This growing demand, simultaneous requirements to reduce greenhouse gas emissions, and escalating social concern about environmental

degradation are accelerating efforts to exploit low carbon renewable energy resources for our future electricity needs. The magnitude and immediacy of the requisite shift from fossil fuels to renewables are daunting; a 70% cut in present carbon dioxide emission by 2050 is necessary in order to stabilize the earth's climate, keep the global temperature rise this century below 2 degrees Celsius above pre-industrial levels, and prevent further global warming [5], [9].

Governments worldwide are currently implementing policies to increase the development of renewable energy; in 2015, 164 countries had renewable energy support policies (Goledemberg, 2006; World Energy Council, 2017). Currently, renewables comprise 9.6% of the world's primary energy consumption (6.8% from hydro, 1.44% from wind, 0.45% from solar and 0.89% from others), see Figure 1.1[3]. These market shares are increasing: the deployment of renewable energies (mainly wind and solar) increased globally by 200 GW between 2013 and 2015, and the trend of increasing renewables is expected to continue in the future [2]. However, as renewable technology deployments scale up they begin to encounter challenges, such as competing land uses, significant energy ramping events, and new environmental concerns; for instance, the substances released from photovoltaic (PV) production for solar energy could contaminate water resources. The increasing demands and challenges faced by existing land based renewables encourages the diversification of the renewable energy portfolio and has sparked worldwide interest in wave energy [4], [8], [10], [11].

1.2 Wave Energy Characteristics

Wave energy has a number of natural, intrinsic advantages over other renewables. Ocean waves are generated from winds as they blow over the ocean's surface, which provides a convenient and natural concentration of wind energy in the ocean surface layer. These winds are a function of temperature and pressure differences across the earth caused by the uneven distribution of solar energy. Therefore, waves can be considered as a tertiary stage of an energy transformation process that sequentially concentrates the energy originally delivered to the Earth's atmosphere via solar radiation. Due to the density of seawater,

ocean waves have a high energy density and there are minimal energy losses when waves travel from their region of origin to a coastline [2], [8], [12]–[16].

From the electricity consumer and utility perspective, wave energy benefits from both low grid integration costs and high predictability when compared against other variable renewables. Regarding the former, when grid integration costs are quantified by calculating balancing reserves, wave reserve costs are less than half of those of wind and solar costs [17], [18]. Regarding the latter, waves can be forecast with greater accuracy; waves are relatively insensitive to short term fluctuations in local weather patterns due to the immense inertia in ocean waves [14], [19], [20]. Furthermore, wave energy exhibits seasonal variations, with low resource availability in summer and high resource availability in winter in WCVI region. These seasonal variations align with the peak heating loads in the North American winter and can offset losses in other renewable technologies that occur in this season, such as solar photovoltaic devices. Therefore, wave energy has the potential to flatten out the 'net load' on the grid (net load is the load less the renewable sources considered) [8], [17].

1.3 Motivation and Objective

To exploit the energetic wave resources in British Columbia (BC), a comprehensive understanding of the wave climate and present-day wave energy conversion technologies is necessary but insufficient. A carefully executed site selection process is essential for identifying the optimal wave energy conversion sites; this process must account for the influence of Wave Energy Converter (WEC) deployment on all pre-existing marine activities and on marine ecosystems. At present, no research in BC has taken such external impacts into account when selecting wave energy sites. The goal of this thesis is to identify the strategically important sites for wave energy development along the WCVI in BC. The strategically important sites are the places that should be considered first and foremost when choosing locations for wave energy projects. Wave energy projects, like any energy industry, typically involve large machinery, extended construction periods, and large operating costs. These projects require coordinated commitments from multiple

stakeholders including commercial investors, government regulators, public funding bodies, conservationists, local communities, etc. Each stakeholder has their own priorities, for example: commercial investors focus more on economic potential of the wave energy projects, while government regulators are likely to pay more attention to the impacts of the wave energy projects on other marine users. It is important to identify strategically important sites that can strike a good compromise between competing stakeholder priorities; 'strategic' sites have both great economic potential and minimum impact on existing economic uses and ecosystems. In order to achieve this goal, the major objectives of the present work include:

1. Develop new metrics that can represent the quality and magnitude of BC wave resources based on the naturally occurring resource and also on technological limits on how that resource can be extracted; as an example, there are limits on the directions and frequencies of waves that WECs can harness.

2. Evaluate the influence of distance to coastline and electrical transmission grid, market size (utility grid scale or remote community scale), and wave farm physical layout on the selection of wave energy sites in BC.

3. Build a Multi-criteria GIS framework and develop a 'scenarios study' to assist stakeholders in identifying strategically important wave sites that can strike a reasonable compromise between competing priorities for the same ocean region.

1.4 Literature Review

The global WEC research community has been active in quantifying wave resources and identifying the potential WEC deployment sites. The majority of existing research can be classified into two categories. The first category is assessments of wave resources which involves large scale (e.g. global scale) models of wave resources, accurate models and measurements of wave conditions at regional scale, and the resulting predictions of power production from wave devices in the highest energy locations. The second category is wave

energy site selection which considers competing socioeconomic factors (e.g. proximity to coastline and transmission infrastructure, fisheries, marine traffic etc.) and environmental factors (e.g. marine parks and ecosystems) to identify priority locations.

1.4.1 Assessment of Wave Resources

Utilizing the wave energy resource and deploying WEC technologies requires a comprehensive understanding of the naturally occurring wave conditions and wave climate. Since the early 1970s, coincident with the modern period of WEC technology development, accurate wave resource assessments have been pursued by WEC developers. At the early stage, wave assessments rely on data collected by direct in-situ measurement, e.g. shipborne wave recorders, wave buoys and observation stations [21]–[25]. These measurements provide information about the wave conditions at specific locations, but they lack spatial and temporal continuity. Later, researchers shifted their interests onto numerical wind-wave models to overcome the problems faced by in-situ measurement; these models include: WaveWatch 3 model (WW3), Oceanweather's 3rd generation wave model (OWI3G), and WAve Modeling (WAM) [13], [16], [26], [27]. These numerical wind-wave models are able to predict wave conditions on a large scale, and when verified against in-situ measurements, have reasonable accuracy at off-shore ocean areas. However, when waves propagate into coastal areas, where it is feasible to deploy WECs, predicting wave heights becomes more complicated due to bottom effects (e.g. shoaling, refraction, diffraction). The bottom effects distort wave amplitudes and directions [12], [28], [29]. Coastal wave models, such as the Simulate WAve Nearshore (SWAN) and wind-wave Mar3G models, are designed to calculate these effects, the generation of waves due to local winds, and additional dissipation effects that happen in shallow waters. These coastal wave models can provide a spectral representation of the wave conditions and this level of fidelity is important in subsequent calculations of WEC performance. However, the cost of acquiring these near-shore predictions is that the topography of the seabed (i.e. the bathymetry) must be supplied at sufficient spatial resolution. All wave models used today can be divided into two categories: phase resolved and phase averaged [30]–[32]. The phase resolved model is able to capture the phase for each constituent wave, whereas the phase

averaged model assumes that the phases are uniformly distributed. The phase averaged models, such as SWAN, are widely adopted in wave resources assessments, as it can be applied on broader spatial scales with a low computation expense. The phase averaged model also provides spectral representations that are able to account for the diffraction and wave-breaking processes, which is sufficient to characterize wave resources in coastal regions.

Wave resources assessments have been developing in Canada and British Columbia (BC). This initial exploration started with three notable research projects: a National Research Council Canada assessment on wave energy flux near Tofino, BC and Logy Bay, Newfoundland and Labrador [24]; a Transport Canada study quantifying wind speeds, wave heights, and wave periods at different geographic regions [16]; and an estimation of wave power off the BC coast using data collected by eleven buoys [33]. However, there was no consistent and comprehensive estimation of all Canada's waters until the 2000s. Cornett et al. quantified the wave resource in both Canada's Pacific and Atlantic waters by analyzing the data from three sources: direct wave measurements (collected from over sixty stations) and two wind-wave hindcast models (OWI3G model and WW3 model) [16]. The direct wave measurements presented the frequency of occurrence and the energy flux for each combination of significant wave height (H_s) and peak wave period (T_p,) at each station. In those wind-wave hindcast models, several important variables (e.g. H_s , T_p, wave energy flux, mean and primary wave direction, wind speed, wind power density) were produced at 3-hour intervals for a three-year period (between October 2002 and September 2005). The measurements and models utilized provide a reasonable estimation of the wave resource at Canadian off-shore sites, but they only cover a short period of time and lack precision in coastal water areas due to a coarse model grid and the fact that the model software used did not account for the bottom effects.

Extending the offshore wave energy resource assessments, an investigation using the near shore SWAN wave model was undertaken for the WCVI near Ucluelet and Tofino, BC [34]. That SWAN model (being a third-generation spectral wave model) simulated the nearshore wave propagation and transformation for 338 different sea-states (i.e. 338 distinct and static combinations of H_s , T_p, and peak direction θ_p) over a 136 km by 90 km

rectangular region, centered on the Pacific Rim National Park (see Figure 1.2 (a)), at 3-hour intervals. Maps of wave energy flux for a five-year period were post-processed.

More recently, a series of detailed wave resource assessments using the SWAN model was conducted by the West Coast Wave Initiative (WCWI) research group at University of Victoria. The SWAN model grid used by WCWI expanded on Cornett's study area to cover a larger section of the WCVI region, which extended from the continental shelf to the coastline of the Vancouver Island and covered a 450 km stretch of BC and Washington coastline (see Figure 1.2 (b)). The WCWI assessments started with a sensitivity study [35] that examined the impact of different boundary conditions and bathymetry grid discretizations on the SWAN model performance. An unstructured grid (i.e. a grid with variable spatial resolution based on water depth) and operation in non-stationary mode were identified as the best options to model the wave climate on WCVI. Omni-directional wave boundary conditions were obtained from the European Centre for Medium Range Weather Forecasts (ECMWF) and wind boundary conditions were obtained from the Fleet Numerical Meteorology and Oceanography Centre's (FNMOC's) Coupled Ocean/Atmosphere Mesoscale Prediction System (COAMPS) model. The spatial and spectral resolution of wind and wave boundary conditions were shown to have significate effect on wave parameter estimates. Boundary conditions were first improved by synthesizing directional wave spectra from parametric wave data values (H_s , T_p, and θ_p) from a WW3 model operated by National Centre for Environmental Prediction (NCEP) [36]. The boundary conditions were then further enhanced by using the best-fitting full directional wave spectra chosen from 17 publicly available global wind models [37]. These enhancements along with the application of the Westhuysen's quadruplet wave interaction solvers [38] and the continuous improvement of nearshore spatial resolution enable the SWAN model to assess the wave resource along WCVI with great detail and accuracy [36].

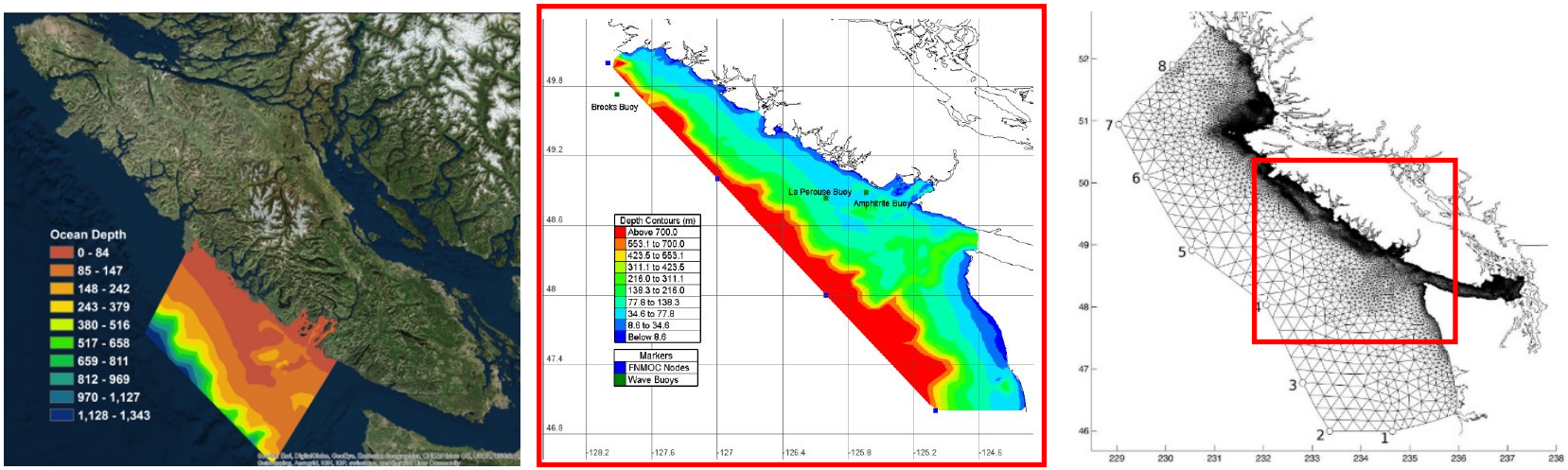

(a) *(b)* *(c)*

Figure 1.2 Computational domain of studies conducted by (a) Cornett and Zhang (2008), (b) Hiles et al (2011), and (c) Robertson et al (2014); the red box in (c) indicates the extent of (b).

The developments in [36] also expanded the SWAN model to a 1500km stretch of coastline encompassing an area of 410 000km^2 of water (see Figure 1.2 (c)). The temporal domain was extend to eight years (2005 – 2012) [36], [37]. As well as the omni-directional wave energy flux, additional metrics (e.g. spectra width, directional co-efficient) were developed to account for the frequency and direction distribution of energy within the wave spectrum; these are important for accurate estimation of the WEC device performance and characterization of wave resource for WEC developers [36], [37], [39]. With the extended study area, the longer temporal duration, and the additional metrics, a comprehensive understanding of gross wave resource along the entire WCVI region was achieved.

Building on these gross wave resource assessments, the wave energy industry is seeking highly resolved and accurate estimations of power production from farms of deployed wave devices. The initial estimations on wave power production started with calculating the theoretical wave farm outputs based on the local wave conditions and the generic WEC performance metrics [1], [14], [37]; the performance metrics are characterized by a two parameter (H_s - T_p,) histogram, and generated following the standard method introduced in the International Electrotechnical Commission (IEC) TC 114 Technical Specification 62600-100: Electricity producing wave energy converters – Power performance assessment [40] . These estimations of wave power production were then improved in later works to include: numerical simulations on how different types of WECs react to the various wave conditions [41], [42], sensitivity studies on how different wave resource characterization methods influence the power production estimations [43], and the influence of WEC array layout on the cumulative array power production [30]. These studies significantly improved the precision of estimations of wave power production, but the methods used rely on having wave conditions described in detail for a specific location. It is impractical to apply these methods to assess the wave energy production potential over broad coastal regions.

Some WEC power performance prediction methods, such as that of Luczko et al. [30] can be implemented within a SWAN model framework and thus can be applied to larger regions. But Luczko's approach relies on specific performance characteristics of the WEC

technology being defined and results generated using that method are specific to a choice of WEC device and farm layout.

Prior to implementing a method such as Luczko's, a method for assess broad coastal regions to determine a much smaller focused set of locations is required; at those focused locations, a more detailed assessment of wave energy production can be applied using any of the existing methods mentioned above. In the initial search for focused locations, the assessment should avoid being tied to power output calculations that are specific to one technology. Rather, a representation of overarching technological limits on WEC performance should be applied. In the current study, such limits will be applied through screening of wave frequencies and directions based on observations on how several different types of WECs perform.

1.4.2 Wave Energy Site Selection

In the existing literature, WEC deployment site selections are mainly based on the gross or extractable wave energy, and the proximity to coastline and transmission infrastructure [14], [37], [44], [45]. Dunnett et al. compared the extractable power from three different types of WECs at hundreds of different locations along both Atlantic and Pacific coast of Canada. Two Atlantic and three Pacific sites were selected as potential wave farms and at each site the devices operated with more than 20% capacity factor, and were close to urban or industrial areas [44]. In the WCVI region, Robertson et al. ranked all possible sites according to the magnitude of the annual average wave energy flux. By comparing the distances between sites of high rank and the current electrical transmission grid from BC hydro, a subset of ten reasonably distributed sites were selected as potential locations for wave farms; a 'wave farm' in that work was comprised of an array of ten WECs deployed at the same location. [37]. However, these studies identified WEC deployment sites only based on the energy conversion and grid integration opportunity - any competing socio-economic or environmental characteristics were not considered.

Wave energy projects usually require enormous investments, and thus economic value becomes an important factor when selecting locations for wave farms. Finding appropriate locations where devices can operate efficiently with low construction cost is an essential step to gain commerical acceptance and to develop wave energy industry. Other factors that influence the construction costs and the potential revenue, such as the water depth, distance to land, ports to support installation, and market conditions, have been considered in different studies [19], [46]. Astariz and Iglesias developed an approach to select the optimal wave farms in the water off the Danish coast [46]. In their approach, hourly wave hindcast data from 2005 to 2015 was implemented by SWAN model to identify the locations that provide the best available resources and power variability. In addition to the wave resource, the technical limitations of water depth and distance to coast have been assessed in a holistic way in their work, and two sites on the northern coast were identified as the the optimal locations for wave farms.

Coastal areas are typically densely populated and have already been utilized for various activities for centuries. Today's growing demands for ocean space make conflicts and competing among different marine users more serious. Large projects such as commercial wave farms will impose restrictions on other marine activities and stress the risk of conflicts with other marine space users. In the case of WEC deployment, minimizing impacts on existing economic uses and avoiding excessive ecological impacts is essential to win public acceptance, which may hold the key to project approvement. However, previous studies have considered the coast as open and empty by ignoring these existing uses and ecological factors, which is not the case in reality. Multiple studies have started to account for socio-economic or environmental factors in their process of selecting sites for wave farms. Iglesias et al. assessed the wave resource off the Galician coasts (Spain) based on a three-hourly interval WAM model data covering the period 1996 – 2005, and selected a total of 18 points that have the highest annual wave potential [47]. These sites were then overlapped with socio-economic information, such as the location of ports, navigation routes, and fishing and aquaculture zones, to find areas that have great energy potential with minimum conflict with other uses. The region from Cape Finisterre to Cape San Adrian, and the region from Cape Ortegal to Cape Estaca de Bares were identified as

potential locations for wave farms in Spanish coasts. Kim et al conducted a spatial overlap analysis to study potential spatial conflicts between areas with potential for wave farm and areas with pre-existing uses and important ecological features along the WCVI [48]. The harvestable wave energy was first estimated based on four wave energy absorption performances from four types of devices, using a three-hour interval WW3 model data covering period 2005 – 2010. The Net Present Value (NPV) for wave farms was then evaluated based on a capital investment analysis. In the last step of the work by Kim et al, the areas with positive NPV for wave farm were identified and overlaid with various marine uses and ecological features one at a time; marine uses include shipping and transport, tenures and offshore energy, tourism and recreation, and commercial fisheries. All areas with positive NPV were found to overlap with at least one existing human use or ecological feature. These simple overlay exercises help to identify the regions where the wave farms need to work together with multiple pre-existing users and the regions where wave farms are likely to be less affected.

The busy marine environment has necessitated a shift in marine spatial planning from a single section management approach (i.e. each area only occupied by one user) to an integrated multiple-use management (i.e. each area used by multiple users collaboratively). The Multi-Criteria Decision Analysis (MCDA) is a decision-making tool that enables multiple criteria to be considered simultaneously and explicitly by providing a logical, structured method to identify and prioritize the factors from diverse social, economic, technological and environmental aspects [49]–[52]. MCDA is effective at addressing complex problems featuring diverse data forms, conflicting objectives, high uncertainty, and multiple interests and perspectives, such as identifying strategic sites for wave energy projects. In this work, strategic sites are the places that compromise or trade-off between the wave energy development and existing human uses and marine ecosystems, unlike the traditional single section approach, in which suitable sites are only evaluated in terms of the priority of energy extraction (or wave resources).

Multiple studies have adopted the MCDM in their site selection process and demonstrated that the MCDM framework can support the identification of suitable sites for wave farms

[50]–[52]. Ghosh et al. developed a model based on MCDA to predict the suitability of different locations with respect to their potential for installation of wave farms [51]. Their study attempted to propose a suitability indicator that could account for various technical, socio-economic and environmental factors, such as wave height, wind speed, ocean depth, turbulence, coastal erosion, shipping density, tourism potential, etc. The performance of the model was validated by a sensitivity analysis that showed the model was sensitive to each of the input parameters (factors) which could influence the decision objective. Last, the suitability analysis conducted by the MCDA model was applied at two sites as case studies: one site is situated in the UK and the other is situated in Jamaica in the West Indies. Their analysis shows the UK is more suitable for wave energy projects than the sites in Jamaica. Kilcher and Thresher applied a MCDA to assess wave energy opportunities at 100 different sites along the entire U.S. coastline [19]. Their MCDA accounted for five criteria, which included wave resource characterized by the annual average energy flux based on a 51-month WW3 model; the market condition which considered both market size and manufacturing capacity; the water depth as regulatory requirement; the distance to the transmission grid; and shipping cost to support installation, operation and maintenance. All criteria were first scored and then summed up to create a composite suitability index, and a rank was generated based on this index among the 100 sites. The Pacific Northwest, which includes Oregon, Northern California, and Washington, was found as the best place for wave energy development without consideing the energy price. After taking energy price into consideration, the Hawaiian Islands of Oahu and Kauai climbed to the top of the suitability index rank, and Northern California maintained its top position on the list. These studies proved that MCDA is an effective method incorporating multiple conflicting factors to predict the suitablity for wave farm sites. However, the suitability analyses were only conducted at limited pre-selected locations in these studies, e.g. two sites in the Ghosh et al. and a hundred sites in the Kilcher et al. study.

A more effecitive site selection of wave farms should apply the MCDA to larger regions with higher density sample sites, or even a continuous study region. This huge amount of sample sites requires enormous effort to collect, store, process, analyze, and accurately represent the geospatial data related to the site selection criteria. The Geographic

Information Systems (GIS) can meet this requirement by providing a comprehensive framework with various spatial analysis tools that can efficiently manage and visualize the digital geo-spatial data [53]. Each site selection criterion is represented by a layer in GIS; a layer is a map that has a scalar value at each site that indicate the goodness based on one criterion. The MCDA is implemented in GIS by setting weights (a numerical indication of importance) to each criterion-layer and combining these layers through various map algebra functions.

The GIS incorporated with the MCDA, referred to as 'multi-criteria GIS' in this thesis, have been previously adopted to identify suitable sites for wave farms in several studies [4], [53]–[56]. A multi-criteria GIS analysis, which included a wide variety of technical, economic, environmental and administrative factors, was developed to identify suitable locations to deploy wave farms along the southwest coast of Portugal [56]. Each factor (such as wave climate, water depth, distance to shore, distance to the electric grid, distance to ports, sea bottom geology, and environmental impact) is first represented by a layer, then assigned different weights according to its importance. A suitability map was generated by summing up the weighted layers to help identify the location with great potential for wave farm deployment. Another geo-spatial multi-criteria approach was developed along the Basque continental shelf to minimize the installation and maintenance costs of WEC farms together with the environmental impact on that area [54]. Compared to the work of Nobre et al., more factors (a total of 17 factors) have been considered in the study of Galparsoro et al. However, these factors were all weighted equally, which may not reflect the real-world situation. The *Waveplam* project for Intelligent Energy Europe [55] describes a similar methodology to the studies of Nobre et al. and the study of Galparsoro et al. The *Waveplam* project also made a detailed list of the factors covering technical, environmental and socio-economic aspects that should be considered when selecting sites for wave farms. Building on the Waveplam project, a more detailed study combined MCDM methods and GIS to identify the most suitable marine renewable energy areas in Greece [53]. Their advanced weighting method, named the Analytical Hierarchy Process, determines the importance of each factor based on a pair-comparison process, rather than having the layer weights directly assigned by users. In North America, the Pacific Northwest National

Laboratory and Parametrix, Inc. conducted a multi-criteria GIS analysis to evaluate the site suitability for marine renewable energy development on the Washington coast [57]. In their analysis, a total of eight criteria, which cover the quality of resources, water depth, distance to the grid connection, and distance to ports, were considered for the evaluation of a site's suitability for three types of WEC. The choice of the criteria and their assigned weights were determined by industry experts via a weight additive algorithm [58]. The southern half of the Washington coast was found to be more suitable for wave energy development than the northern half, due to its proximity to the transmission grids. Their study comprehensively incorporated basic technical and economic criteria into the selection of wave energy sites but didn't account for any socioeconomic and environmental criteria. In all of these prior studies, wave farm deployment site suitability was calculated based on a single set of weighting values.

WEC deployment site suitability strongly relies on the choices of weighting values for the criteria (layers) chosen in the analysis, and thus the multi-criteria GIS analysis should not be limited to the results made based on a single set of weighting values; a single set of weighting values is defined as a 'single scenario'. Analogous to the need to incorporate multiple criteria (layers) in the decision-making process, there should be a mechanism to consider how these multiple criteria are prioritized by different user groups (or stakeholders). For this purpose, an analysis that is built on combining different sets of weighting factors, which is referred to as 'multi-scenario', should be incorporated to the GIS analysis. The multi-scenario GIS analysis that evaluates the suitability of wave sites based on the set of weighting in each of the scenarios has started to draw researchers' attention. Flocard et al. applied a range of scenarios in their multi-criteria GIS evaluation along the southeast Australian coast to assess how sensitively the model reacted to each input criterion and validate the robustness of the resulting suitable sites [4]. The suitability of the sites was evaluated based on five criteria which include the wave resource, the distance to infrastructure, environment influence, seabed characteristics, and existing marine users. Eight scenarios were developed by manipulating the weighting value for each criterion. By spatially comparing the results from different scenarios, the model proved to be effective since the results do not overly rely on the weighting choice from one specific

criterion, and an area of 700 km^2 off the coast of Portland, South East Australia was identified as being highly suitable for WEC deployment. The study developed by Flocard et al. represents the current state-of-the-art analysis for wave energy site selection.

This thesis follows a similar approach as Flocard et al. by using a multi-scenario GIS analysis, but conducts the analysis at the WCVI region (see Figure 1.2 c). Unlike the scenarios in Flocard et al. study, scenarios in this thesis are designed to represent multiple stakeholders with different priorities. In each scenario, the priorities of each stakeholder are described by a unique set of weighting values (which refers to a weighting scheme). The *Rank Ordering Weight* method [59], which is an effective way to convert the priorities of the stakeholders to numerical values, is applied to decide the weighting scheme for each scenario. This proposed process will lead to the identification of 'suitable' sites that balance the concerns of all stakeholders, which will be the strategically important sites for wave energy projects. This study will be the first time that a suitability analysis, incorporating GIS and MCDA to account for all technical, environmental, social, and economic factors, has been applied to the identification of strategically important sites for wave energy along WCVI region.

1.5 Contributions

While the overarching objective of this thesis is to identify the strategically important wave sites within the WCVI region, progress towards that objective will also develop novel metrics for wave resource assessment, as well as new methods for the economic evaluation of WEC deployment sites. These metrics and methods are not limited to the specific WCVI region. Additionally, the multi-criteria GIS framework is not limited to wave energy. The major contributions of this thesis are summarized as follows:

1. New wave energy metrics that account for the influence of wave frequency and direction on the potential wave energy extraction are developed. Rather than studying one specific WEC operating with device specific directional and spectral energy conversion behaviour, this thesis considers various types (four types) of WECs to generalize the extractable

portion of the wave energy flux at each site (e.g. the frequency and the directional limits are set based on examination of the characteristics from all types of WECs). The new metric allows the vast and comprehensive wave dataset used as an input to the study to be condensed within a finite set of layers in ArcGIS[1].

2. An economic metric is established through a detailed calculation process to represent the economic feasibility (which includes the potential cost and revenue) at each wave site. The economic analysis includes the distance to the coastline and transmission grid, market size, and wave farm physical layout, but does not include the WEC cost; there is insufficient data in the public domain on which to build a meaningful WEC cost model. Rather than giving an absolute measure in dollars, this economic analysis evaluates sites by a relative value, which is more useful for comparing the economic feasibility on a site-to-site basis. As will be detailed later in the thesis, the immense differences between integration into the utility grid or remote communities led to two different implementations of this new economic metric – one for each paradigm.

3. A scenario based, multi-criteria GIS framework to identify strategically important wave sites is developed. This framework assists stakeholders in negotiating for important wave sites that strike a reasonable compromise between competing economic and environmental priorities. Despite the focus on the wave site selection in this thesis, this framework can be adapted to assist solving any site selection problem influenced by multiple conflicting factors.

1.6 Thesis outline

The remainder of this thesis is laid out as follows:

Chapter 2 first introduces the data source of wave information (SWAN data) used in this thesis and WEC technologies considered when processing the wave data. A detailed description about constructing a frequency filter and a directional filter is then presented in

[1] Maps throughout this thesis were created using ArcGIS® software by Esri. ArcGIS® and ArcMap™ are the intellectual property of Esri and are used herein under license. Copyright © Esri. All rights reserved.

this chapter. The spatial distribution of gross, frequency filtered, and frequency-direction filtered wave resources is presented in a GIS layer format by the end of this chapter.

Chapter 3 presents a detailed economic evaluation of WEC sites that accounts for all the influence of wave resources, distance to coastline and transmission grid, market size, and wave farm physical layout. Two specific cases are demonstrated in this chapter: one is utility grid market scale and the other is remote community market scale. The resulting economic potential is measured by the Net Revenue Index (NRI), and a GIS layer of NRI for each of the market scales is presented at the end of this chapter.

Chapter 4 introduces other factors that influence the choices of wave sites, such as existing human uses and marine conservations. This chapter includes three sections: the commercial fishery, the marine vessel traffic, and the marine conservation. Each section includes a briefly introduction of the importance for that factor, the data source, and the data processing.

Chapter 5 first explains the process of the multi-criteria GIS evaluation. The competing criteria chosen in this evaluation are then presented in detail. Later, a 'scenarios study' is introduced to estimate different stakeholder perspectives on the choice of wave energy sites. The strategically important wave sites along the WCVI are identified at the end of this chapter.

Chapter 6 summarizes the major conclusions and the limitations of this thesis as well as provides recommendations and guidelines for future work.

Chapter 2 Gross and Technical Extractable Wave Resource Assessment

The wave resource assessment developed in this work is based on wave climate data, obtained from a computational wave propagation model for the computation domain referred to as West Coast of Vancouver Island (WCVI) region (shown in Figure 2.1), that is built from the Simulating WAves Nearshore (SWAN) software. The SWAN wave model is operated by the West Coast Wave Initiative (WCWI) at the University of Victoria and has been validated against wave buoy measurements collected from seven buoys within the study area. Three of the buoys are directional wave measurement buoys maintained by the WCWI, the rest are maintained by the Environment Canada (EC) and the National Ocean and Atmospheric Administration (NOAA) [1]. This thesis focuses on the wave resource assessment using the wave data produced by the SWAN model developed by [37].

2.1 SWAN Model Overview

SWAN is a third-generation phase-averaged Eulerian numerical wave model that is widely used for simulating and calculating the wave conditions in near-shore regions [1], [12], [60]. SWAN is preferred for modelling near-shore wave conditions given its ability to represent the propagation, refraction and diffraction of waves in depth-limited regions; all are important physical processes in coastal waters. The SWAN grid used in this study covers a 410,000 km^2 area of the WCVI water and a 1500 km stretch of the BC and Washington coastlines. The northern edge of the grid starts from the Queen Charlotte Sound; the southern edge ends at Astoria Canyon (U.S.); the outside boundary extends about 200km westward from the coastline. The grid also includes the Strait of Juan de Fuca (see Figure 2.1).

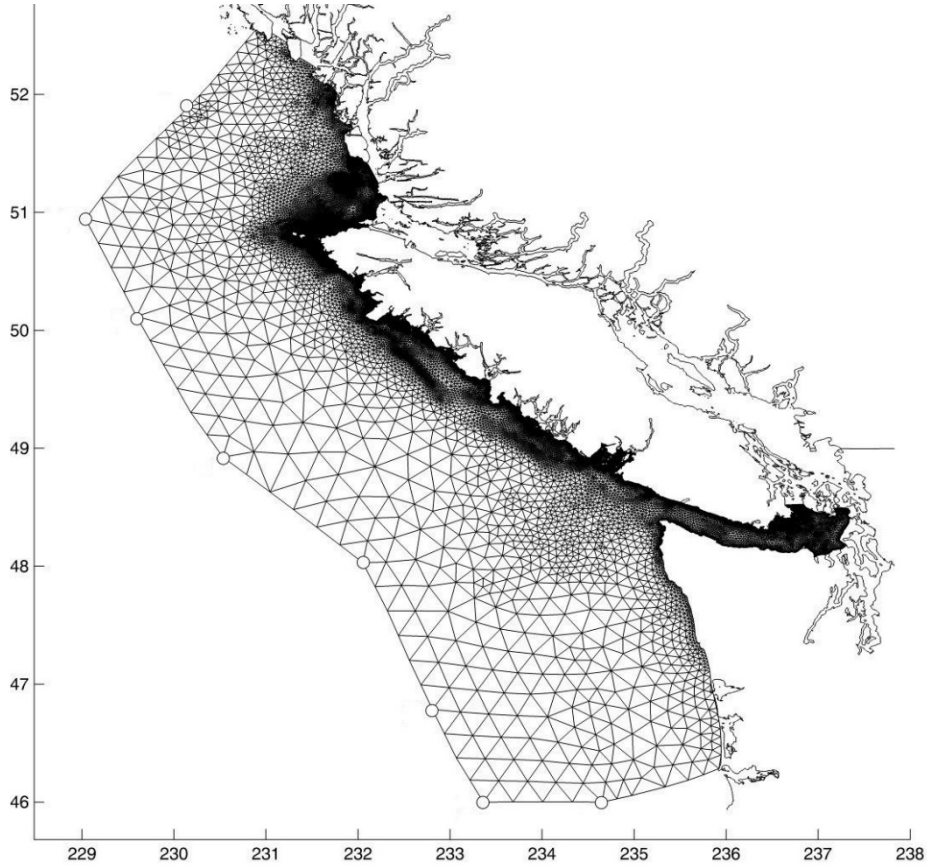

Figure 2.1 SWAN grid and computation domain [37].

The SWAN model uses an unstructured computational grid and the grid spatial-resolution increases with decreasing water depth to ensure an accurate representation of wave transformations in the near-shore areas while maintaining computational efficiency. In the extreme, a 50 m resolution was adopted for near-shore shallow regions to capture small scale wave effects caused by the interaction with the ocean floor; this resolution also follows the guideline of the International Electrotechnical Commission (IEC) TC 114 Technical Specification 62600-101:Wave energy resource assessment and characterization (IEC TS 62600-101) [39]. A lower resolution (e.g. more than 40 km spacing between grid points at the outer boundary) was applied in deep water to reduce the computation time. In transition regions, the grid resolution was proportional to ocean depths and seafloor slope.

The SWAN model is operated in a non-stationary mode [12]. In addition to the grid resolution and operation mode, the input wind and wave boundary conditions have

significant influence on the model performance. The SWAN model utilizes a combination of the European Centre for Medium Range Weather Forecasts (ECMWF) WAve Modeling (WAM) wave boundary conditions and Coupled Ocean/Atmosphere Mesoscale Prediction System (COAMPS) wind fields [1]. The ECMWF WAM model provides full directional spectra that meet the requirement for coastal modeling given in the IEC TS 62600-101. At the same time, the temporal and spatial resolution of the COAMPS wind forcing field are sufficient for accurate simulation of the generation and dissipation of waves in wind seas. The Westhuysen method [38] is chosen from three different quadruplet wave interaction solvers that are available in the SWAN model; the three solvers are the methods of Komen [61], Janssen [62], and Westhuysen. The combination of the Westhuysen solver and bottom friction is believed to provide the optimum performance on calculating the wave transformations [36].

2.2 SWAN Model Outputs

The SWAN model was used to compute a full directional variance density spectrum $E(f,\theta)$ (where f is the frequency and θ is the propagation direction measured relative to North) at each node point of the computational grid for a 10-year period (2004 -2013) using a time step of 3-hours. The SWAN model discretizes the continuous wave spectrum into 37 frequency-bins and 36 direction-bins to characterize sea-states [63]. The spectral-directional grid used to define the wave spectra at each node point is shown in Figure 2.2. The domain of the frequency-space is in the range of 0.035Hz - 1Hz, and the grid resolution is not uniform; the frequency is logarithmically distributed according to Eq. 2.1. The domain of directional-space covers a full 360° with a uniform of 10° bin resolution. In the following discussion, all integral operations on $E(f,\theta)$ are executed in a discrete manner within the SWAN calculations.

$$\Delta f = \left(-1 + \left(\frac{1}{0.035}\right)^{\frac{1}{n-1}}\right) f \qquad 2.1$$

In Eq. 2.1 Δf is the frequency-bin width, f is the bin center frequency, and n is the total number of frequency-bins in the model (n = 37).

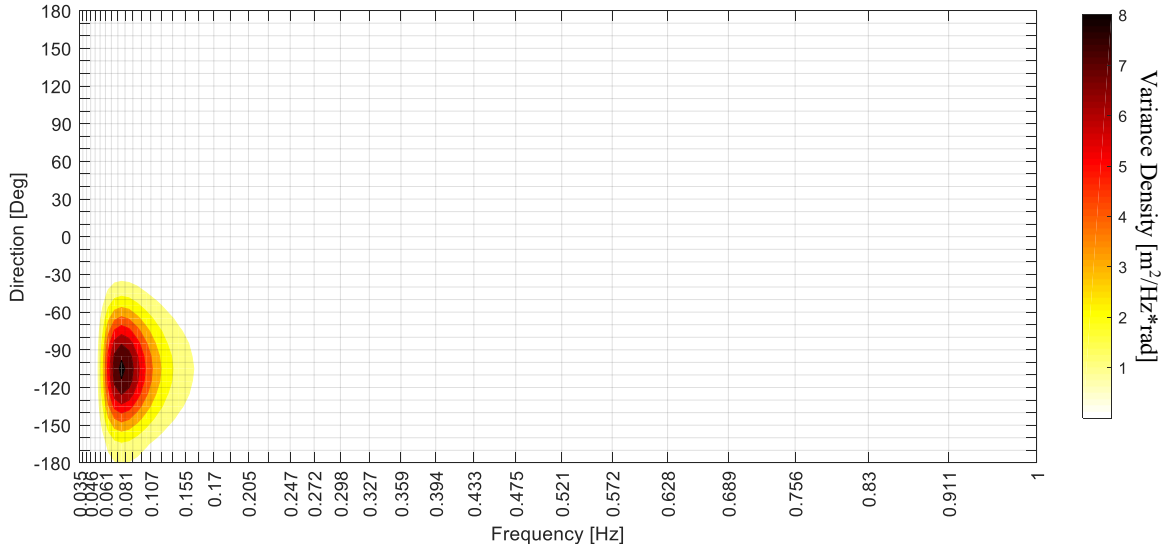

Figure 2.2 The spectral and directional discretization used by the SWAN model.

During model execution, SWAN tracks the full variance density spectrum at each grid point. However, the shape of the full spectrum is discarded as the model evolves; an excessive amounts of computer memory is required to store the full spectra. The full spectra are only recorded at 19 sites which are shown in Figure 2.3. These spectra are used for comparing with WCWI and EC buoy data in validation studies on the SWAN model.

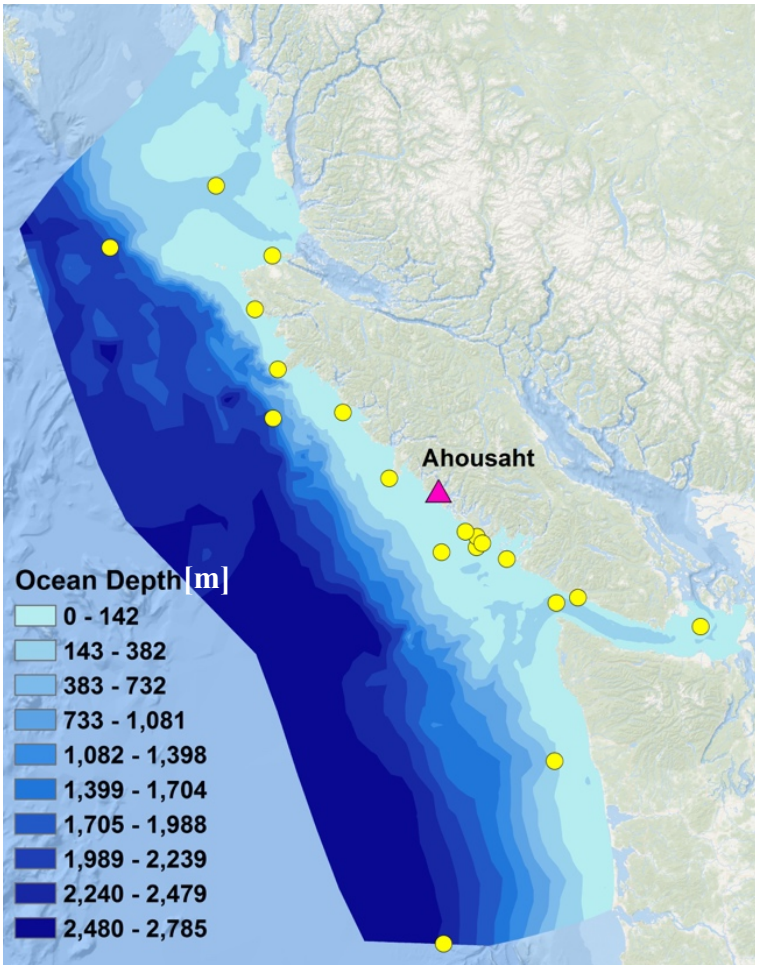

Figure 2.3 The sites where full frequency directional spectra are recorded in SWAN.

At the rest of the SWAN model grid points, the SWAN model retains a statistical summary of the wave characteristics. The summary data includes: Significant Wave Height (H_s), Energy Period (T_e), Peak Wave Direction (θ_p), Directional Spreading of the waves (δ_θ), Energy Flux (J) etc. The SWAN model calculates the H_s and T_e based on Eq. 2.2 and Eq. 2.3.

$$H_s = 4.004\sqrt{m_0} \qquad 2.2$$

$$T_e = \frac{m_{-1}}{m_0} \qquad 2.3$$

where m_n is the n^{th} spectral moment and can be calculated at any grid point from the discrete variance density spectrum through Eq. 2.4, for the non-directional case.

$$m_n = \int_0^{\infty} f^n E(f) df \quad (2.4)$$

As well as H_s and T_e, the SWAN model also parameterizes the directional characteristics of waves. The peak wave direction (θ_p), which is the direction-bin with the maximum variance density, is extracted from the directional wave spectrum. The directional spreading (δ_θ) of the waves is calculated through Eq. 2.5.

$$\delta_\theta^2 = \int_{-\pi}^{+\pi} \left(2 \sin\left(\frac{1}{2}\hat{\theta}\right)\right)^2 D(\hat{\theta}) d\hat{\theta} \quad (2.5)$$

where $\hat{\theta}$ is taken relative to the peak wave direction (θ_p) and can be defined by $\hat{\theta} = \theta - \theta_p$, and $D(\hat{\theta})$ is the directional distribution and can be calculated through Eq. 2.6.

$$D(\hat{\theta}) = \frac{E(f, \hat{\theta})}{E(f)} = \frac{E(f, \hat{\theta})}{\int_0^{2\pi} E(f, \hat{\theta}) d\hat{\theta}} \quad (2.6)$$

Finally, the omni-directional wave energy flux (J) is calculated in the SWAN model through Eq. 2.7.

$$J = \rho g \int_0^{2\pi} \int_0^{\infty} C_g(f) E(f, \theta)\, df d\theta \quad (2.7)$$

where ρ is the sea water density, g is the gravity acceleration, $E(f, \theta)$ is the variance density, and $C_g(f)$ is the group velocity and can be calculated via Eq. 2.8.

$$C_g = \frac{g}{2\pi f} \tanh kd \left[\frac{1}{2}\left(1 + \frac{2kd}{\sinh 2kd}\right)\right] \quad (2.8)$$

where k is the wave number and d is the water depth.

For irregular wave conditions, in deep water, the energy flux (J_{DW}) can be roughly estimated using H_s and T_e via Eq. 2.9 [12]. Note that this approximation is independent of the shape of the true spectral distribution $E(f, \theta)$.

$$J_{DW} = \frac{\rho g^2}{64\pi} H_s^2 T_e \quad (2.9)$$

2.3 Re-generating a Wave Spectrum from Summary Statistics

The omni-directional wave energy flux (defined by Eq. 2.7) is a required resource assessment output by IEC TS 62600-101 [39]. While the omni-directional wave energy flux provides an understanding of the magnitude of the naturally occurring wave energy, it represents an upper bound on the level of energy that could be extracted and converted into a usable energy commodity by technology. Wave energy flux is distributed unevenly in both frequency and directional spaces and given that frequency and directionality characteristics significantly affect the performances of WECs, these characteristics need be considered when assessing the wave energy production opportunity. To apply knowledge of technological bandwidths in terms of frequency and direction, a full directional variance density spectrum at each model grid point is needed.

A full directional spectrum at any SWAN model grid point can be regenerated using the limited wave parameters in the SWAN outputs and an assumed spectral shape. A single peaked spectrum with a Pierson-Moskowitz shape has previously been found to most closely match the wave resource at the WCVI region [43]. The frequency spectrum can be generated following Eq. 2.10.

$$\hat{E}(f) = \alpha g^2 (2\pi)^{-4} f^{-5} exp\left[-\frac{5}{4}\left(\frac{f}{f_p}\right)^{-4}\right] \qquad 2.10$$

where $\hat{E}(f)$ is a synthetic non-directional variance density spectrum, f is the wave frequency in Hertz, f_p is the peak frequency, α is an energy scale to ensure that the overall variance of the synthetic spectrum matches the variance of the original, but unrecorded, spectrum. The total variance of the original spectrum can be calculated via Eq. 2.11.

$$\int_0^\infty E(f)df = \frac{H_s^2}{16} \qquad 2.11$$

The directional distribution of variance is set according to Eq. 2.12.

$$D(\hat{\theta}) = \beta \cos^{2s}(\frac{1}{2}\hat{\theta}) \qquad 2.12$$

where $\hat{\theta}$ is taken relative to the peak wave direction, s is a width parameter that decides the width of the directional distribution and can be calculated via Eq. 2.13.

$$s = \frac{2}{{\delta_\theta}^2} - 1 \qquad 2.13$$

β is a normalization coefficient to ensure the total direction distribution

$$\int_0^{2\pi} D(\hat{\theta})\, d\hat{\theta} = 1 \qquad 2.14$$

and β can be calculated via Eq. 2.15.

$$\beta = \Gamma(s+1) / \left[\Gamma\left(s + \frac{1}{2}\right) 2\sqrt{\pi}\right] \qquad 2.15$$

where Γ is the Gamma function and is defined in Eq. 2.16.

$$\Gamma(s+1) = (s)! \qquad 2.16$$

The regenerated full directional variance density spectrum is then binned to the resolution that matches the computational spectral grid used in the SWAN model, which characterizes the sea-states with 37 frequency-bins and 36 direction-bins. As an example, the synthetic spectrum for a site near the Ahousaht (at 24:00, Mar 30, 2012) (see Figure 2.2) is plotted in Figure 2.4.

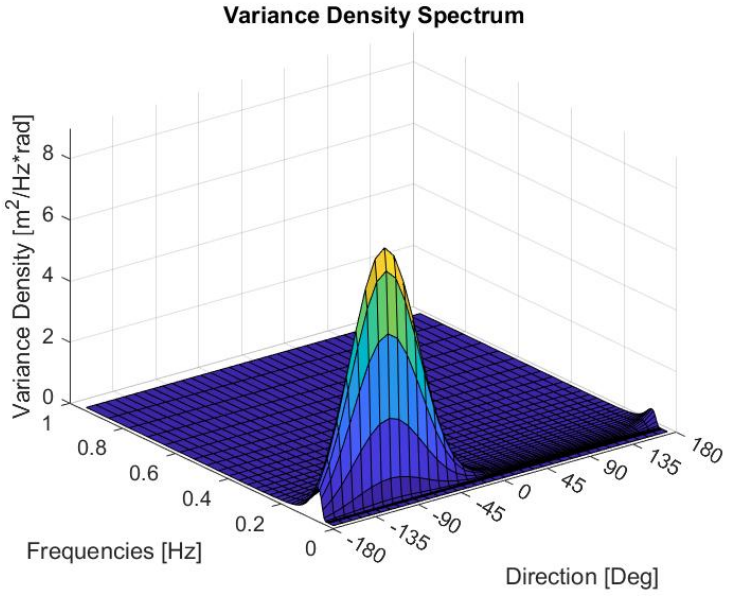

Figure 2.4 The synthetic full directional variance density spectrum.

The regenerated variance density spectrum is based on some assumptions and will be different than the original spectra that are calculated inside SWAN at each grid point and time step. The difference between the synthetic spectrum and the original spectrum can be

measured by comparing the energy flux (J) calculated in the SWAN model and the energy flux (J_{syn}) calculated via Eq. 2.17, based on the synthetic spectrum.

$$J_{syn} = \rho g \int_0^{2\pi} \int_0^{\infty} C_g(f) \widehat{E}(f,\theta)\, df d\theta \qquad 2.17$$

The difference between the J and J_{syn} can be quantified by the Relative Error (ER) defined by Eq. 2.18. The ER for each grid node is represented by the average ER throughout year.

$$ER = \frac{\left|J_{syn} - J\right|}{J} \qquad 2.18$$

The Relative Error (ER_{DW}) between the J and the deep-water approximation J_{DW}, estimated using the SWAN output H_s and T_e via Eq. 2.9, is calculated through Eq. 2.19 as a comparison.

$$ER_{DW} = \frac{\left|J_{DW} - J\right|}{J} \qquad 2.19$$

The average, standard deviation, first quartile, second quartile, and third quartile of the annual ER and ER_{DW} are shown in Table 2.1.

Table 2.1 The Average, standard deviation, and quartiles of the ER and ER_{DW}.

	Synthetic	Deep-water
Average	19.05	24.71
Standard Deviation	19.28	38.84
First Quartile	9.54	5.97
Second Quartile	17.92	10.80
Third Quartile	23.20	23.85

The average of the ER for the synthetic spectral is 19.05%, whereas the ER_{DW} for the conventional deep-water approximation is 24.71%. The energy flux calculated from deep-water approximation, which is commonly used, contains more error than the energy flux calculated from synthetic spectra. As such, the difference between the synthetic spectral

and the real spectral is acceptable. The synthesized spectra are the best available descriptions about the energy flux distribution in the frequency and directional space.

2.4 Overview of Wave Energy Conversion (WEC) Technologies

Individual WEC architecture reacts to the waves differently due to inherently different operational characteristics and power production concepts. Identification of future wave farm locations needs to account for the performance limitations of the full population of WEC technologies. In this work, the 'population' of WECs is represented using four WECs spanning for different classes of WEC technology: a Two-Body Point Absorber (2B-PA), a Pitching Surging Flap (PS-flap), a Buoyant Raft (Raft), and a Backwards Bent Duct Buoy (BBDB). These WECs have different energy recovery concepts, required deployment depths, and rated power levels. By combining their performance characteristics in a unionized representation of WEC performance the goal is to implement technological limitations while still remaining device-agnostic. As will be shown in Section 2.4, the devices actually demonstrate similar frequency response characteristics based on available performance data, which eases the task of combining spectral performance characteristics.

The electrical power that can be recovered from each device is assessed at each sea-state using the commercial software ProteusDS and MathWorks' Simulink package [42]; the sea-state is characterized by each H_s - T_e pair that has been standardized according to the IEC TS 62600-100 [39]. The wave climate is simulated using each H_s - T_e pair with a Pierson-Moskowitz spectral shape. A uniform directional spread for each sea-state is created using a cosine squared that is suggested by the [64]. For each sea-state, a 20-minute simulation was conducted. In the simulations, the wave condition is represented with 140 different wave segments composed of 7 different direction-bins and 20 different frequency-bins, which is recommended by IEC TS 62600-101. The electrical power (measured in kW) for all the representative sea-states is presented in a power matrix format.

Two-Body Point Absorber

The two-Body Point Absorber (2B-PA) is an axis-symmetric two-body WEC developed as a research platform by the University of Victoria (shown in Figure 2.5 (a)) and its typical

operating depth is 40 - 60 m. [65]. The main structure is composed of a cylindrical (15m diameter) buoyant float coaxially aligned with a spar (39m tall). The spar has 6 degree of freedom movements whereas the float is constrained to move along the common central axis. Wave energy is converted by harnessing the relative motion (going in both directions) between these two bodies. This structure is slack-moored (e.g. multiple catenary mooring lines) to the seabed. The power matrix of 2B-PA is shown in Table 2.2.

Table 2.2 The power matrix for 2B-PA[2].

Significant Wave Height [m] \ Wave Energy Period [s]	5.5	6.5	7.5	8.5	9.5	10.5	11.5	12.5	13.5	14.5	15.5	16.5	17.5
0.25	0.696	1.09	1.33	1.22	0.958	0.737	0.599	0.476	0.34	0.328	0.261	0.208	0.172
0.75	6.48	10	11.4	11.8	9.55	6.55	5.78	4.29	2.76	2.99	2.48	1.97	1.49
1.25	17	25.6	31.1	29.4	24.9	20.9	16.3	13.8	8.92	9.94	6	5.11	3.63
1.75	33.2	52.7	53	58.2	45.3	32.2	29	22.4	19.6	18.1	12.2	11.7	8.33
2.25		84.6	82.8	99.6	79.7	58	46.9	40.9	36	26.6	20.1	14.9	14.6
2.75		116	104	128	122	97.9	58.4	52.5	46.3	38.2	34.2	24.2	19.7
3.25		156	137	168	163	128	86.8	76.1	61.5	56.8	47.2	40.4	29.6
3.75		214	196	190	192	167	142	111	72.4	71.8	71.6	53.1	37.2
4.25			229	235	255	216	179	147	128	98.8	71.8	50.7	49.1
4.75				309	254	241	219	143	146	109	94.2	92.6	66.7
5.25					368	322	272	212	170	151	104	93.1	78.9
5.75						336	247	251	180	143	150	105	84.8
6.25						394	321	283	260	203	149	99.8	106
6.75						350	357	300	254	229	163	121	145
7.25						476	466	287	260	236	180	153	133
7.75						464	379	418	292	285	231	171	143

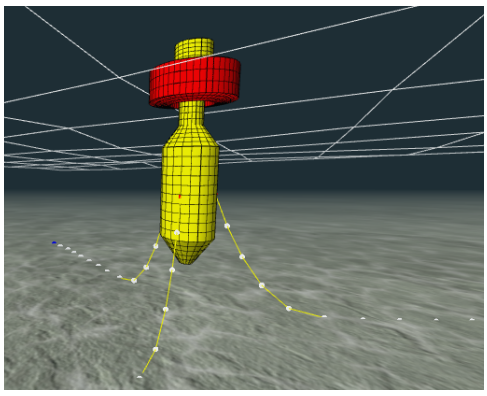

(a) 2B-PA

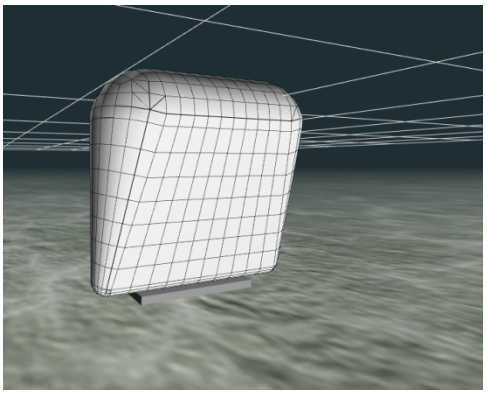

(b) PS-flap

[2] The matrices are obtained from WCWI

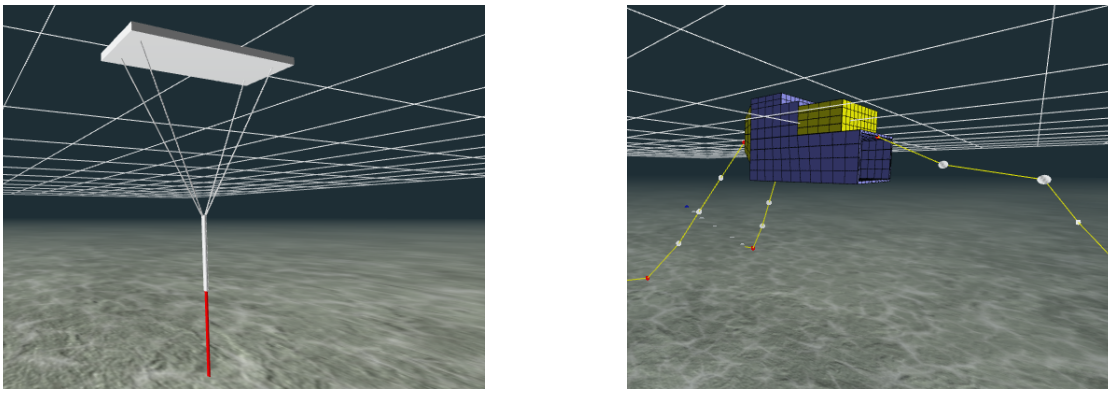

(c) Raft (d) BBDB

Figure 2.5 Four types of WECs (shown in ProteusDS environment).

Pitching Surging Flap

The Pitching Surging Flap (PS-flap) typically operates in shallow water (8 -15 meter), and is shown in Figure 2.5 (b) [66]. The buoyant flap has dimensions of 8m in width and 7.5 m in height, and rotates around a fixed axis rigidly attached to the seabed. A hydraulic cylinder is placed between the flap and its fixed base. The power is generated by compression and expansion of the hydraulic cylinder caused by the pitching oscillations of the flap. The electric power generated by the PS-flap for each sea-state is presented in the power matrix shown in Table 2.3. In the power matrix, blank cells indicate H_s - T_e conditions in which the device produces no power. There are two reasons for the absence of the values. First, the power is negligible at the sea-states with such small H_s, and the device may not even activate in these small H_s conditions. Second, the devices are in a shutdown mode at some of these sea-states, and thus no power is generated.

Table 2.3 The power matrix for PS-flap.

Significant Wave Height [m] \ Wave Energy Period [s]	7.5	8.5	9.5	10.5	11.5	12.5	13.5	14.5	15.5	16.5	17.5
0.25			1.8	1.6	1.3						
0.75	11.2	10.4	11.7	9.24	9.29	7.38	5.63	4.75	3.68		
1.25	25.7	31.1	22.4	23.9	18.4	17.5	15.6	13.4	10.1	8.78	
1.75		44.4	38.6	38.8	31	33	31.4	22.6	18.3	15.9	
2.25		70.6	59.9	49.2	48.1	44.5	40.1	36.8	29.9	28.2	21.1
2.75		85.2	78.8	77.3	72.9	62.9	52.3	47.4			
3.25			117	89.9	83.9	83.8	59.4	56.7			
3.75						113	111	88.3			
4.25							117	111			
4.75								130			

Buoyant Raft

The buoyant raft (Raft) is a surface following floating WEC designed by Seawood Designs Inc (shown in Figure 2.5 (c)) [67] and its typical operation depth is 40 - 60 meter. The main structure is composed of a buoyant rectangular pontoon (24m length, 7m width and 1m height) attached to a hydraulic cylinder via a static bridle. The buoyant rectangular pontoon has 5 degrees of freedom in any motions except yaw. The hydraulic cylinder is fixed at its bottom to the seabed, but the cylinder is able to rotate around the fixed point. The wave power is produced by the expansion (only on upstroke) of the hydraulic cylinder. The power matrix is presented below.

Table 2.4 The power matrix for Raft.

Significant Wave Height [m] \ Wave Energy Period [s]	6.5	7.5	8.5	9.5	10.5	11.5	12.5	13.5	14.5	15.5
0.75		19.4	11	10.9	12.1	7.99				
1.25	58.6	85.2	83	94	85.5	69.3				
1.75	147	164	167	174	156	141	139			
2.25	209	209	235	233	213	205	196	179		
2.75	298	310	313	308	271	236	233	216	218	
3.25		379	364	359	335	315	295	265		
3.75		435	431	420	401	368	366	317		
4.25			507	473	445	435	388	376		
4.75			583	564	492	482	445	414	380	
5.25				596	553	527	479	447	410	
5.75				625	588	545	526	479	457	417
6.25					626	555	558	504	461	443
6.75					664		585	529	501	

Backwards Bent Duct Buoy

The Backwards Bent Duct Buoy (BBDB) is an Oscillating Water Column WEC featured in the US Department of Energy Reference Manual (shown in Figure 2.5 (d)) and its typical operation depth is 60 - 150 meter [68]. The BBDB is composed of an internal air chamber and a rigid hull. The back of the rigid hull (with a 17.5 m draft, a 27 m beam and a 35 m length) is set to face the wave propagation direction and fixed with a 3-point mooring system. The entrained water is excited to oscillate with the incoming waves. The oscillation of the entrained water drives compression or expansion of the air trapped inside the hull, and thus creates a pressure differential between the air chamber and the external environment. This pressure differential cause air flow through an air turbine mounted to

the hull, and thus a rotating generator to produce power. The power matrix is presented below [42].

Table 2.5 The power matrix for BBDB.

Significant Wave Height [m] \ Wave Energy Period [s]	5.5	6.5	7.5	8.5	9.5	10.5	11.5	12.5	13.5	14.5
0.75	0.0388	0.838	3.59	5.7	8.05	7.39	7.43	5.68		
1.25	0.621	3.76	13.8	19.9	27.3	28	24.6	20.7		
1.75	2.03	11	31.4	52.5	57	52.7	51.3	40.4	34.7	
2.25		22.7	57.8	88.2	94.6	88.2	85.1	70	64.7	
2.75		34.2	83.1	120	128	123	117	106	84.1	
3.25			115	158	177	165	162	129	119	
3.75			152	204	203	209	182	169	147	143
4.25				234	253	229	232	201	181	156
4.75					277	272	261	227	197	180
5.25						303	240	252	252	
5.75						296	296	279		

2.5 WEC Spectral and Directional Performance Characteristics

The four presented WECs have very different physical architectures and operating concepts, yet a device-agnostic representation of WEC performance characteristics is required in order to identify strategically important sites for wave farms. Since only a portion of the wave energy flux can be captured by WECs, it is important to apply performance limits in the resource assessment stage. As examples, the wave frequency delivering the peak wave energy flux and the frequency at which a WEC is most efficient will not necessarily match, and some wave energy flux will be delivered at frequencies at which WECs cannot operate.

The naturally occurring omni-directional wave energy flux could present a biased estimate of a site's 'goodness'. The gross wave resource is described by the omni-directional wave energy flux (J) output from the SWAN model, and it does not account for the impacts of frequency and direction on WEC performance.

As a first step, a frequency filter is developed to help screen the omni-directional wave energy flux by removing energy flux delivered by waves at frequencies at which a WEC cannot operate. This filter is based on power performance matrices of the four aforementioned WECs. Equation 2.9 shows that the wave energy flux is highly dependent

on H_s and T_e. Since this study focuses on investigating how the devices react to different wave frequencies, i.e. the relationship between the devices extractable power and the wave period, the rows of the power matrix of each WEC are normalized by ${H_s}^2$ to remove the influence of the wave height on the magnitude of the extracted power. Each performance matrix is then compressed to the wave period axis by averaging the normalized entries within each column. A cosine bell shape was created to fit the normalized power vs. wave period of the data points for each type of WEC. The peak of the cosine bell is set at the wave period corresponding to the maximum normalized power. The cosine bells are created in terms of the wave period, but are redefined in terms of frequency to facilitate the application of the filters to the spectra produced using the procedure outlined in Section 2.3 (see Figure 2.6).

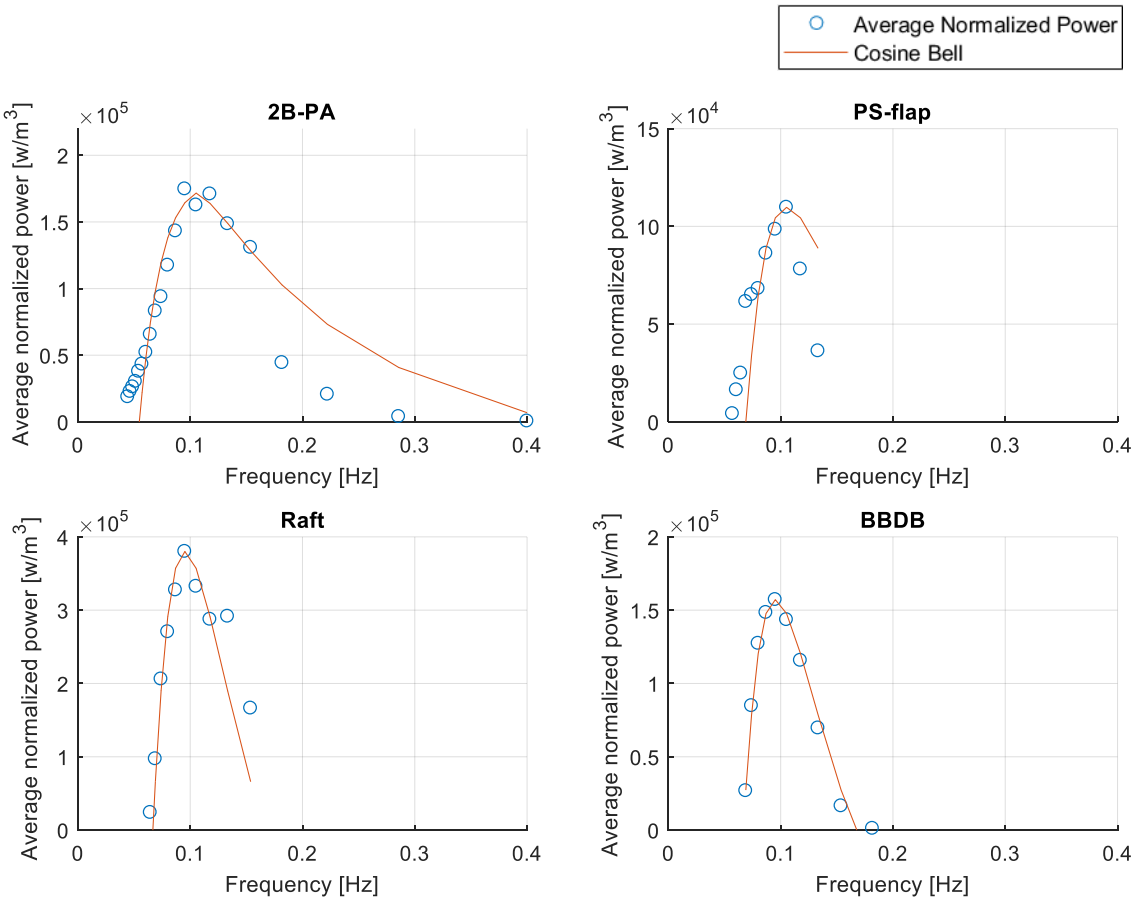

Figure 2.6 The cosine bell shapes that comprise the frequency response for each of the four WECs.

The cosine bell for 2B-PA features a peak at 0.105Hz and has boundaries at 0.044Hz and 0.4Hz. The cosine bell for PS-flap features a peak at 0.105Hz and has boundaries at 0.057Hz and 0.133Hz. The cosine bell for Raft features a peak at 0.095 Hz and has boundaries at 0.065 Hz and 0.154 Hz. The cosine bell for BBDB features a peak at 0.095Hz and has boundaries at 0.069 Hz and 0.182 Hz. The cosine bells are able to represent the normalized power from the Raft and BBDB data effectively. The cosine bells show some differences to the 2B-PA and PS-flap data, but still capture the trends near the frequency with the highest power concentration (0.065Hz to 0.12Hz).

Instead of creating an individual filter for each device, a frequency filter that can capture the trends for all the four cosine bell curves is required. The extractable power varies significantly from one device to another due to different operational characteristics, power production concepts, and dimensions of the devices. Since this study focuses on the relative performance of devices among different frequencies, rather than the precise amount of power that can be extracted, the cosine bell curves are normalized again to ensure peak values of 1. The frequencies that exceed the device operation range and have no extractable power are assigned a 0 score. The scaled data points from each device's cosine bell curve are plotted in Figure 2.7 as well as a single average curve for comparison.

By comparing the scaled cosine bell curve data points, the single average cosine bell shape ($W_f(f)$) with a peak at 0.095Hz and boundaries at 0.065Hz and 0.154Hz does represent the generic WEC responses to waves of different frequencies; moving forward, this shape is used as the frequency filter and is described by Eq. 2.20. For this study, this single filter allows WECs to capture all (100%) energy at the peak frequency and no energy beyond the boundaries. The filter matches the performance of devices well at the frequency between 0.069Hz and 0.153Hz where most power can be extracted by WECs (see Figure 2.7). This filter slightly underestimates the power at higher frequencies, but those higher frequencies only contain a small amount of the overall wave energy flux at any site.

$$W_f(f) = \cos\left(\frac{\pi}{15.5 - 6.5}\left(\frac{1}{f} - 10.5\right)\right) \qquad 2.20$$

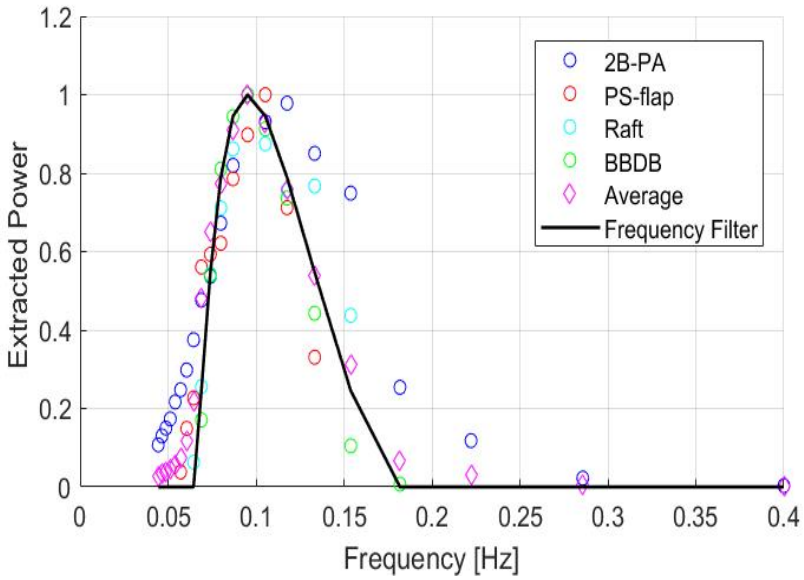

Figure 2.7 Frequency filter and scaled power.

In addition to frequencies, certain WECs are also sensitive to wave directions. For examples, the PS-flap and DDBD must be deployed so that they face into the predominant wave direction whereas the 2B-PA is axis-symmetric and can be moored at any orientation. A directional filter is developed here to emulate the degradation of some WEC's performance with changing relative wave directions. This directional filter is applied to the wave resources data after the frequency filter has been applied. Since no simulation of the WEC performance has accounted for the wave direction yet, this directional filter is generated following the IEC TS 62600-101[39]: a standard cosine window with a width of 180-degrees is used (see Figure 2.8). This filter is represented by Eq. 2.21.

$$W_D(\theta) = \cos(\theta - \theta_D)\delta \begin{cases} \delta = 1, & \cos(\theta - \theta_D) \geq 0 \\ \delta = 0, & \cos(\theta - \theta_D) < 0 \end{cases} \qquad 2.21$$

In Eq. 2.21, θ_D is the dominant wave direction of the year. The θ_D varies at different grid points, and the identification of the θ_D is introduced here.

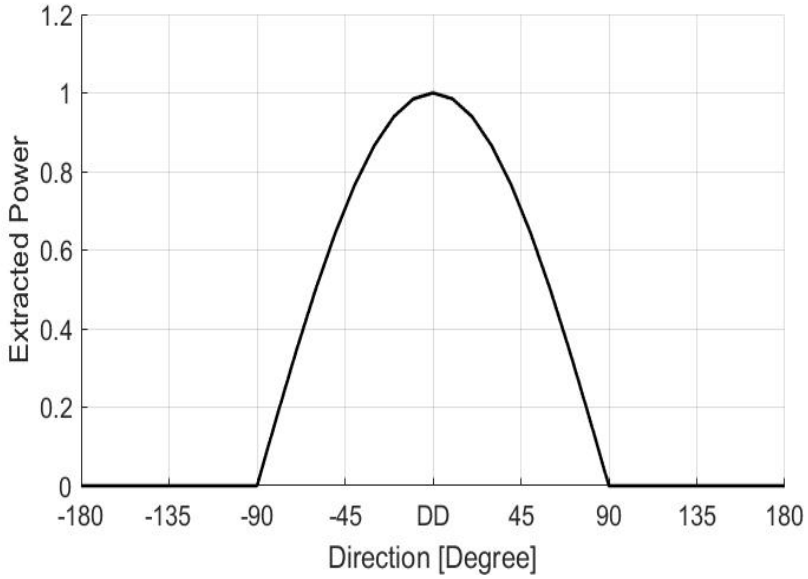

Figure 2.8 Directional filter (DD stands for the Dominant Direction of the year).

The dominant wave direction (θ_D) is the direction where the majority of energy is delivered during a year. In order to understand how the accumulated energy through a year is distributed among different directions, the directional energy flux spectrum for each time step is required. The spectrum at each step can be calculated through Eq. 2.22 [12], with the knowledge of the full directional variance density spectrum; the variance density spectrum can be synthesized following the method in Section 2.3. As an example, the energy flux spectrum for the site near Ahousaht (at 24:00, Mar 30, 2012) is shown in Figure 2.9, where the total energy flux for this record is 68 kW/m.

$$J_{bin}(f,\theta) = \rho g \int_{\theta_1}^{\theta_2} \int_{f_1}^{f_2} C_g(f) \widehat{E}(f,\theta)\, df d\theta \qquad 2.22$$

where J_{bin} is the energy flux within frequency-direction bin, C_g is the group velocity, $\widehat{E}(f,\theta)$ is the variance density, and θ_1, θ_2 , f_1 and f_2 are the boundary of each frequency-direction bin which is shown in Figure 2.2.

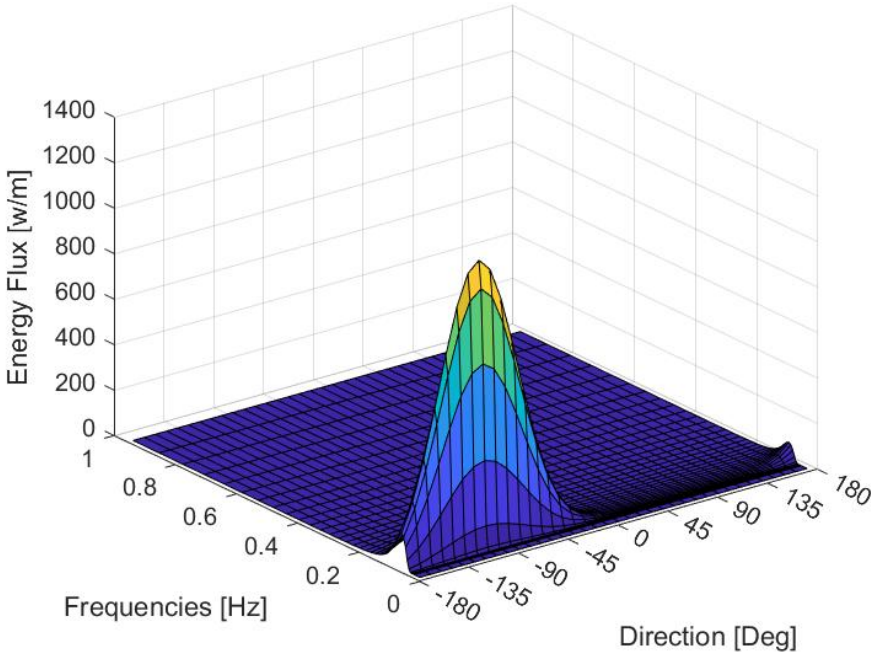

Figure 2.9 Full directional energy flux spectrum.

Since the time-step resolution of the SWAN model is 3-hours, J_{bin} is assumed to be the mean energy flux within the three hours. The annual energy delivery for the bin is calculated by summing up the energy of each 3-hour time step through the year. The annual energy delivery within each bin is shown in Figure 2.10, and the total annual energy delivery for this site is 249 MWh/m. The frequency-direction annual energy delivery surface is then compressed to the direction axis by summing up the energy of the bins with the same direction. The direction-bin corresponding to the maximum annual energy is taken as the dominant wave direction of the year. For this example, the dominant wave direction is at -105°.

In order to understand the relationship between the peak wave direction and the dominate wave direction at one site during a year, the peak wave direction at each time step and the dominant wave direction for the year are plotted in Figure 2.11. In this example, the peak direction has an approximate 125° variation during a year.

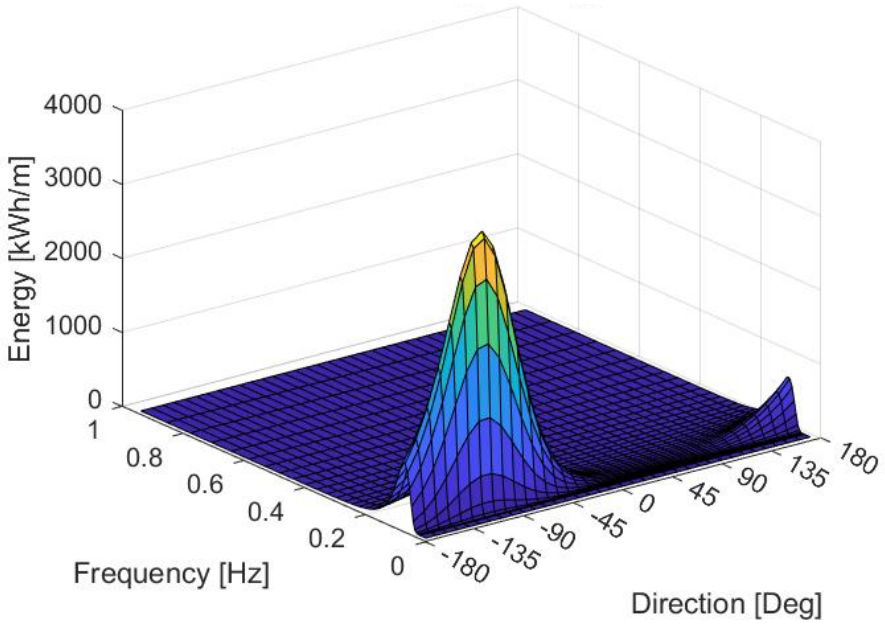

Figure 2.10 Annual energy delivery surface at a site near Ahousaht.

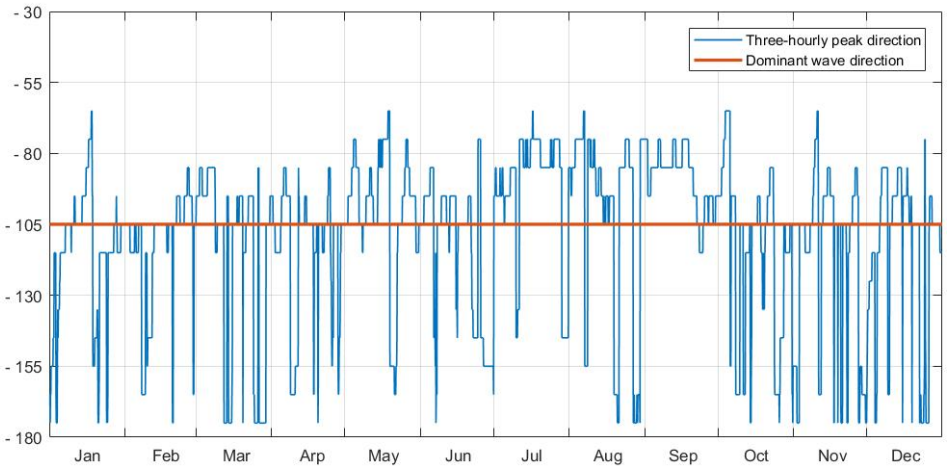

Figure 2.11 The dominant wave direction and the peak directions during a year.

2.6 Gross, Frequency Filtered, and Frequency-direction Filtered Wave Resource Evaluation

The gross wave resource is described by the omni-directional wave energy flux (J) output from the SWAN model, which is at a 3-hour time step throughout the years 2004 – 2013. The procedure for applying the frequency and directional filters to estimate the frequency

filtered and frequency-direction filtered wave resource is introduced as follows. Note that the order of application is the frequency filter first and then the directional filter. Since all WECs have frequency limits but only some WECs have directional limits, it is impractical to apply the directional filter without also applying the frequency filter. As a demonstration, the frequency and directional filters are only applied for the data of 2012 considering the computational space and time. The time for processing one-year data is around two weeks, which makes it impractical to apply the filters for all ten years of data given the project time.

First, a full directional variance density spectrum is synthesized, following the method in Section 2.5. The frequency filter (Eq. 2.20) is then applied to remove energy flux that cannot be captured by WECs. The frequency filtered energy flux (J_f) of each bin can be calculated following the Eq. 2.23.

$$J_f = \int_0^{2\pi} \int_0^{\infty} \mathrm{W}_f(f)\, J_{bin}(f,\theta)\, df d\theta \qquad 2.23$$

As an example, the gross and frequency filtered energy flux for a site near the Ahousaht (at 24:00, Mar 30, 2012) is plotted in Figure 2.12 to demonstrate the effect of this frequency filter. In the plot, the filtered energy flux spectrum is compressed to the frequency axis only. The frequency with peak energy flux is at 0.077Hz, whereas the frequency where WECs are most productive is at 0.095Hz; these two do not match perfectly, which reduces the extracted energy flux. In this example, only 51% energy flux can be captured.

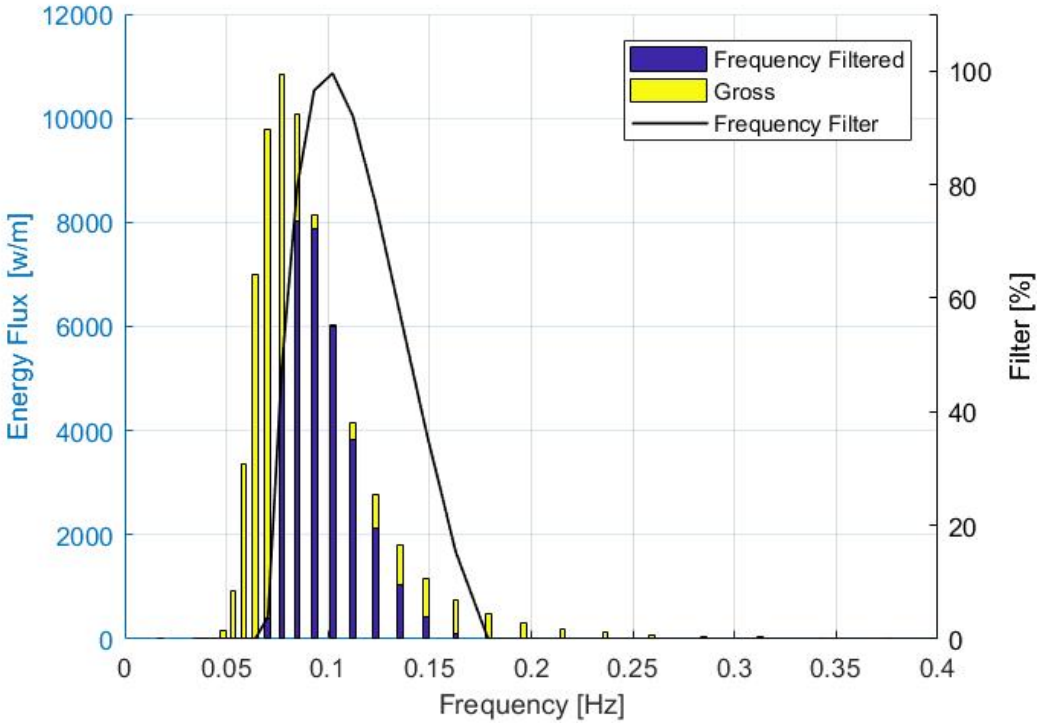

Figure 2.12 Frequency filtered energy flux.

To represent the potential power capture degradation that would result from using WECs sensitive to wave direction, the directional filter is subsequently applied in a similar manner. Assuming devices can be aligned to the dominant wave direction (the direction with the maximum energy delivery over a year), the frequency-direction filtered energy flux ($J_{f\theta}$) is calculated following Eq.2.24.

$$J_{f\theta} = \int_0^{2\pi} \int_0^{\infty} J(f,\theta)\, \mathrm{W}_f(f) \mathrm{W}_D(\theta - \theta_P)\, df d\theta \qquad 2.24$$

where θ_P is the dominate wave direction for the year of 2012.

The direction filter and the frequency-direction filtered energy flux at different times for the same site near Ahousaht are plotted in Figure 2.13. The direction filter is fixed to be aligned to the dominate wave direction (-105°) of the year, but the peak of the directional spectrum varies throughout the year. The peak direction in March (shown in (a)) perfectly matches the dominant direction, whereas in June (shown in (b)), the peak direction shifts to – 85º.

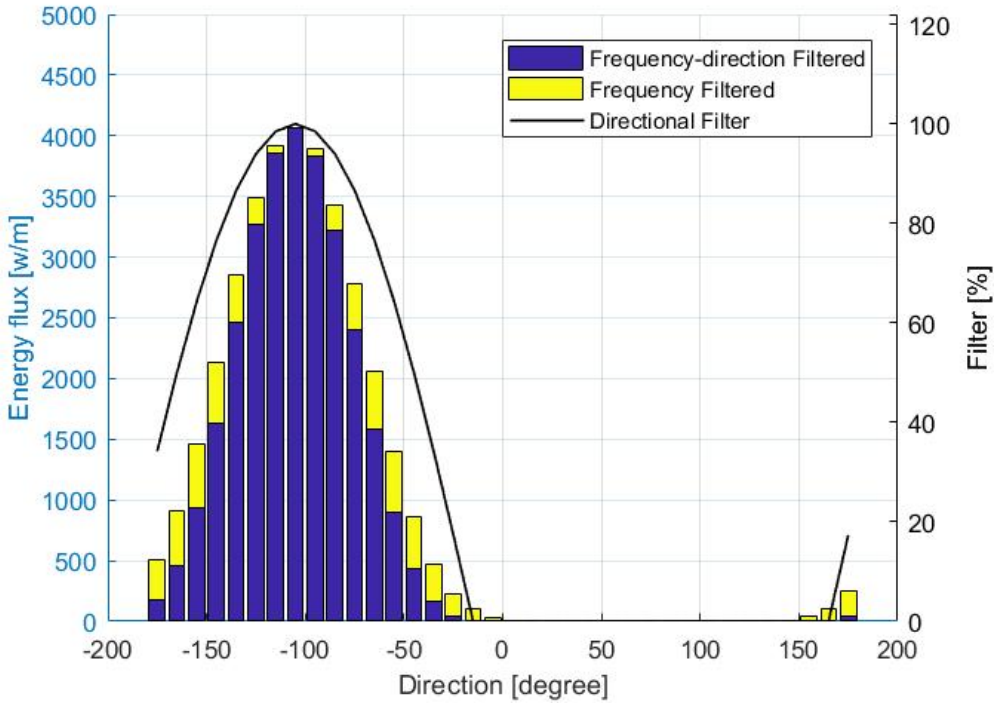

(a)

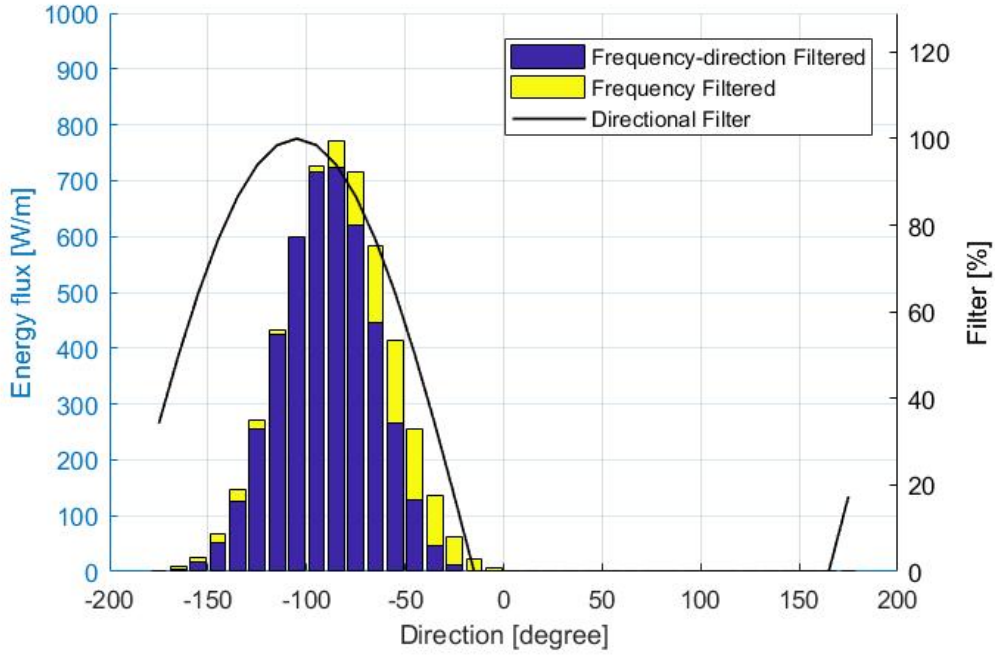

(b)

Figure 2.13 Frequency-direction filtered energy flux sampled in (a) March and (b) June.

2.7 The Spatial Distribution of Wave Resources

For each node in the SWAN grid, the yearly average of the annual gross wave energy flux (J), the frequency filtered energy flux (J_f), and the frequency-direction filtered energy flux ($J_{f\theta}$) are calculated. This information is best displayed in a map format to demonstrate the spatial distribution of the wave resource along WCVI. The gross and filtered wave energy flux is shown Figure 2.14.

Note that the gross wave energy flux, the frequency filtered energy flux, and the frequency-direction filtered energy flux are displayed with a common color scale to easily visualize the effect of the two filters. As will be discussed further in Chapter 4, data beyond 20km from the coastline, or deeper than 200m are eliminated from this study, due to the considerable costs for deployment and moorage constraints for WECs.

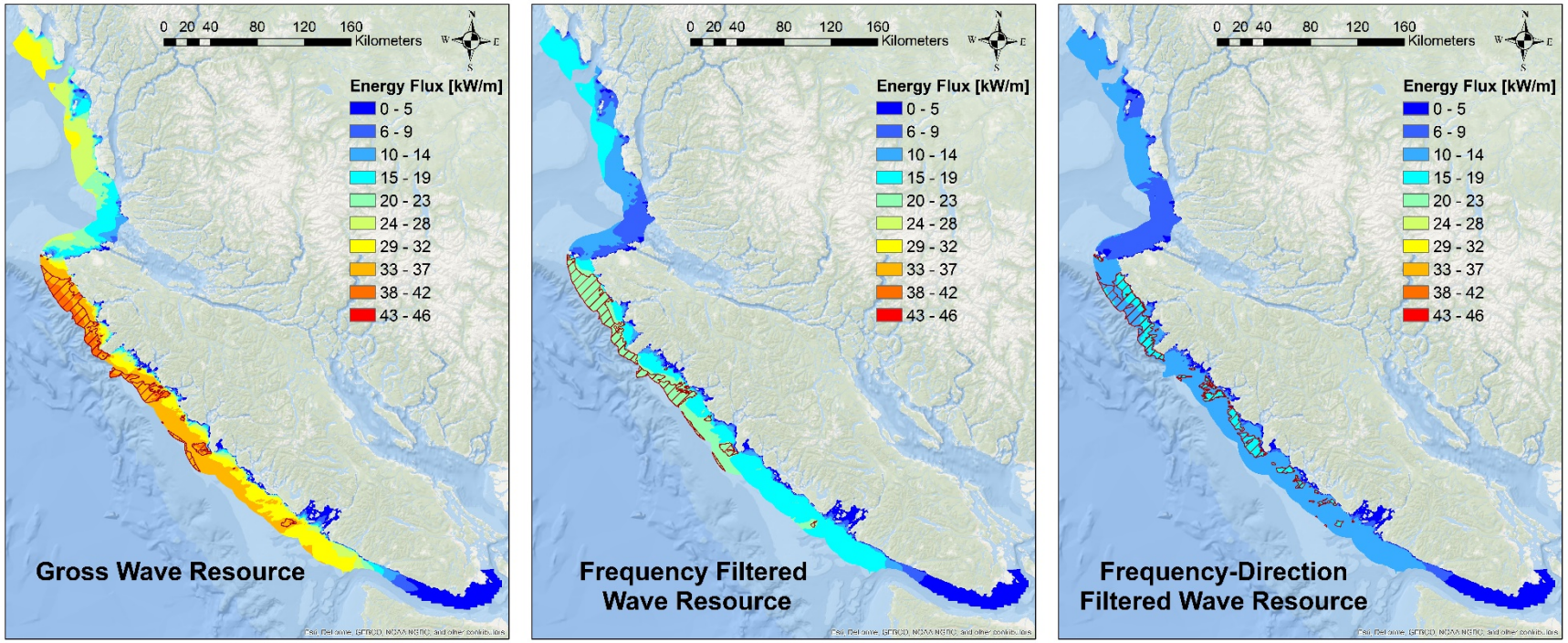

(a) *(b)* *(c)*

Figure 2.14 (a) Gross, (b) frequency filtered, and (c) frequency-direction filtered energy flux.

(Sites with energy flux in excess of 90th percentile are shown as the red-dashed region.)

The original data from the SWAN model is provided with Geographic Coordinate System named *World Geodetic System (WGS) 1984* and needs to be transformed into a Projected Coordinate System. The *North American Datum (NAD) 1983 Universal Transverse Mercator (UTM) Zone 10N* is selected for this study; this system is suitable for the use in North America between 126°W and 120°W. A spatial resolution of 100m by 100m is utilized considering the storage space and processing time.

In general, the wave resource is abundant on the north end of WCVI region, whereas the wave resource is inadequate in the Strait of Juan de Fuca. The frequency filter reduces the extractable wave resource significantly, from the average of 23.86 kW/m to the average of 13.03 kW/m. Given the filtering order, the directional filter has less impact than the frequency filter, but it still reduces the wave resource by 25% overall, and the average frequency-direction filtered energy flux is 9.79 kW/m. This is partly due to the assumption that WECs can be aligned to match the dominant wave direction at each grid point, which improves the WECs' efficiency.

In order to highlight the spatial distribution of wave sites with great power production potential, sites with 90^{th} percentile of gross, frequency filtered, and frequency-direction filtered wave resources are presented in Figure 2.15. The average wave energy flux and total filter resource area with each zone are shown in Table 2.6. Comparing areas with 90^{th} percentile of wave resources, the frequency filtered resource is reduced by 46%. The frequency-direction wave resource reduces it another 28%. In addition, the areas with 90^{th} percentile of gross wave resource and the areas with 90^{th} percentile of frequency filtered wave resource are highly correlated. The frequency-direction filter shifts the areas with 90^{th} percentile of wave resources southward.

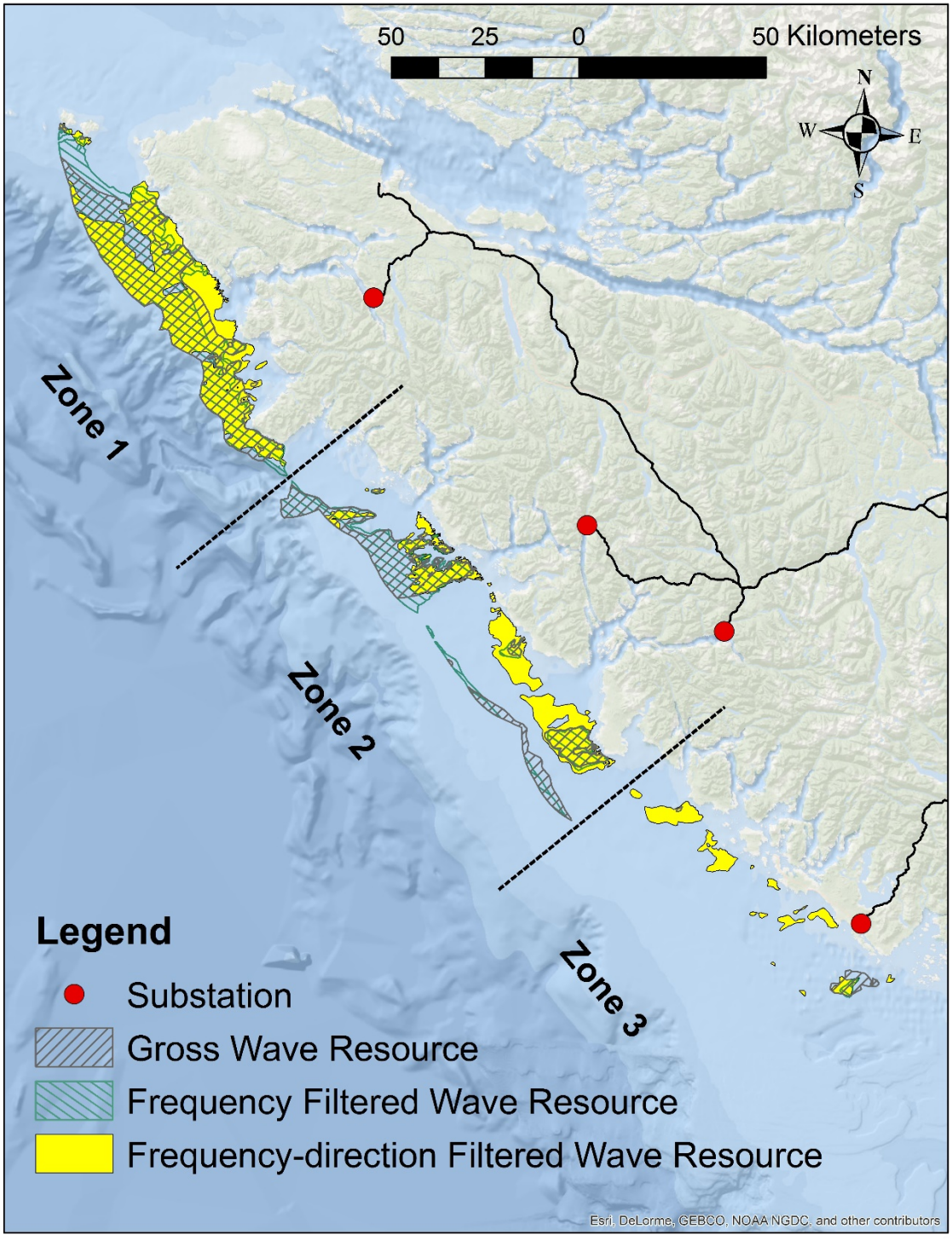

Figure 2.15 Areas with 90th percentile of gross, frequency filtered, and frequency-direction filtered wave resource.

Table 2.6 The average wave energy flux and area of each zone.

	Zone 1		Zone 2		Zone 3	
	Energy Flux [kW/m]	Area [km^2]	Energy Flux [kW/m]	Area [km^2]	Energy Flux [kW/m]	Area [km^2]
Raw	37.05	1040	36.67	595	36.25	47
Frequency Filtered	19.83	1145	19.59	601	19.22	11
Frequency-direction Filtered	14.15	1098	14.38	547	14.04	176

In conclusion, the frequency and frequency-direction filters effectively filter the gross wave energy flux to account only for energy that can be captured by the WECs. These filters not only reduce the amount of the wave resource, but also shift the boundaries of regions where 90^{th} percentile of resources occur. These sorts of filters are necessary to better represent the true opportunity for wave energy power production.

Chapter 3 Economic Evaluation of Wave Energy Sites

The potential economic return of wave energy farms is influenced by many factors beyond just the quality and magnitude of the gross wave resource. While the previous chapter described a device-agnostic assessment of the available wave energy resource, this chapter presents a device-agnostic assessment of revenues and costs associated with the size of the nearby electricity markets (both utility and remote community market scales) and the current cost of power in those markets, the distance to the coastline and the transmission grid and site specific installation costs. This study focuses on the economic returns expected at a site from a wave farm, an array of WECs at the same location, rather than a single device. The cost for the WECs are not considered in the economic analysis, since the number of the devices in the farm and the technology unit cost varies significantly among different types of WECs that could eventually be deployed. Rather cost, farm size and capacity benchmarks are set for each site considered by applying capacity limits associated with the subsea transmission infrastructure.

3.1 Vancouver Island Electricity Demands

The electricity demand for Vancouver Island is significant, with approximately 9069 GWh each year comprising 15% of the total British Columbia electricity load. The existing generation facilities on Vancouver Island can only supply 51% of the Island's demand, and the remainder is met by power transmitted from the Lower Mainland [69], [70]. This dependency is expected to only increase in the future in order to meet the growing demand. Unless additional on-island generation capacity is developed, significant expansion to the transmission network will be necessary by 2023 [71], and the cost of the expansions will be considerable. For example, it took approximately $230 million in 2008 to add a 600-MW of capacity on a 230-kV transmission circuit between Arnott and the Vancouver Island Terminal (which location is shown in Figure 3.5) [72]. Wave energy development off the West Coast of Vancouver Island (WCVI) has the potential to reduce the gap between the future demand and the current capacity and mitigate the necessity of transmission upgrades.

The current Vancouver Island power generation is dominated by hydroelectric generation. For instance, the capacity of the hydroelectric system is 459MW in 2003, which can supply up to 87% of the on-island generation capacity [73]. Each year in the winter, especially from December to January, the water inflow to BC Hydro reservoirs is minimal, whereas the provincial demand is at its peak. This makes both the net load and the cost for BC Hydro acquiring the power goes up [74]. The seasonal trends of the wave resource in WCVI region, which is energetic during the fall and winter, could be an excellent supplement to overcome the winter supply shortfall caused by the hydro-dominated BC electricity grid.

The utility grid is not the only source of demand. There are 40 remote communities on Vancouver Island that are not connected to the BC Hydro transmission network [75]. Most of them rely on diesel generators for electricity production. However, the inflated prices, high transportation costs, and the high operational cost of diesel generation create an energy poverty situation and eliminate future economic development opportunities for these communities; new commercial enterprises require a robust energy supply. At the same time, diesel generation also causes air pollution (through greenhouse gas emission during both the long-distance fuel transportation process and fuel burning process), soil pollution (though diesel fuel spills and leaks), and noise pollution. These problems have sparked interest in renewable energy development in BC's remote communities [76]. Many of these communities are coastally situated, and the seasonal supply makes wave energy stand out from other alternative energy options.

3.2 Wave Energy Farm Sizing and Costing

The economic evaluation in this study is at a wave farm scale rather than a device scale; a wave farm is a collection of WECs deployed in the same place to optimize the cost of construction and maintenance by sharing the transportation, subsea transmission infrastructure, deployment infrastructure, etc. In this study, the capacity of the wave farm is measured in terms of Power Producing Units (PPUs). PPU represents a collection of WECs deployed in a cabled network that achieve a set capacity of generation; the capacity is set by the limits of the subsea transmission infrastructure as defined in Section 3.2.1. In

this chapter, the transmission infrastructure, technical specifications, and the cost for each component is based on the WEC Infrastructure Review provided by MacArtney Underwater Technology [77].

3.2.1 Subsea Transmission Infrastructure and Power Producing Units (PPUs)

The subsea transmission infrastructure includes: cable hang-offs, bend stiffeners, Distributed Buoyancy Modules (DBMs), touchdown productions, in-line terminations, cable distributions (hubs), subsea cables, etc. [77]. Each WEC requires a cable hang-off clamp to fasten the structure of the device with the dynamic cable and an in-line termination to connect the dynamic cable with the output cable to bring the generated electricity to shore; for a single device case see Figure 3.1 (a). For a multiple devices case (see Figure 3.1 (b)), a hub can help to join multiple dynamic cables from different devices to a single output cable, so these devices can share the same export cable. In order to join cables to the hub, it requires a half-inline termination at the cable end.

When deploying the subsea transmission infrastructures, a bend stiffener is utilized to protect the cable from bending tighter than its minimum bending radius. A bend stiffener is especially critical for the connection between the cable and the structure of the WEC and the connection between the inline termination and the hub. The bend stiffener also requires a reusable tip clamp for installation; one tip clamp is sufficient to install all bend stiffeners within the scope of this study. In addition, DBM is utilized to compensate for the movements caused by different wave heights. Last, a touchdown production is applied to where the cable touches the seabed to avoid damage caused by the movements and frictions between the dynamic cable and seabed.

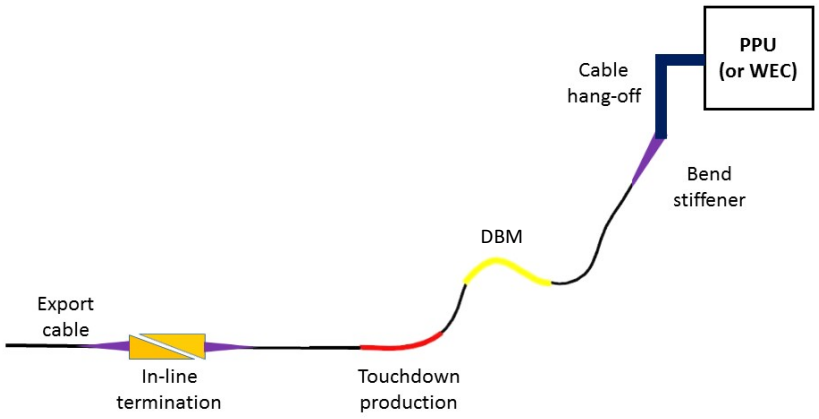

(a) the electrical infrastructure for a wave farm with single PPU.

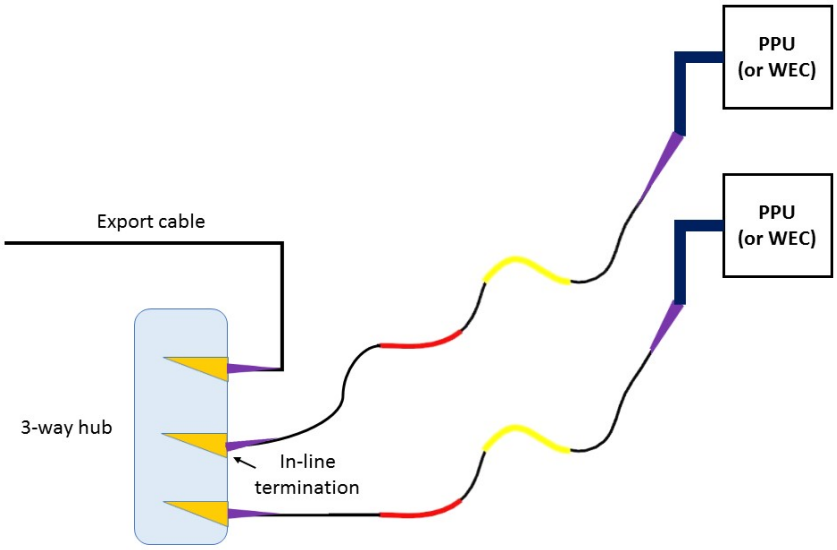

(b) the electrical infrastructure for a wave farm with multiple PPUs.
(use two PPUs as example)

Figure 3.1 The electrical infrastructures used for connections.

Three types of underwater cables (SILEC Dynamic, SILEC Export, and NSW Export) and one type of on-land cable are used in this study (see Table 3.1) [48], [77]. A dynamic cable provided by SILEC Cable, S.A.S. (referred as SILEC Dynamic cable) is generally used to connect devices to the in-line terminals or hubs. The dynamic cable can also act as an

export cable to transport the generated electricity to shore, when electricity is less than 2.17 MW. A larger capacity cable provided by SILEC Cable, S.A.S. (referred as SILEC export cable) is used as an export cable to transmit less than 8.69 MW of electricity to shore. If electricity exceeds 8.69 MW, an export cable provided by Norddeutsche SeekabelWerke (NSW) (referred as NSW export cable) is used. For on-land transmission, a uniform cable with a 20 MW capacity is selected in this study, based on the economic parameters in the analysis conducted by Kim et al [48].

Table 3.1 The Export cables and their properties.

Cable Type	Maximum PPU	Capacity (MW)	Price (US$/m)
SILEC Dynamic	1	2.17	133.5
SILEC Export	4	8.68	233.6
NSW Export	8	17.36	330.0
On-land	8	20	65.0

The PPU is intended to optimize the capacity of the subsea transmission infrastructures and thus lower the total cost of WECs deployment. Among all infrastructure components, the cost for underwater cable is significant, especially for sites away from the coastline. The PPU is thus defined by the capacity of the underwater cables; a 2.17 MW capacity of SILEC dynamic cable which has the lowest cost among underwater cables is selected. The total capacity of the WECs within a PPU should therefore reach 2.17 MW. This suggests the number of the WECs for each PPU varies at different locations due to the different wave condition at each site. For instance, a PPU contains fewer WECs to meet the 2.17 MW capacity at a site with adequate wave resources than a site with insufficient resources.

Since the number of the WECs for each PPU is not fixed, the cost analysis only considers the electrical infrastructure components connected with the PPU. The components utilized to connect the WECs within each PPU are not accounted for in this study. The wave farm sizes considered in this study are from one-PPU to eight-PPU. The upper limit of the wave farm is constrained by the maximum capacity of the underwater cable, where the capacity of an eight-PPU farm matches the capacity of the NSW export cable (Table 3.1).

3.2.2 Wave Farm Sizing

The gross wave energy flux is used in this chapter to drive the sizing and costing calculations. In order to prevent infrequent extreme wave energy events from influencing the sizing calculations, the peak wave energy flux values with less than a 10% probability of occurrence are removed from the original wave energy flux time series ($\underline{J_{or}}$). The original energy flux time series ($\underline{J_{or}}$) at a site near Ahousaht, BC is shown in Figure 3.2. The extremes filtered energy flux time series ($\underline{J}$) is used to calculate the electric output of the WEC farm. The maximum value of the energy flux ($\underline{J}$) occurring at a specific site is referred to as the maximum energy flux (J_M) and this maximum value determines the power extraction length (l_e) associated with the site. The power extraction length is the length of wave crest that the farm works off of during an occurrence of maximum energy flux J_M to deliver the maximum power of the PPUs; 2.17 MW for each PPU as limited by the SILEC dynamic cable rating. The calculation of the power extraction length is shown in Eq. 3.1.

$$l_e = \frac{C_p}{J_M} = \frac{n \times 2.17 \times 10^6\, W}{J_M} \qquad 3.1$$

where the C_p is the capacity of the wave farm, and n is the number of PPUs, which can vary between one to eight at each site.

The electricity output ($\underline{E_{op}}$) of each wave farm is then derived from scaling the energy flux ($\underline{J}$) by the l_e, following Eq.3.2. The resulting $\underline{E_{op}}$ for the one PPU wave farm at a site near Ahousaht is shown in Figure 3.2, as an example.

$$\underline{E_{op}} = l_e \times \underline{J} \times \frac{1\, kW}{1000\, W} \times 1h \qquad 3.2$$

Finally, a characteristic farm length (l_F) can be calculated via Eq. 3.3. Here, WECs are assumed to have a 10% energy conversion efficiency (e_c) and to be spaced at a single device-space apart. In this framework, the farm length is inversely proportional to the local wave resources. It requires larger farm lengths at a site with insufficient wave resources than a site with abundant wave resources to reach the same capacity. The farm length can grow to unlimited size at locations where wave resources are extremely insufficient.

However, the large farm lengths will be penalized in the revenue analysis which is introduced in Section 3.3.

$$l_F = l_e \times \frac{2}{e_c} = l_e \times \frac{2}{10\%} \tag{3.3}$$

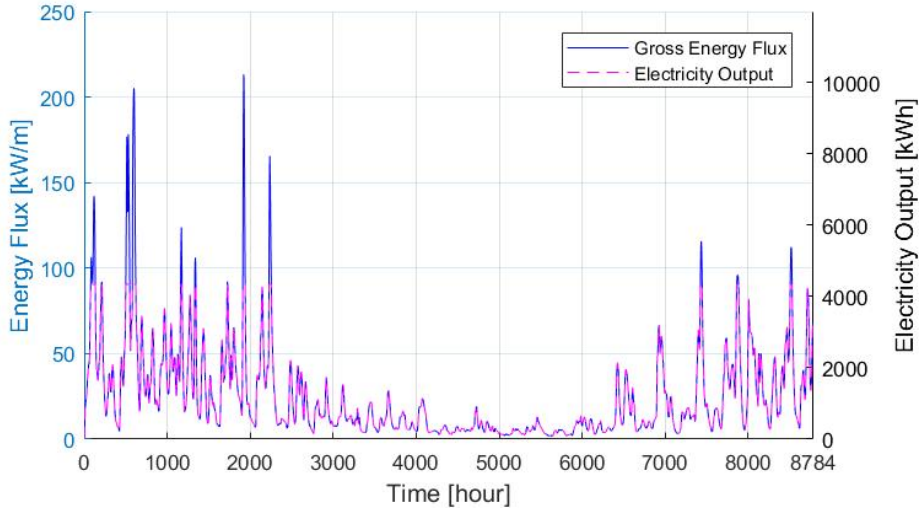

Figure 3.2 Gross energy flux and electricity output of a wave farm (with one PPU) near Ahousaht.

3.2.3 Wave Farm Cost Estimation

A Cost Index (CI) is introduced which facilitates comparison of the potential costs to construct a WEC farm at different sites. This cost index accounts for three major parts: the export cable (C_{EC}) between the electricity market and the wave site; the inter-connection cable between PPUs within the wave farm (C_{IC}); and the cost for electrical infrastructure (C_{EI}). However, the cost index does not include the cost for the WEC technology, installation costs, or on-going operation and maintenance costs. The cost index is not a high-fidelity model of actual project costs; rather, it is a representative measure that is used strictly to compare different sites (we expect a lower cost index to occur for sites that would have relatively lower actual costs). The cost index can be calculated through Eq. 3.4, and each component of the cost index is introduced in the following section. The costs are initially evaluated in US$, and converted to CA$ with the rate US$:CA$ =1:1.3; the average exchange rate of 2017 [78].

$$CI = C_{EC} + C_{IC} + C_{EI} \quad (3.4)$$

The export cable cost (C_{EC}) is influenced by the capacity of the wave farm (number of PPUs), the distance to the coastline, and terrestrial distance to the electricity markets. As previous noted, three different types of export cables are used for underwater transmission based on their capacities. The cable types and their prices, the maximum PPUs that cables are able to connect to, and the corresponding capacities are presented in Table 3.1 [77]. For on-land transmission, a cable with 20MW capacity, whose price is 65US$/m, is applied regardless of the capacity of wave farms [48]. The cable routes with the lowest construction cost can be found using the Cost Distance tool in ArcGIS. This tool calculates the least accumulative cost distance for each wave site to its nearest electricity market; rather than the shortest Euclidean distance. As an example, the cost distance, calculated based on an eight-PPU wave farm, from each site to its closest substation is shown in Figure 3.3. In addition, two sites are selected to demonstrate the optimal routes with the lowest construction cost (see Figure 3.3).

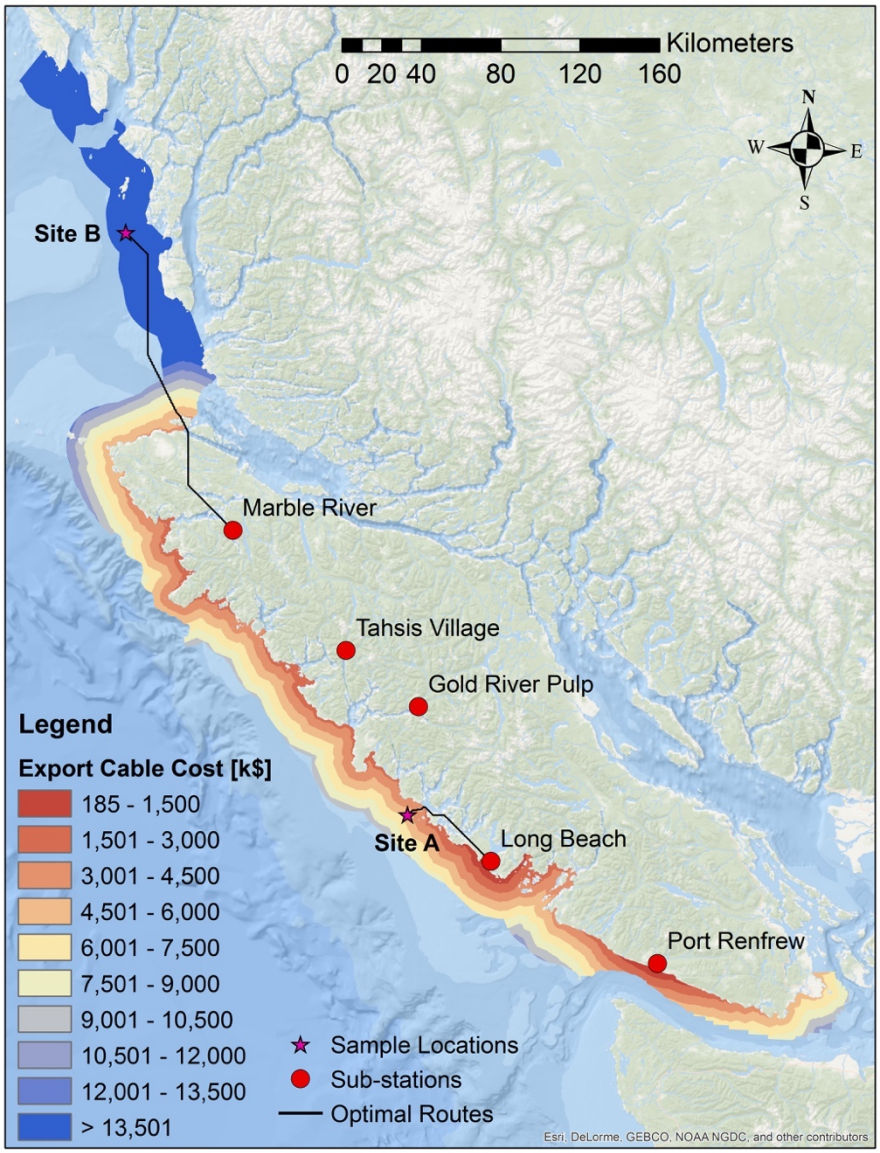

Figure 3.3 The cost distances to substations and the optimal cable routes.

The costs for electrical infrastructure and the inter-connection cable are calculated based on estimations from MacArtney Company [77]. A WEC farm with six PPUs is used to demonstrate the estimate of these costs, see Figure 3.4. When connecting a WEC farm to an electricity market, the PPUs need to be connected to each other via subsea hubs. Two types of hubs are available: a hub with three connections (referred to as a 3-way hub) and a hub with five connections (referred to as a 5-way hub). In order to join the six PPUs together, it requires one 5-way hub to connect four PPUs together and one 3-way hub to

connect the other two; the length of SILEC dynamic cable used for connection is equal to $\frac{2}{3}$ of the farm length (l_F). Later, a 3-way hub is used to connect the two aforementioned hubs together; the SILEC export cable with larger capacity is used for this connection, and the length is the half of the l_F.

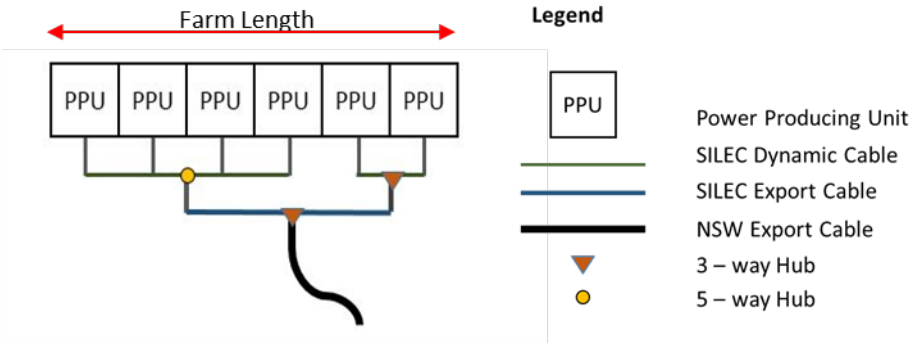

Figure 3.4 The configuration of a WEC farm with six PPUs.

For a wave farm with six PPUs, the number of each electrical infrastructure component, the lengths and types of cable used for the inter-connection are summarized in Table 3.2; the price of each component is also presented in the table. For a six-PPU case, the cost for all electrical infrastructures is $1,247,800. The inter-connection cable cost is location dependent, and it can be calculated via Eq. 3.5.

$$C_{IC} = p_{sd} * \frac{2}{3} * l_F + p_{se} * \frac{1}{2} * l_F \qquad 3.5$$

where p_{sd} is the price for the SILEC dynamic cable, and p_{se} is the price for the SILEC export cable.

Table 3.2 The summary of costs for electrical infrastructure components and inter-connection cables for a six-PPU WEC farm.

Items	Price [$]	count
Non-recurring engineering costs	41,150	1
Components at PPUs		
Cable hang-off	8,500	6
Reusable tip-clamp	12,370	1
Dynamic bend stiffer with tip-clamp at structure entrance point	21,200	6
Half in-line termination with bend stiffer for SILEC dynamic cable	33,100	6
Cable protection equipment		
Distributed module (10 per unit)	5,653	60
Uraduct cable protection (30m per unit)	5,300	6
Components at intermediate hubs		
Half in-line termination with bend stiffener for SILEC export cable	38,600	2
3-way hub	49,600	1
5-way hub	99,200	1
Components at export hubs		
Half in-line termination with bend stiffener for SILEC export cable	38,600	2
3-way hub	99,200	1
Half in-line termination with bend stiffener for SILEC export cable	44,100	1
Total cost for electrical infrastructures	$1,247,800	
Inter-connection cables		
SILEC dynamic cable	133.5 /m	2/3 l_F
SILEC export cable	233.5 /m	1/2 l_F
Total cost for inter-connection cables	$\$\ l_F * 205.75/\text{m}$	

The configurations of WEC farms with other number of PPUs, and the cost of electrical infrastructures and inter-connection cables for these farms are summarized in Appendix A.

3.3 Revenue Analysis

In reality, not all electricity output will always be utilized to meet the demand. Given that there is no specific storage technology considered in this study, electricity that cannot be immediately used to meet the demand will be discarded and will not generate any revenue. Therefore, it is important to determine the portion of electricity output from a WEC farm that is utilized productively; this portion of the WEC extracted energy is referred as *net*

generation in this thesis. A Revenue Index (RI) is then introduced to represent the potential revenue of the wave farm, and this revenue index is estimated based on the net generation.

In the end of this section, a Net Revenue Index (NRI) that incorporates both cost index and revenue index is established to measure the potential economic return from wave farms. The net revenue index will be estimated in two cases: utility market scale (i.e. all energy generated from WEC farm will be utilized) and remote community market scale (i.e. energy utilized is limited by finite community demand).

3.3.1 Utility Grid Market Scale Revenues

The utility grid of Vancouver Island is located at the southwestern corner of BC and consists of 15 substations, see Figure 3.5 [74]. The substations are the locations with significant load, power generation facilities or interconnections between transmission lines, which are the potential locations that wave power can be easily integrated into. Each substation is connected to others by bi-directional power lines. The BC utility grid on the lower mainland is represented by a single substation - Lower Mainland substation. The utility grid of Vancouver Island is connected to the BC utility grid at Lower Mainland substation, by two bi-directional power lines via Dunsmuir and Vancouver Island Terminal. The four substations close to the west coastline (Long Beach, Marble River, Tahsis Village, and Gold River Pulp) are selected as locations for wave energy integration (see Figure 3.6). In addition to the existing substations, a site close to Port Renfrew is proposed due to its proximity to the ocean and existing transmission infrastructure. When electricity is intergraded into the grid, it is assumed to transfer anywhere in the grid without any cost. As such, the ‘demand’ at each substation is assumed to be limited by the capacity of transmission-level power lines (see Table 3.3) [79]. Since the lowest demand (20 MW) among the substations is larger than the capacity of NSW export cable (17.36 MW), all the electricity generated by a wave farm will be used productively regardless of which substation it is connected to. The five substations provide the same revenue potential, and thus the transmission grid is treated as a whole in this analysis. As such, the wave farm is always connected to the closest substation to reduce the cost of transmission cables.

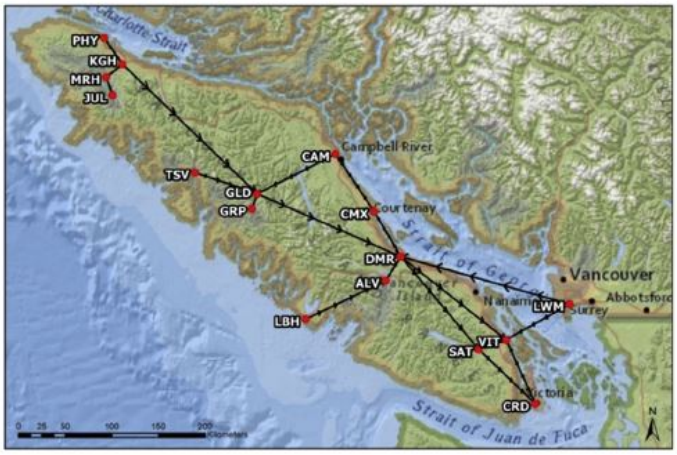

Bus	Location/Name
ALV	Alberni Valley
CAM	Campbell River
CMX	Comox
CRD	Capital Regional District
DMR	Dunsmuir
GLD	Gold River
GRP	Gold River Pulp
JUL	Jeune Landing
KGH	Keogh
LBH	Long Beach
LWM	Lower Mainland
MRH	Marble River
PHY	Port Hardy
SAT	Sahtlam
TSV	Tahsis Village
VIT	Vancouver Island Terminal

Figure 3.5 The transmission grid on Vancouver Island [74].

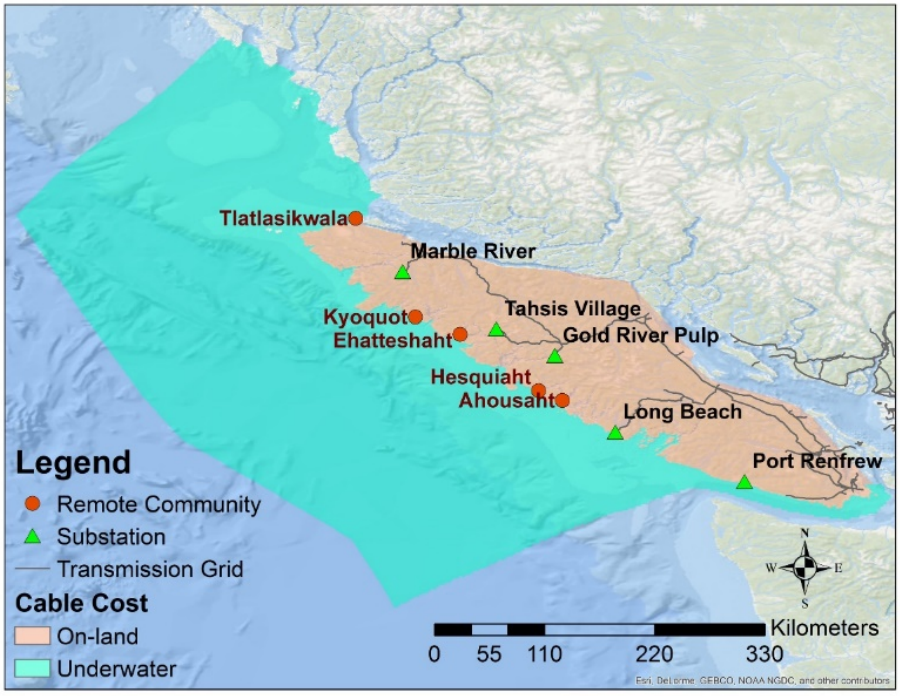

Figure 3.6 Locations of substations and remote communities.

Table 3.3 Substations and capacity of power lines [79].

Substation	Transmission Capacity (Demand)
Long Beach	35 MW
Marble River	80 MW
Tahsis Village	108 MW
Gold River Pulp	88 MW
Port Renfrew	20 MW[3]

All wave farms are unified to contain eight PPUs to match the significant demand at utility market scale. The demand at utility market scale is such that all the electricity output will be used productively. Here, Port Renfrew, which has the smallest capacity, is used as an example to demonstrate the magnitude of demand versus the electricity output (see Figure 3.7). The electricity output is always below the demand curve, and thus the net generation is the area (blue region) under the electricity output curve - the sum of electricity output ($\underline{E}_{op}$) from a wave farm with eight PPUs. The net generation for the utility market scale can be calculated via Eq. 3.6.

$$E_{net} = \sum \underline{E}_{op} \qquad 3.6$$

[3] The information of transmission capacity of Port Renfrew is not available, 20 MW is assumed, which is also the capacity of the on-land cable used in this study.

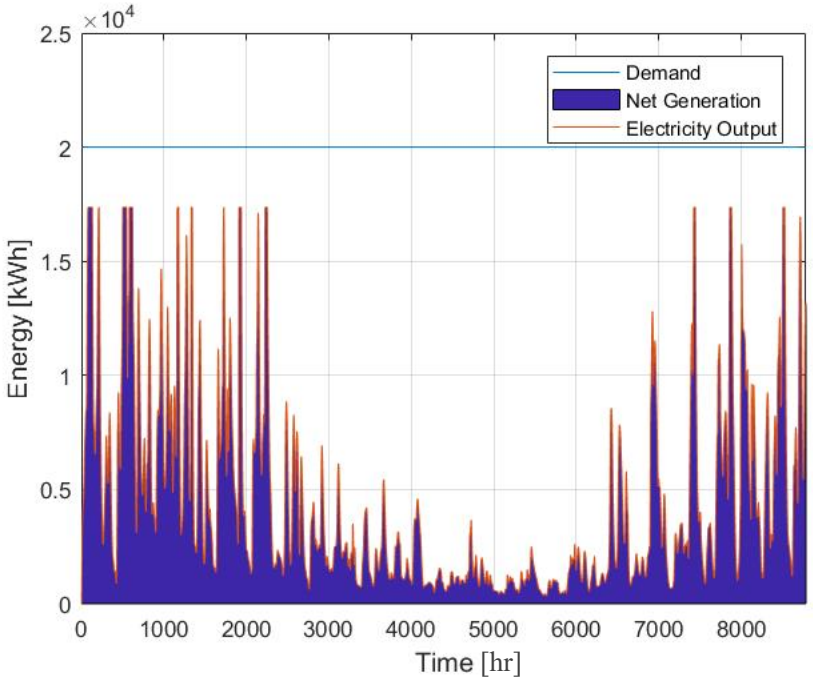

Figure 3.7 The demand, electricity output, and net generation at a site near Ahousaht that is connected to the Port Renfrew Substation.

The majority of the revenue for a wave energy farm comes from selling the electricity output, and thus the Revenue Index (RI) is proportional to the net generation. In this analysis, the revenue index is defined by the present value (R_n) of the revenue earned each year. The revenue index for each site can be calculated via Eq. 3.7 and is based on a 15-year lifespan wave farm.

$$RI = \sum_{i=1}^{15} R_n = \sum_{i=1}^{15} \frac{E_{net} \times p_n}{(1+r)^n} = E_{net} \times \sum_{1=1}^{15} \frac{p_n}{(1+r)^n} \qquad 3.7$$

where r is the nominal interest rate of 3.73% (the average rate of 2001- 2016 from [80], [81]. p_n is electricity rate for the year of n. The electricity rate for the first year is 0.1$/kWh according to the rates from BC Hydro in 2017[4], and the electricity rate will increase by the rate (i) of 3% every year [82], [83]. The electricity rate (p_n) for the future years can be calculated from the Eq. 3.8.

[4] The BC Hydro 2017 electricity rate varies from 0.0858 to 0.1287 CA$ per kWh depending on purpose and volume; residential, commercial and governmental customers are billed for consumption in excess of a set limit per month;

$$p_n = p_1 * (1 + i)^{n-1} \quad 3.8$$

The economic opportunity is not just about how much profit is made at each wave site, but also how much required to be invested for the wave site and how spatially efficient the wave site can make the profit. Therefore, Net Revenue Index (NRI) accounts for the cost, the revenue, and farm length and is indicative of the near-term economic opportunity of a wave site. The NRI can be calculated through Eq. 3.9, and has units of $/m. In the NRI, the numerator represents the potential net revenue for a 15-year WEC farm, and the denominator reflects the farm length (l_F).

$$NRI = \frac{RI - CI}{l_F} \quad 3.9$$

where RI is the revenue index, CI is the cost index.

3.3.2 Remote Community Market Scale Revenues

A remote community (also known as an off-grid community) refers to a permanent settlement (usually longer than 5 years) with more than 10 dwellings and is not currently connected to the North-American electrical grid, nor to the piped natural gas network [75]. Currently, there are a total of 86 remote communities with a population of 24,068 people in BC. The electricity rates for these communities are usually much greater than for utility grids, due to delivery costs, high diesel fuel prices, and high operation and maintenance costs of the generators [84]. The mean electricity rate for remote communities in BC was 0.37$ /kWh in 2005 [75]. Considering the recent inflation, 0.5 $/kWh is used as the electricity rate for the initial year, and it would follow the same increase rate (3%) as the rate used for the utility market scale.

Five communities (Ehattesaht, Kyoquot, Ahousaht, Hesquiaht, and Tlatlasikuala) are selected in this study due to their proximity to the ocean (see Figure 3.6). The demand of each community is assumed to be proportional to its population, and the average demand for a person who lives in a BC remote community is 9.9 MWh for a year [85]. The population and the demand for each community are shown in Table 3.4.

Table 3.4 The population and annual demand of each community.

Remote Community	Population	Demand (MWh)
Ehattesaht	489	4,841
Kyoquot	570	5,643
Ahousaht	2143	21,216
Hesquiaht	733	7,257
Tlatlasikuala	65	644

The demand is not evenly distributed through a year. An hourly demand curve is important and can be created by scaling the BC hourly demand curve by the annual demand of the community [70]. The hourly demand curve of Ahousaht is used as an example and presented in Figure 3.8

In contrast to the utility market scale, the demands of remote communities are significantly lower and the wave-generated electricity output is not necessarily useful at the time of generation. The net generation is decided by both the electricity output and the demand, and calculated through Eq. 3.10 and Eq. 3.11. The resulting net generation at Ahousaht is shown in Figure 3.8.

$$\underline{E}_{net} = \begin{cases} \underline{E}_{dem}, & \underline{E}_{dem} < \underline{E}_{op} \\ \underline{E}_{op}, & \underline{E}_{dem} \geq \underline{E}_{op} \end{cases} \quad 3.10$$

$$E_{net} = \sum \underline{E}_{net} \quad 3.11$$

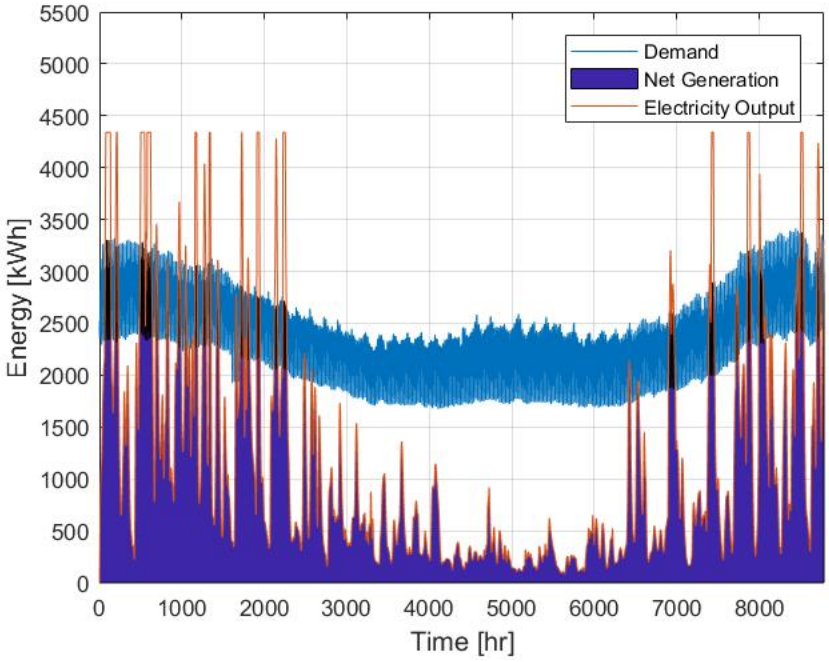

Figure 3.8 Net generation (using a WEC farm with two PPUs as example).

The net generation does not necessarily increase proportional to the number of PPUs, due to the uneven distribution of the demand. Further, the NRI does not always increase when additional PPUs are built in a wave farm; a larger farm capacity also increases the cost caused by more complicated connections between each PPU and the requirement of the export cable with larger capacity.

It is important to determine the size of the wave farm (i.e. number of PPUs) that provides the maximum NRI. For this reason, the NRI is evaluated individually for the wave farms with different PPUs, from one PPU up to eight PPUs, for each community of interest. Comparing NRI among the farms that contain different numbers of PPUs at each site, the one with the maximum NRI is selected to represent the NRI for the community, and the size of the wave farm (the number of PPUs) which provides the maximum NRI is also recorded. The resulting maps show the maximum NRI and the corresponding wave farm size for each of the five remote communities are presented in Appendix B.

3.4 Spatial Distribution of Net Revenue Index

The Net Revenue Index (NRI) for the utility and remote community market scale is presented in Figure 3.9 and Figure 3.10 respectively. For the utility market scale, the maximum NRI is $18,860/m, and the average is $8,940/m. The wave sites with great NRI are concentrated at several spots: Lawn Point and Brooks Peninsula, close to Marble River substation; Catala Island, close to Tahsis Village substation; Hesquiat Peninsula, close to Gold River Pulp substation; and Ucluelet, close to Long Beach substation. However, no site with great NRI is found around the Port Renfrew substation.

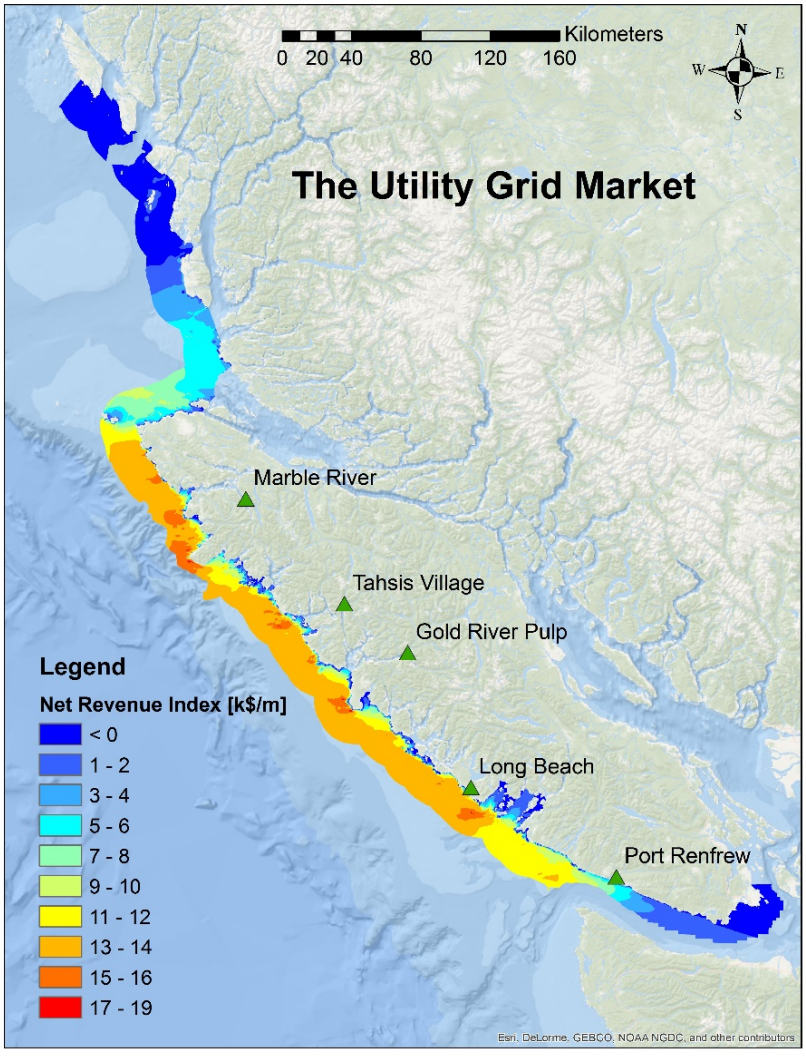

Figure 3.9 The net revenue index at utility market scale.

The remote communities are independent from each other. The NRI is estimated for each remote community, for each of one up to eight PPUs farm, individually. Figure 3.10 illustrates the greatest NRI among the five communities; generated by comparing the five

maximum NRI maps shown in Appendix B, which are selected from comparing different numbers of PPUs for each remote community. Finally, the maximum NRI for the remote community market scale is $94,260/m, and the average is $30,080/m. It is worth noting that the NRI should only be compared within each market scale, rather than comparing the utility market scale against the remote community market scale.

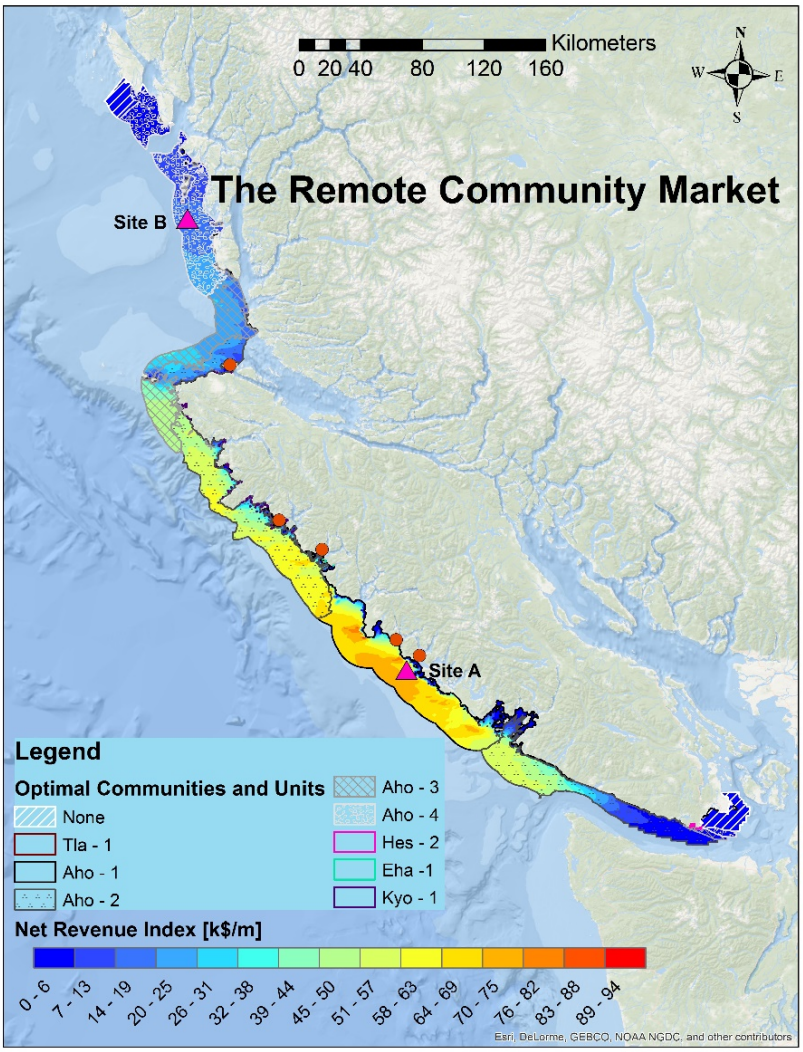

Figure 3.10 The net revenue index at remote community market scale.

(In the legend, none stands for the area with zero NRI value; Tla - 1 stands for Tlatlasikwala with one PPU; Aho – 1 stands for Ahousaht with one PPU; Aho – 2 stands for Ahousaht with 2 PPUs; Aho – 3 stands for Ahousaht with 3 PPUs; Aho – 4 stands for Ahousaht with 4 PPUs; Hes – 2 stands for Hesquianht with 2 PPUs; Eha – 1 stands for Ehatteshaht with one PPU; Kyo – 1 stands for Kyoquot with one PPU)

Rather than just presenting the NRI, Figure 3.10 also indicates the community to be connected to and the size (the number of PPUs) of the initial farm, when supplying wave energy to remote communities. In this map, Ahousaht dominates almost the entire study area. This is because Ahousaht has the biggest population, almost three times bigger than the second largest community Hesquaht, and a bigger population has a larger demand and makes greater revenue.

Interestingly, wave sites closer to Ahousaht have higher NRI with less PPUs; when compared to sites distant from Ahousaht. This observation was unexpected and to confirm the reasons why two sites were pulled out as examples to further investigate the cost and revenue calculations for wave farms of different PPUs. The locations of the two sites are shown in Figure 3.10. These two sites are: Site A located around 12 km from the Ahousaht and 8 km from the coastline, with a 24.69 kW/m annual average energy flux and a 90.52 kW/m maximum energy flux; and Site B located at the north end of study area and extreme far away from the Ahousaht, with a 22.92 kW/m annual average energy flux and a 99.79 kW/m maximum energy flux.

Ahousaht is selected as the electricity market in the following analysis. For both Site A and Site B, the percentage of demand met (r_{met}) and the percentage of electricity output used (r_{used}) are calculated based on the data summarized in Table 3.5 through Eq. 3.12 and Eq. 3.13. In addition, the percentage of electricity output used for each added PPU (r_{AU}) is calculated to illustrate the effectiveness of that PPU. The results are shown in Figure 3.11 and Figure 3.12.

$$r_{met} = \frac{E_{net}}{\sum \underline{E}_{dem}} \tag{3.12}$$

$$r_{used} = \frac{E_{net}}{C_p \times 24h/d \times 365d} \tag{3.13}$$

Table 3.5 The farm length, the net generation, and the total generation of wave farms with different PPUs at Site A and Site B.

Number of PPUs	Site A			Site B		
	Farm Length [m]	Net Generation [MWh]	Total Generation [MWh]	Farm Length [m]	Net Generation [MWh]	Total Generation [MWh]
1	479	4,930	4,930	435	4,120	4,120
2	959	8,980	9,870	870	7,560	8,250
3	1,440	11,600	14,800	1,310	9,950	12,400
4	1,920	13,300	19,700	1,740	11,700	16,500
5	2,400	14,600	24,700	2,180	12,900	20,600
6	2,880	15,700	29,600	2,610	13,900	24,700
7	3,360	16,500	34,500	3,040	14,700	28,900
8	3,840	17,200	39,500	3,480	15,300	33,000

The r_{used} of first two PPUs at both site A and site B is greater than 90%; however, they can only supply around 40% of the community's demand. The third and fourth PPUs increase the r_{met} to 50 – 60% but reduce the r_{used} to around 70%. For the first three PPUs at both sites, the r_{AU} is greater than 50%. However, when the fourth PPU is built in, the r_{AU} drops to 35% and 41% at site A and site B respectively, which indicates that the added PPU is not efficient. This suggests that a wave farm with three or four PPUs keeps a good balance between r_{used} and r_{met}.

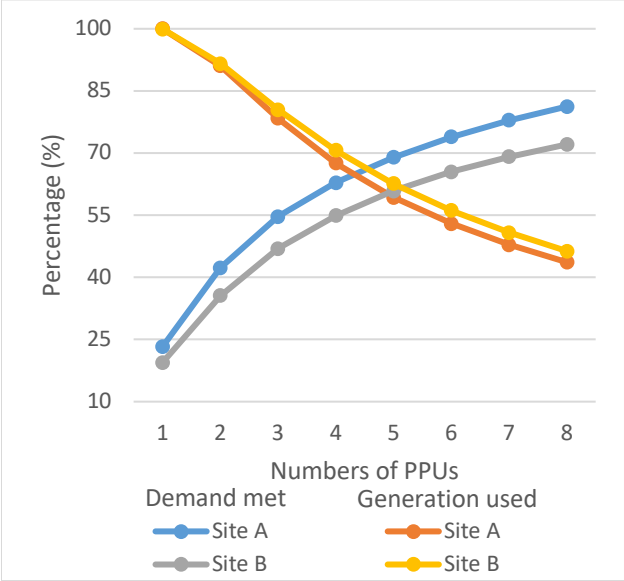

Figure 3.11 The percentage of demand met and generation used.

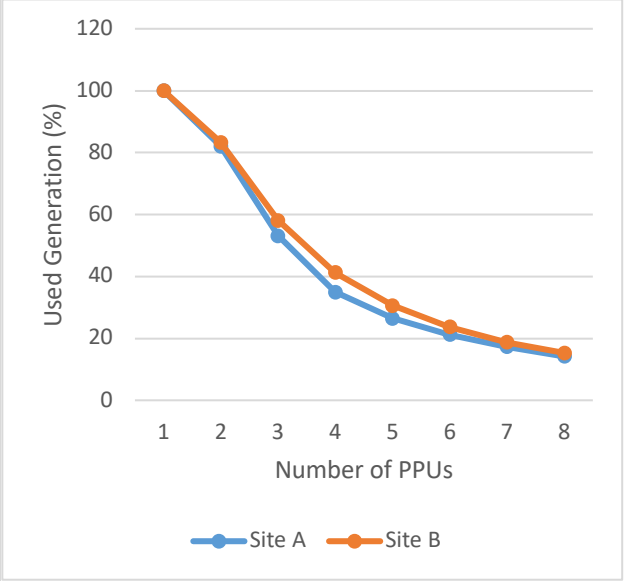

Figure 3.12 The percentage of generation used for each added PPU.

The composition of the costs, calculated using the method introduced in Section 3.2.3, for sites A and B is shown in Figure 3.13.

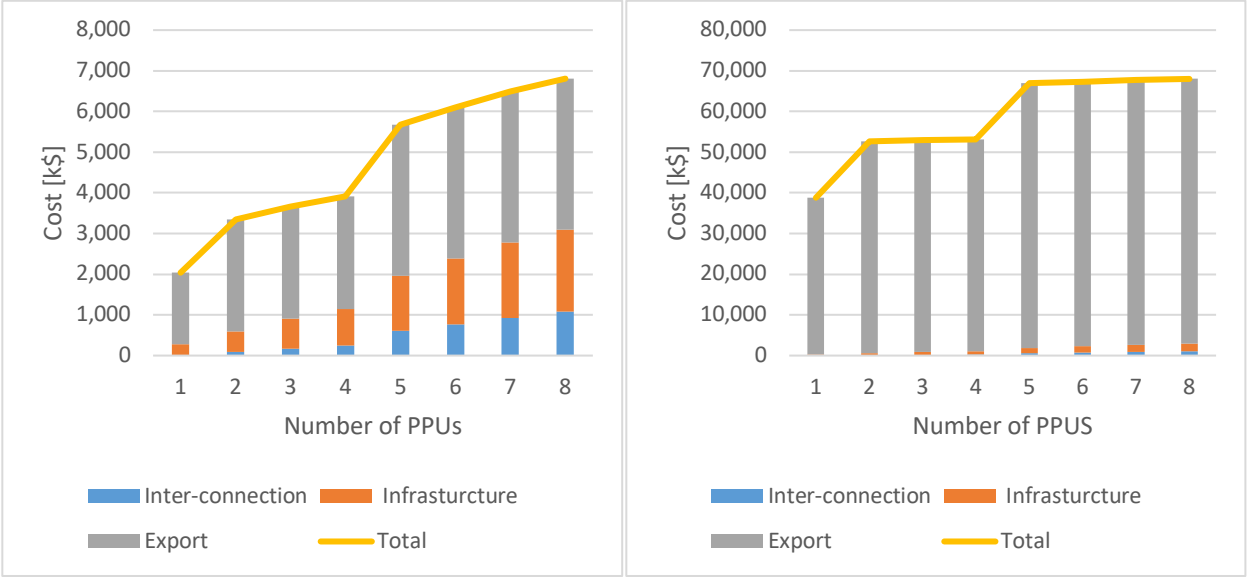

(a) *(b)*

Figure 3.13 The composition of the cost at (a) site A and (b) site B.

The costs increase dramatically when building the second and fifth units. When these additional units are built, an underwater cable with a larger capacity is required and the costs increase significantly. In addition, the structure of the connections between PPUs is more complex and costly for a wave farm with more than four PPUs (details of the wave farm configuration are shown in Appendix A).

The revenue index (RI) and the cost index (CI) for site A and site B, calculated using the methodology introduced in Section 3.3, are plotted in Figure 3.14. These plots compare the impact of the distance to the community on the potential economic return. The revenue index for the two sites are in the same magnitude, although the revenue index at site A is slightly higher. However, the cost index at site B is almost 10 times larger than at site A.

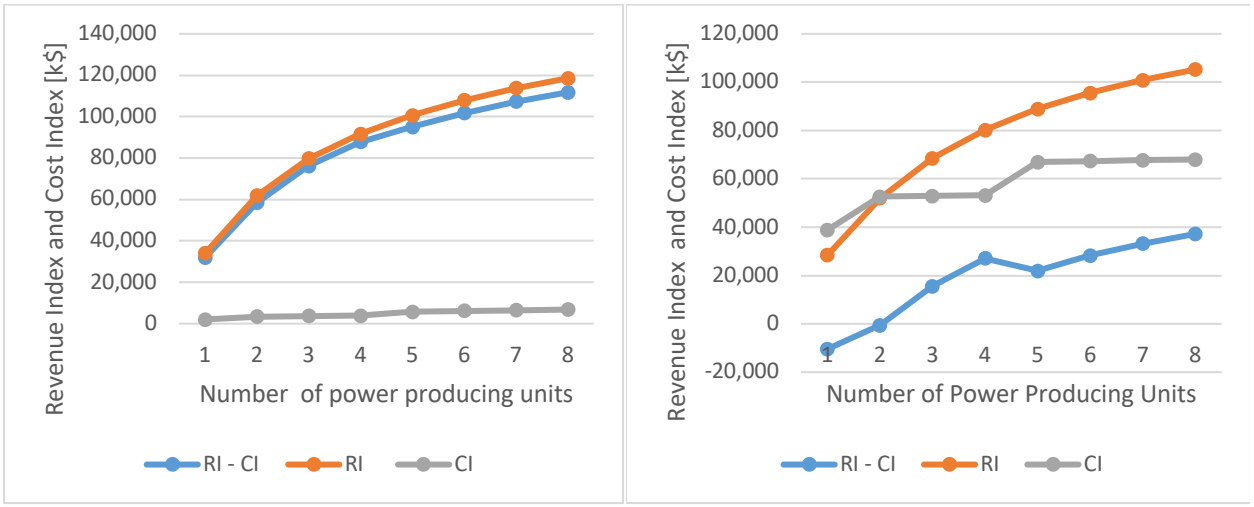

(a) *(b)*

Figure 3.14 The cost index and revenue index at (a) site A and (b) site B.

Finally, the NRI for the two sites is shown in Figure 3.15. At site A, the NRI for a wave farm with one PPU is about $ 67,000/m, but the NRI continually decreases with more PPUs built in. At site B, the NRI initially is negative but increases when the first four PPUs are built in. However, the NRI decreases significantly when the fifth PPU is built in, due to the requirement for an export cable with a larger capacity. After that, the variation of the NRI is minor.

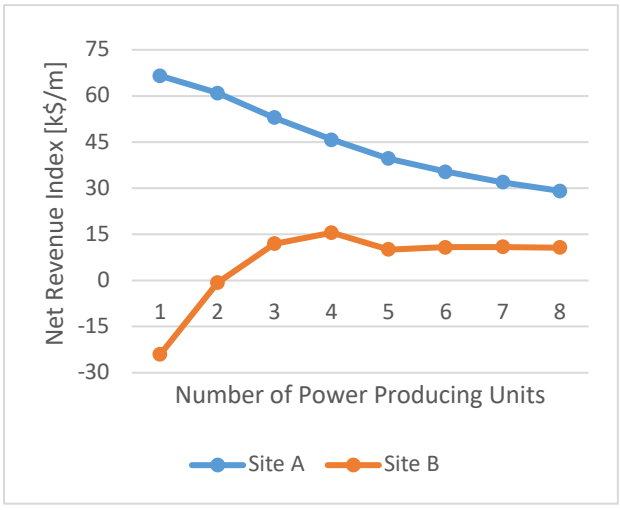

Figure 3.15 The net revenue index for WEC farm with different PPUs.

The rest of this study focuses on the locations which maximize NRI, yet the above analysis can provide investors with relatively complete information about the efficiency and economic opportunities of wave sites, and to choose a wave farm to match their distinct requirements.

3.5 Summary

At the end of this chapter, the map of net revenue index for the utility market scale (Figure 3.9) and the map of net revenue index for the remote community market scale (Figure 3.10) effectively describe the economic feasibility along the WCVI region. These two maps are used as input data in the GIS analysis in Chapter 5, together with the factors introduced in the next chapter, to seek the trade-off between the economic potential and impacts on the existing human uses and marine ecosystems.

Chapter 4 Pre-existing Human Use and Marine Conservation

For centuries, coastal areas have been utilized for many activities such as: fisheries, industry, recreation and shipping. The development of WEC farms will impose restrictions on other marine activities, and the selection of WEC deployment locations that present minimal conflict with pre-existing human uses is a significant challenge. In addition, some sections of the coastline possess sensitive marine ecosystems and have high conservation value. The objective of this chapter is to introduce high value pre-existing human uses and marine conservation principles as criteria and constraints on the identification of BC's strategic wave energy sites.

The pre-existing human uses include: the commercial fishery, which will be introduced in Section 4.1, and marine vessel traffic, which will be introduced in Section 4.2. The marine conservation criterion will be introduced in Section 4.3. Each criterion introduced in this chapter will be accounted for in Chapter 5, in a multi-criteria GIS framework. The considerations introduced in this chapter compete with the wave resource layers (criteria) described in Chapter 2 and Chapter 3 for priority within the weighting schemes described in Chapter 5 – each weighting scheme comprises a particular stakeholder *perspective*.

4.1 Study area and data sources

The study area in this thesis is constrained by costs for transmission cables, typical operation depth for WECs, designs of mooring systems and anchors, and the technology for installation. Considering transmission costs, a 20 km contour from the coastline is selected as the outside boundary of the study area. The cost for a 20 km underwater cable (NSW export cable) is 6.6 million USD [77], which is a considerable expense for a wave energy project, and thus the sites beyond this contour are eliminated from this study. The typical operation depths for the WECs, introduced in Section 2.4, vary from shallow regions (e.g. between 8m to 15m) to deep ocean waters (around 150m). Developing a wave farm in the deep ocean waters increases the technical challenges associated with the installation, such as efficient designs of mooring lines and anchors, and increases the cost

related to the operational maintenance of the WEC farm. A 200-meter depth is sufficient for the operation of the WECs considered in this study. As such, waters within 20 km from the coastline and shallower than 200 meters are decided as the study area and are shown in Figure 4.1.

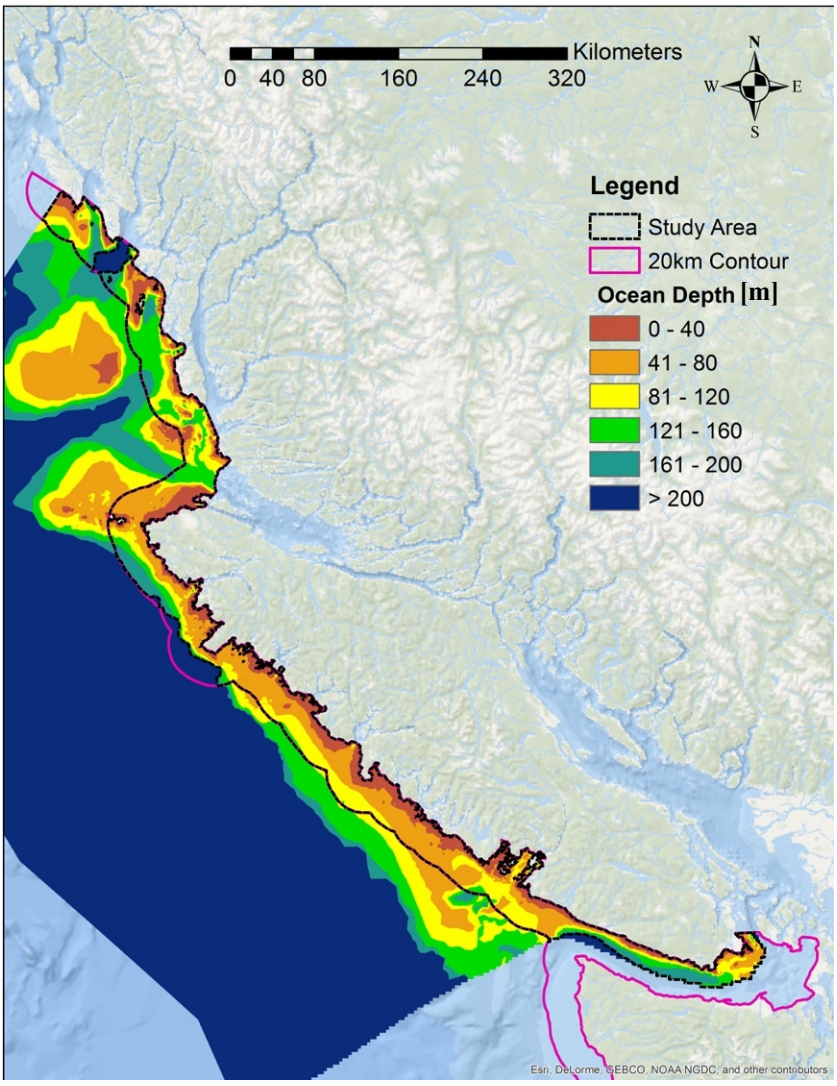

Figure 4.1 Study area, the 20 km contour from the coastline and the bathymetry.

The spatial data used in this chapter is obtained from the British Columbia Marine Conservation Analysis (BCMCA) [86]. The BCMCA is a collaborative project that focuses on integrated marine management and marine spatial planning to assist decision-making

for the west coast of Canada. From 2006 to 2013, the BCMCA developed projects to identify marine areas of high conservation value and marine areas important to human use in Canada's Pacific Ocean. Identifying areas important to human use includes six sectors that focus on different human use objectives, two of which are commercial fisheries, and shipping and transportation. BCMCA collected best available data from various sources and drew the knowledge and expertise from diverse background to provide integrated marine management, and their results include ecological resource data and human-use data collected through state-of-the-art research processes. As such, the data collected by BCMCA and the results from BCMCA analyses are used as input data for the spatial analysis in this thesis. The data used in Section 4.2 are datasets collected in BCMCA commercial fisheries sector. The data used in Section 4.3 are datasets collected in BCMCA shipping and transportation sector. The data used in Section 4.4 is the results of the ecological Marxan scenario with expert medium targets. The ecological Marxan analysis is introduced in Appendix D. The spatial data used in this thesis is summarized in Table 4.1.

Table 4.1 Summary of the source data used in the multi-criteria GIS analysis.

Name	Source	Data Type	Date	Spatial reference
Commercial fisheries*	BCMCA	Vector (sampled in 2x2km grid)	2012	Projected Coordinate System_NAD_1983_BC_Environment_Albers
Marine vessel traffic density	BCMCA	Vector (sampled in 5x5km grid)	2010	Projected Coordinate System_NAD_1983_BC_Environment_Albers
Ecological Marxan results Expert Medium (no clumps)	BCMCA	Vector (sampled in 2x2km grid)	2011	Projected Coordinate System_NAD_1983_BC_Environment_Albers
Bathymetry	Triton Consultants Ltd	Triangulated irregular network	2014	Geographic Coordinate System_World Geodetic System_1984
Electricity transmission grid	BC Hydro	Vector (Polyline)	2012	Projected Coordinate System_NAD_1983_BC_Environment_Albers
Remote community locations	GeoBC	Vector (Point)	2016	Projected Coordinate System_NAD_1983_UTM_Zone_10N

* The *Commercial fisheries* is a dataset that includes the data of 35 different species, details are introduced in Section 4.2.2.

The original spatial data is provided with varying spatial references and is transformed into *North American Datum (NAD) 1983 Universal Transverse Mercator (UTM) Zone 10N* projected coordinate system using the *Project* tool provided by ArcGIS. The *NAD 1983 UTM Zone 10N* is suitable for use in North America between 126°W and 120°W. All data obtained from BCMCA is converted to a raster format and is resampled into 100 by100 m cells to match the spatial resolution of the wave resources data. However, the actual resolutions of these BCMCA raster layers are much lower, since the raw data of commercial fisheries collected by BCMCA was estimated by the fishing zones, which vary from 2 square kilometers to hundreds of square kilometers. The original BCMCA marine vessel traffic density data is sampled by the number of vessels moving through each 5 by 5 km cell.

The resampled raster data is converted to a same numerical scale – the suitability value, which is introduced later in this chapter. The suitability value for each criterion will be added together in Chapter 5, following weighting schemes, to generate a Suitability Index (SI) that based on a perspective from a particular stakeholder.

4.2 Commercial fishery

Commercial fishing is an important economic activity in BC and must be considered in any marine spatial planning exercise. However, available data on commercial fisheries in BC focused either on economic value, or on spatial distribution. A map that combines these descriptions will be generated in this section.

4.2.1 Importance of BC's Commercial Fishery

Fisheries provided the foundation for the first European settlement in Canada, and fisheries continue to make a substantial contribution to the Canadian economy and have become an important source of employment [87], [88]. Over the past two decades, commercial fisheries in BC typically produce between 200,000 and 250,000 tons of raw material per year, with a landed value between $300 and 350 million. BC's fisheries also create about 8,000 job opportunities for crew members on around 2000 vessels. Beyond job

opportunities and profits from raw materials, BC fisheries have additional influences on the provincial economy in other direct, indirect, and induced ways. Commercial fisheries generated 260 million dollars Gross Domestic Product (GDP) through direct, indirect and induced means, and they created 154 million dollars income in 2006. The details of the economic impact of commercial fisheries in BC are shown in Table 4.2.

Table 4.2 The economic impact of commercial fisheries in BC.

	GDP [k$]	Employment [Jobs]	Income [k$]
Direct	143,509	434	82,916
Indirect	51,025	656	31,891
Induced	66,142	338	40,183
Total	260,676	1428	154,990

* *based on 2006 data* [87]

4.2.2 Assessing Commercial Fishery Value

Unfortunately, commercial fisheries data taken along the west coast of BC is limited. The two available datasets are from two sources: the federal Department of Fisheries and Oceans Canada (DFO) and the BCMCA. The data published by the DFO shows quantities and values of annual commercial landings for each species in BC, but this data lacks spatial information [89]. On the other hand, the BCMCA provides a feature count map of commercial fisheries which shows the number of commercial fishing features occurring in each of the 2 by 2 km planning units (cells) studied by the BCMCA [86]. The BCMCA map provides spatial knowledge of BC's fishery activities, but the feature count cannot reflect the economic values. Consequently, an assessment that can consider the quantities, economic values, and spatial distributions of commercial fisheries is required. In this work, the DFO data provides the information to calculate the prices of each fishery species, and the BCMCA data determines where each commercial fishery is executed and the average annual catch weight for each species in those areas.

The Pacific Coasts Commercial Landing data published by DFO is collected by federal, provincial and territorial governments [89]. It provides both the volume and value of annual fisheries landings, where the landings refer to the part of the catch that is put ashore. The

landing data is presented in a table format and organized by species, by species groups, and by province. The volume data is recorded by live weight in metric tons, and value data is evaluated in thousands of dollars. The DFO data is collected annually starting from 1990 to 2016. The landing data for 2015, the latest data available when collecting data for this project, is used to calculate the price for each commercial fishery species.

The commercial fisheries data provided by BCMCA includes a total of 35 species. Each of the species data is stored in an individual GIS layer that shows spatial distribution of the fisheries and the total catch in each fishing zone. In addition to the total catch, additional supporting information is provided in an Attribute Table for each GIS layer - the duration of the underlying data for the layer is an example of supporting information.

After screening and sorting, the original data is reduced and combined to 17 species that belong to four species-groups: groundfish, shellfish, herring, and salmon. Each of the BCMCA commercial fishery species and its corresponding price used in this study is summarized in Table 4.3, and a detailed explanation of this screening and sorting process is presented in Appendix C.

Table 4.3 Types of commercial fisheries species and their prices.

	Species (BCMCA)	Years of Data Collection	Species (DFO)	Total catch values (2015) [k$]	Total catch volume (2015) [metric ton]	Price (2015) [$/kg]
Groundfish						
1	Groundfish Trawl	1996 -2004	Ground	146,379	87,049	1.68
2	rock fish	1993 - 2004	Ground	146,379	87,049	1.68
3	Schedule II	1996 - 2004	Cod & dogfish	/	/	1.33
			Cod	2,933	1,460	2.01
			Dogfish	236	365	0.65
4	Sablefish Longline	1996 - 2004	Cod	2,933	1,460	2.01
5	Sablefish Trap	1996 - 2004	Cod	2,933	1,460	2.01
6	Halibut	1991 - 2010	Halibut	59,690	3,710	16.09
Shellfish						
7	Shrimp Trawl	1996 - 2004	Shrimp	42,183	6,168	6.84
8	Prawn Trap	2001 - 2004	Shrimp	42,183	6,168	6.84
9	Crab	2000 - 2004		54,743	4,261	12.85
10	Geoduck	2000 - 2005	Clams	33,427	1,832	18.25
11	Sea Cucumber	2000 - 2005	Sea cucumber	3,610	1,692	2.13
12	Green Sea Urchin	2000 - 2005	Sea Urchin	6,380	4,069	1.57
13	Red Sea Urchin	2000 - 2005	Sea Urchin	6,380	4,069	1.57
Herring						
14	Herring Roe Gillnet	1989 - 2008	Herring	9,809	20,000	0.49
15	Herring Roe Seine	1989 - 2008	Herring	9,809	20,000	0.49
16	Sardines	2001 - 2008	Herring	9,809	20,000	0.49
Salmon						
17	Salmon	2001 - 2007	Salmon	45,072	20,064	2.25

The total catching weight (w_c) of each fishing zone is first divided by the data collection time span (t) to calculate the annual landing (w_a) through Eq. 4.1. The annual landing is then divided by the area (A) of each fishing zone to estimate the annual landing density (D_l) in units of kg/km^2 through Eq. 4.2. Next, the annual landing density of each species is multiplied by its price (p) in Table 4.3 to calculate the annual landing value (V_l) through Eq. 4.3.

$$w_a = \frac{w_c}{t} \tag{4.1}$$

$$D_l = \frac{w_a}{A} \tag{4.2}$$

$$V_l = D_l \times p \tag{4.3}$$

Finally, a map of commercial landing density (D_l) and a map of landing value (V_l) are created by summing up the annual landing density and value of all the 17 species respectively. These calculations are finished using the *Field Calculator* and the *Cell Statistics* tool in ArcGIS. The resulting maps are shown in Figure 4.2. In general, the commercial fisheries are more active in the offshore area rather than open seas.

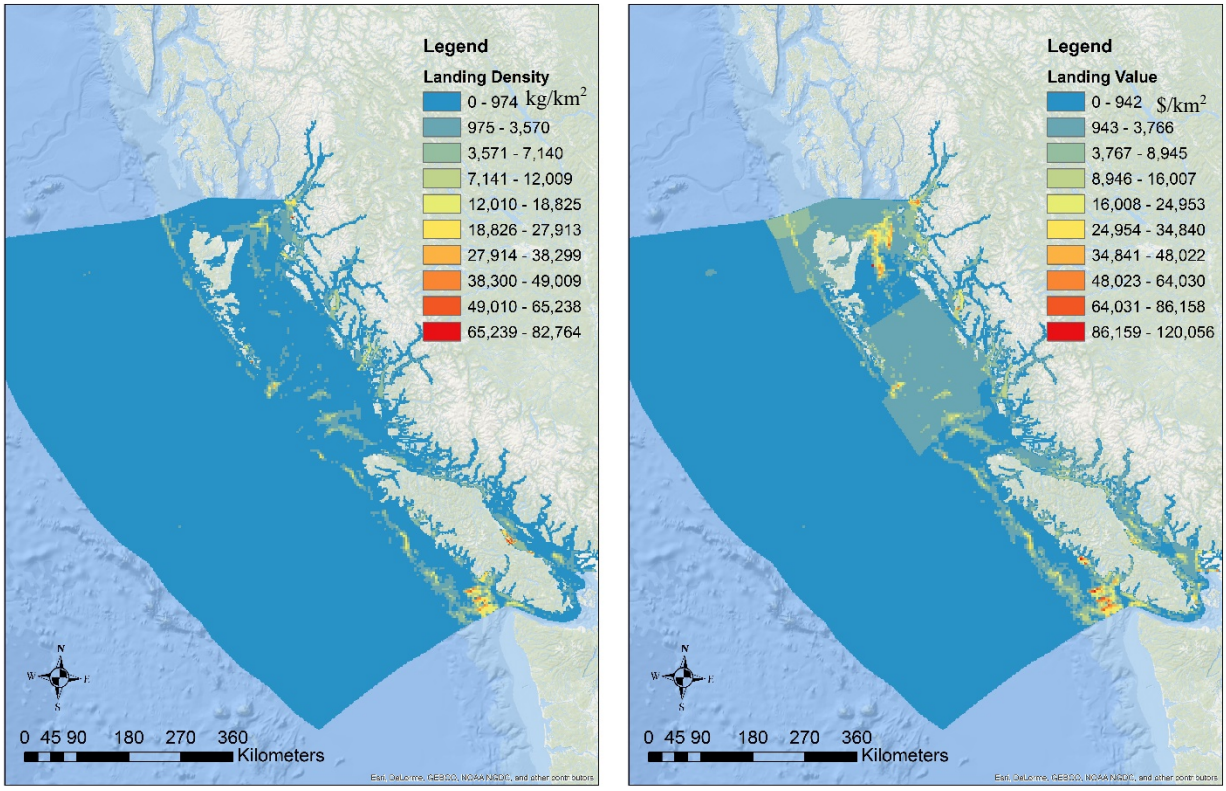

(a) *(b)*

Figure 4.2 The spatial distribution of annual commercial (a) landing density and (b) landing value.

4.2.3 Commercial Fisheries Suitability Value

The prices of fishery species are subject to volatility. The annual commercial landing value can better represent the importance of areas for commercial fisheries and thus is used in the further analysis; this value can adjust to the volatility by updating the price for each fishery species to create updated landing value layers that reflect the current market value. The prices used in this study are from DFO data published in 2015, which is the latest data available.

When inputting multiple criteria into a GIS framework, it is important to normalize all competing criteria to a common numerical scale. A suitability value of 0 - 100 is used in this study to normalize all criteria (e.g. fisheries, marine traffic) to the same scale, where the best condition for deploying WEC farm is rated as '100' and the worst is rated as '0'. For instance, sites with lower commercial landing value are more suitable for WEC deployment, so the sites with no commercial fishery are rated as a 100 value. On the contrary, the sites with landing values larger than 10 k$/m^2 are extremely important for commercial fisheries, and these sites are rated as 0. The rest is linearly assigned a value between 0 to 100 through Eq. 4.4. The resulting suitability value map is shown in Figure 4.3.

$$S_{CF} = \frac{V_l^{max} - V_l}{V_l^{max}} \times 100 \qquad 4.4$$

where S_{CF} is the suitability value for the commercial fisheries, V_l^{max} is the maximum annual landing value (10 k$/m^2), and V_l is the annual landing value at each site.

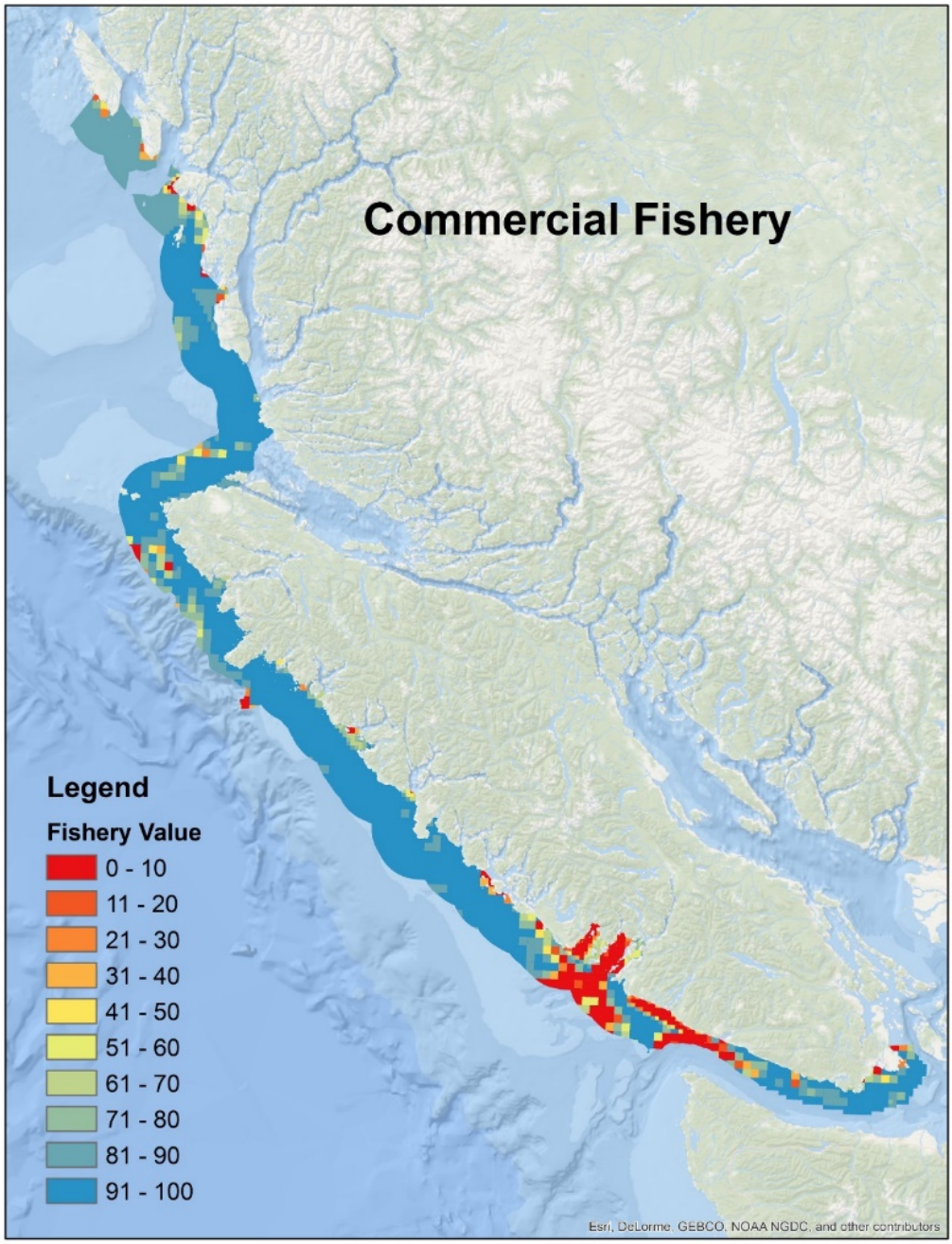

Figure 4.3 Suitability value for commercial fishery.

Most commercial fisheries are concentrated in Imperial Eagle Channel, Loudoun Channel, Barkley Sound, areas close to the entrance of the Strait of Juan de Fuca, and waters next to Outer Central Coast Island. These areas should not be selected as the locations for WEC deployment. Some fishery activities occur at the northwestern tail of Vancouver Island,

and thus those areas have relatively low value for WEC deployment as well. The remaining areas have higher value and are more suitable for WEC farm deployment.

4.3 Marine Vessel Traffic

Canada is a country surrounded by three oceans. Marine transportation is a key transportation mechanism in Canada and offers important social and economic benefits to Canadians [90]. Canada's marine transportation system embraces more than 550 ports, 860 fishing harbors and 120 recreational harbors, which serve as vital links and gateways that facilitate domestic and international economic activities [91]. The marine vessels operating in Canadian water include a wide variety of vessel types such as passenger ferries, cruise ships, bulk cargo, fishing boats, tankers carrying oil and liquid chemicals and tug boats.

4.3.1 Importance of Marine Transportation in BC

The Pacific west coast region is one of the four major geographical lanes for shipping services in Canada. This region boasts a large and diverse fleet of vessels engaged in barging and towing of cargo, as well as ferry services [92]. These marine activities play an important role in BC economy and supply coastal communities. For example, two main Canadian ports are located in this region, the Port of Vancouver and the Port of Prince Rupert. The Port of Vancouver is Canada's largest port in terms of traffic volume, which generated 135.5 million tons (Mt) of traffic in 2016. In the same year, the Port of Prince Rupert handled 18.9 Mt of traffic [91]. In addition, ferries and cruise liners in BC provide an important transportation link for coastal and island communities. *BC Ferries* operated 35 vessels to carry passengers and vehicles on the west coast through 25 routes that connects 47 terminals. The Port of Vancouver benefitted from ocean cruise liners with 199 sailings from 27 vessels, and more than 663,000 passengers [92]. It is clear that the Pacific west coast region is one of the busiest ocean transportation corridors in the world, and marine transportation is the element that cannot be overlooked in marine spatial planning.

4.3.2 Marine Vessel Traffic

The Marine Vessel Traffic Density data, published as a result of BCMCA analysis, is used to define the spatial distribution of marine vessel traffic in this study. The data provided by BCMCA was consolidated from four main sources: (1) the Marine Communications and Traffic Services (MCTS) vessel tracking database by Canadian Coast Guard, (2) Analysis of Canadian Coast Guard data by Canadian Wildlife Service, (3) Maritime Activity and Risk Investigation Network (MARIN) by Dalhousie University, and (4) Coastal Resource Information Management System (CRIMS).

The Marine Vessel Traffic Density data defines the hours that a particular type of marine vessel spent in transit within each 5 by 5 km cell for 2010. The traffic counted includes the vessels which visit ports along the BC coast, as well as those just travelling through Canadian waters on their way to ports in other countries. The marine traffic is summarized in seven different types of vessels: fishing, government, pleasure and yachts, merchant, tanker, research, and tug and service vessels. Traffic in this dataset is broken down into categories by seasons, vessel length, vessel type (use purpose), year built, and vessel with Flag Convenience or not. The total vessel traffic in each cell is calculated by summing up the hours of all types and categories of vessels that transit. The result is shown in Figure 4.4 .

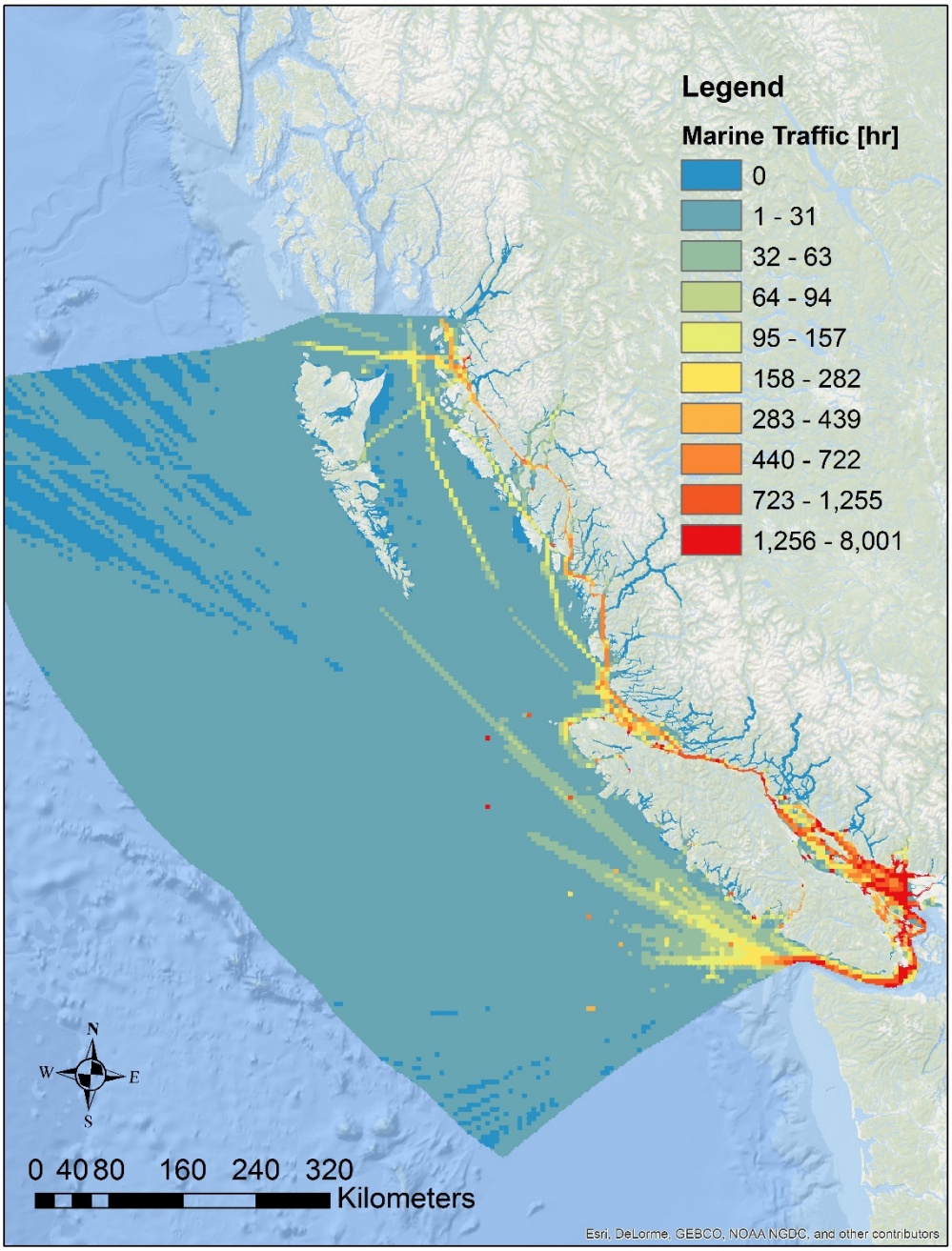

Figure 4.4 Marine vessel traffic density in Pacific west coast region.

The marine traffic at the Strait of Georgia (water between Vancouver Island and Lower mainland) and the Strait of Juan de Fuca (water next to the southeastern end of Vancouver Island) are very busy, because a huge number of ferries and cruise vessels travel in that area. In addition, merchant vessels increase the traffic in the Strait of Juan de Fuca and the traffic in the open ocean next to the west coast of Vancouver Island. The merchant, ferries

and cruise vessels comprise the majority of the recorded traffic around the Port of Prince Rupert, which is relatively active compared to other places. Lastly, some hot-spots are distributed sparsely in the water away from the coastline; they are primarily caused by the occurrence of fishing vessels and tank vessels. Other hot-spots occur inland on the west coastline near the harbours are caused by government vessels, pleasure vessels, and yachts.

4.3.3 Marine Vessel Traffic Suitability Value

WEC farms will interrupt the marine traffic, so sites with less traffic are preferred for wave energy sites. Sites with no traffic are assigned suitability value of 100. On the contrary, sites with busy traffic are not suitable to build WEC farms. Therefore, sites with traffic more than 168 hours (the total hours in a week) are extremely busy and are rated as 0. The remaining sites are assigned a value between 0 to 100 according to Eq. 4.5. The resulting marine vessel traffic suitability value is shown in Figure 4.5.

$$S_{MVT} = \frac{h_{max} - h}{h_{max}} \times 100 \qquad 4.5$$

where S_{MVT} is the suitability value for marine vessel traffic, h_{max} is the maximum hours of the traffic time (168 hours), and h is the traffic hours at each site.

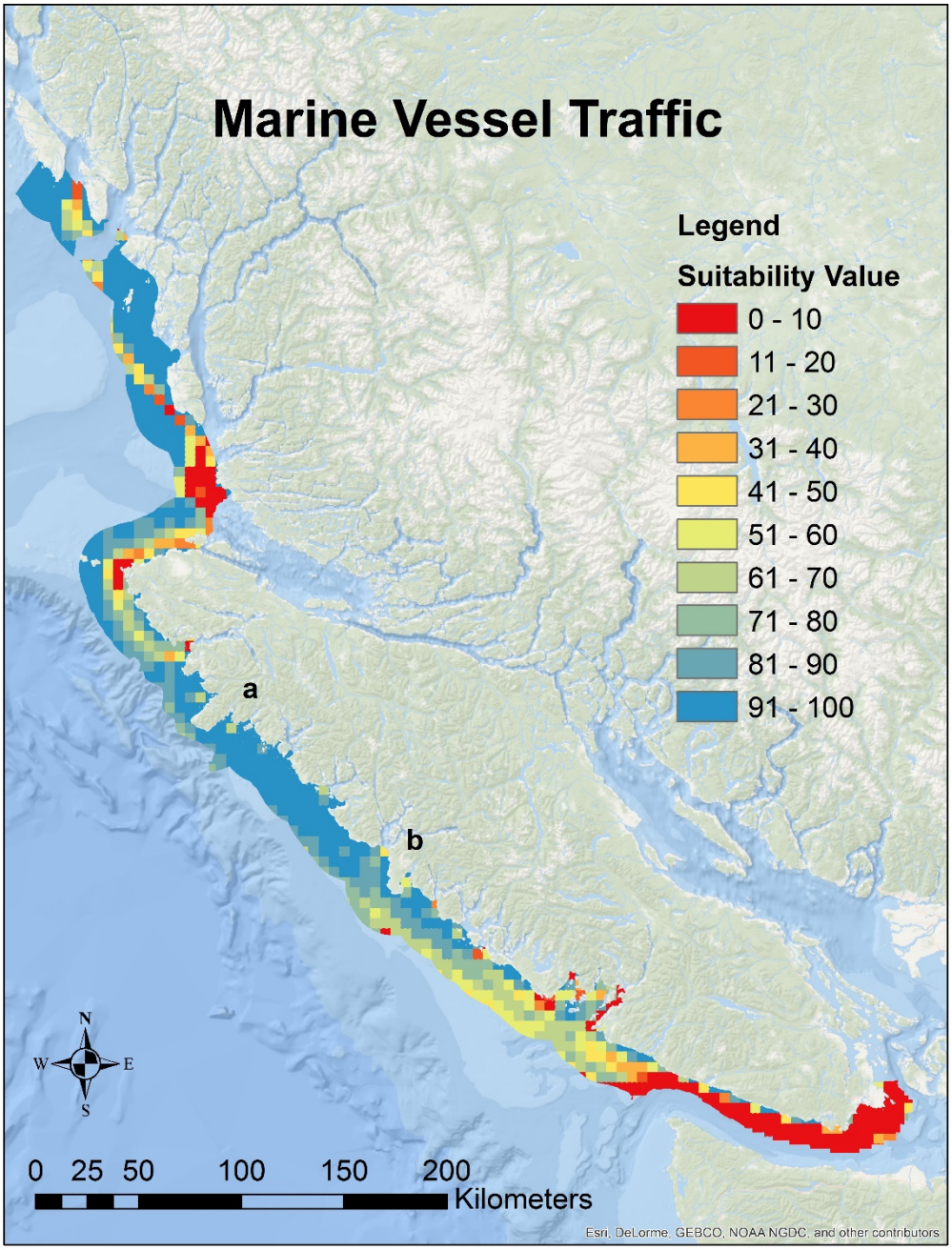

Figure 4.5 Suitability value for marine vessel traffic.

Within the study area, the traffic is concentrated at the Strait of Georgia, and the traffic close to the Barkley Sound is relative busy as well. Traffic will impede the WEC farm development, and thus those areas have a low suitability value. On the contrary, the traffic between (a) the Brooks Peninsula and (b) the Hesquiat Peninsula is very low and thus these areas are more suitable for WEC farm deployment and have a higher suitability value.

Around 30% of the sites have a suitability value between 96 to 100, and around 63% and 75% of the sites have a value greater than 90 and 86 respectively. These sites have less marine traffic and relatively suitable for WEC farm deployment. Overall, only 7% of the sites are extremely busy and have a '0' suitability value.

4.4 Marine Conservation

With approximately 36,000 km of coastline and over 450,000 km^2 of marine waters (internal and offshore), Canada's Pacific Coast possesses one of the most diverse and productive marine ecosystems in the world. These marine ecosystems support BC's economy (e.g. fishing, aquaculture, and tourism) and provide a source of inspiration, rejuvenation, and discovery for people living the province [93]. The wide biodiversity gives marine ecosystems a strong resistance to environmental disturbances and a remarkable resilience to the state before perturbation. However, the increase in human activity has acted to accelerate the rate of marine environment change and has caused significant damage to marine ecosystems [94]. The intention of this study is to minimize the pressure on the marine environment when developing additional wave energy activities on the ocean, and thus prevent the sensitive marine ecosystems from being lost.

The data used in this section is the result of BCMCA ecological Marxan analysis, which covers a total of 169 ecological features and data. The resulting map from BCMCA analysis is presented in a 0 – 100 scale and is shown in Figure 4.6, where '100' stands for sites with extremely important conservation value and '0' stands for sites with low conservation value (details of the BCMCA analysis are in Appendix D).

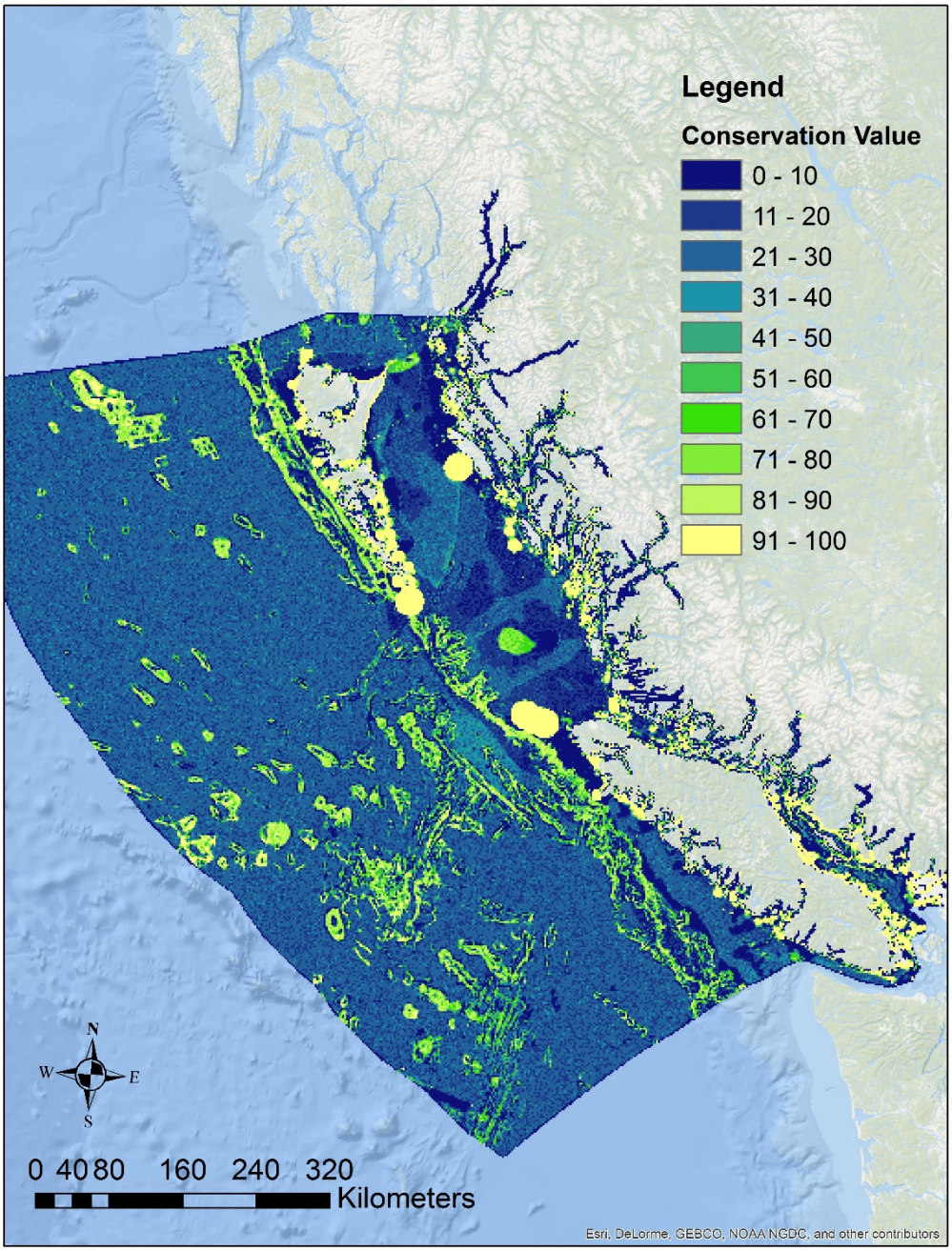

Figure 4.6 Marine conservation value in Pacific west coast region.

The sites with high conservation value (Value > 50) are locally intense and occupy only 15% of the whole study area, but they are widely spread out. However, the sites with extremely high conservation value (Value > 90) are all close to the coastline of Vancouver Island, Haida Gwail and Mainland. The only exception is the hot-spot that covers the

Sartine Islands Province park, Anne Vallee Ecological Reserve, and Lanz and Cox Island Province park, which is next to the Cape Scott Provincial Parks on the northwestern tail of Vancouver Island.

Sites with high conservation value are less suitable for WEC farm deployment, so the conservation value need to be inversed via Eq. 4.6 to match the suitability value scale used for other layers.

$$S_{MC} = 100 - V_{MC} \tag{4.6}$$

where S_{MC} is the suitability value for marine conservation, and V_{MC} is marine conservation value at each site.

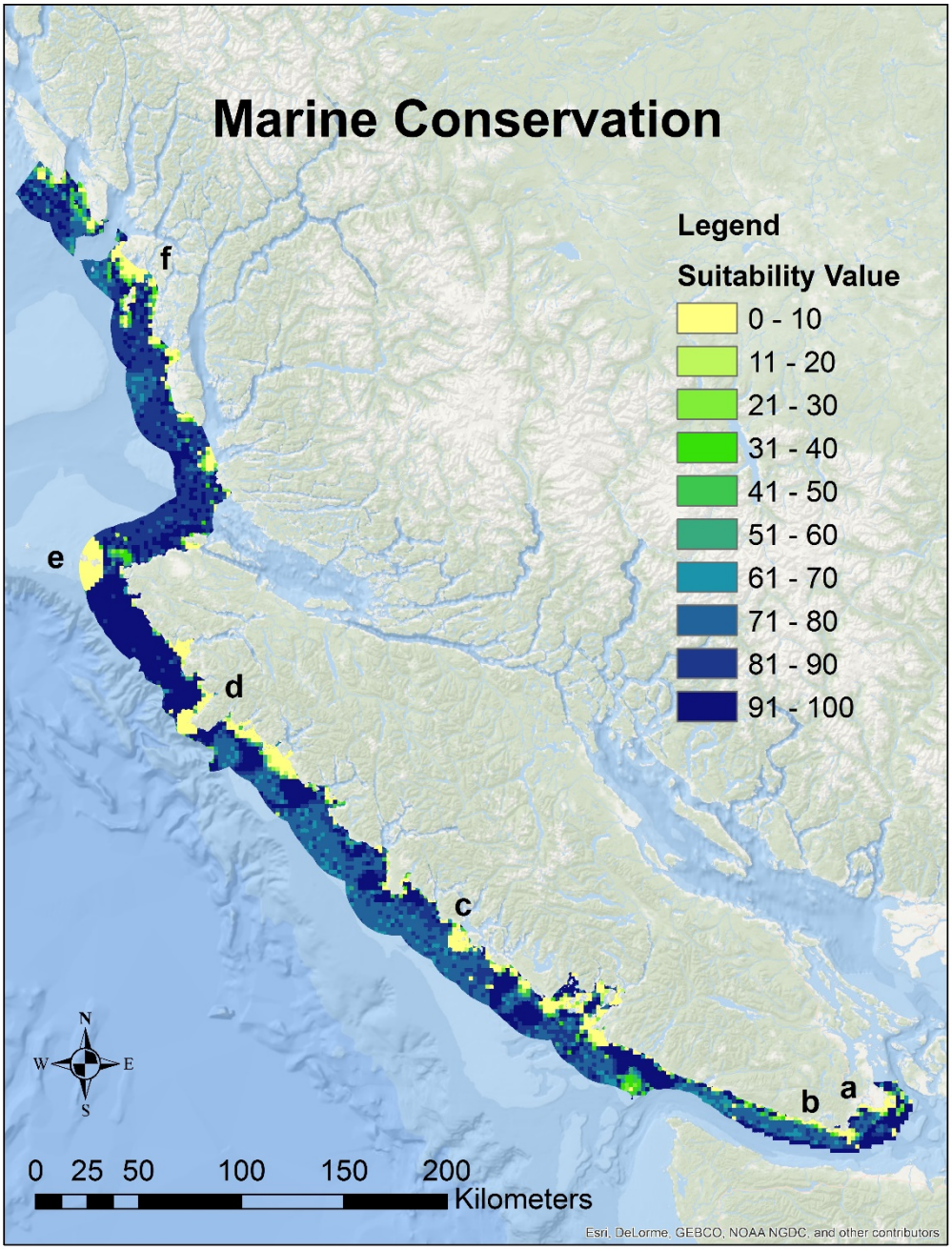

Figure 4.7 Suitability value for marine conservation.

The resulting suitability value is displayed in Figure 4.7. In general, the areas in the north are relatively less important for marine conservation compared to the areas in the south, and thus are more suitable for WEC deployment. The sites with extremely high conservation value are concentrated in a few spots: Imperial Eagle Channel and Loudoun Channel, coastal areas close to (a) Oak Bay and (b) Sooke, water next to (c) Vargas Island,

water close to (d) Brooks Peninsula, water around (e) Lanz and Cox Island, and water close to (f) Outer Central Coast Islands. When choosing the deployment locations for WEC farms, those areas should be avoided.

Chapter 5 Scenario Based Multi-criteria GIS Analysis

As discussed in Chapter 4, the development of WEC farms will impose restrictions on other marine activities and will thus conflict with multiple existing marine users of the BC coastal area. The Multi-Criteria Decision Making (MCDM) framework, with its ability to incorporate different criteria simultaneously and explicitly, is well-suited for a site selection process that seeks to minimize this unavoidable conflict while still maintaining strong potential to generate revenue from wave energy production. The integration of MCDM into GIS (referred as multi-criteria GIS) can extend the decision making process to an enormous number of potential sites [54]. The multi-criteria GIS framework developed in this chapter accounts for the wave resources and economic data produced in Chapter 2 and Chapter 3 and the existing human uses and marine conservation data produced in Chapter 4. Alternative solutions for the WEC deployment site selection can be generated by varying the priorities of these criteria – each set of weighting factors representing a particular stakeholder group's perspective. In this chapter, four theoretical stakeholder perspectives, or *scenarios*, are considered, and strategically important sites are identified by intersecting high value sites from all of the different perspectives.

5.1 Multi-criteria GIS Analysis

The multi-criteria GIS analysis, illustrated in the flowchart of Figure 5.1, consists of the following steps: 1) identifying competing criteria that are important for site selection 2) normalizing all criteria to a common scale – the suitability value 3) assigning a weight to each criterion, with increasing weighting corresponding to higher priority, and summing the weighted criteria to calculate the Suitability Index (SI) for WECs deployment.

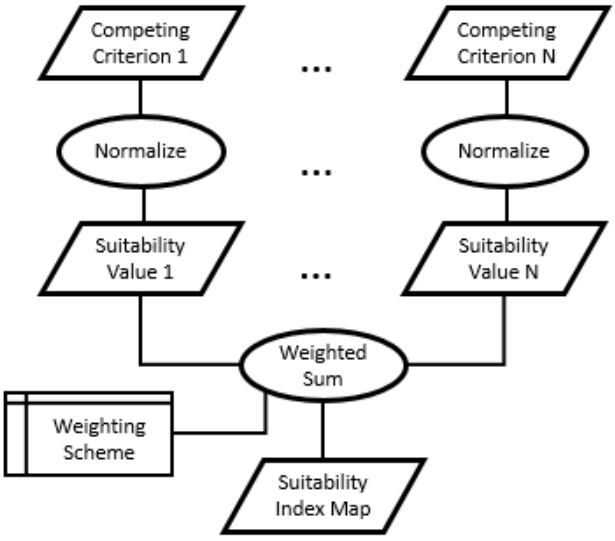

Figure 5.1 The methodology of a multi-criteria GIS analysis for generating a SI map according to a single stakeholder perspective.

The Suitability Index (SI) is calculated through Eq. 5.1; the higher the SI score, the greater the potential for that location to be a WEC farm site.

$$SI = \sum_i w_i S_i \qquad 5.1$$

In Eq. 5.1, the S_i represents a suitability value generated from the i^{th} criteria, and w_i is the weighting for i^{th} criteria so that $\sum w_i = 1$.

The five criteria considered in the analysis are Wave Resource (WR), Net Revenue Index (NRI), Commercial Fishery (CF), Marine Vessel Traffic (MVT), and Marine Conservation (MC). The WR is introduced in Chapter 2, and three different types of wave energy flux (gross, frequency filtered, frequency-direction filtered) are available for consideration here. The NRI is introduced in Chapter 3, and two types of NRI are available: one is calculated at the utility grid market scale, and the other at the remote community market scale. These two NRI are used independently in this analysis; the former is used for the analysis to select wave energy sites for the utility grid, and the latter is used to select wave energy sites for remote communities. The CF, MVT, and MC layers are introduced in Chapter 4. Among these five criteria, the suitability values for CF, MVT, and MC have already calculated in Chapter 4. The conversion to suitability values for the WR and NRI is introduced in the following section.

5.1.1 Suitability Value for Wave Recourse

As stated in Chapter 4, all competing criteria need to be normalized to a common evaluating scale, called the suitability value. For the WR criterion, sites with higher energy flux are more suitable for WEC deployment. As such, sites with the maximum annual average wave energy flux are rated as 100. When finding the maximum energy flux, values in excess of the 99.5 percentile of the energy flux are removed to eliminate extreme values. The maximum energy flux (J_{max}) is 40.57 kW/m for gross wave resource, 21.18 kW/m for frequency filtered wave resource, and 16.41 kW/m for frequency-direction filtered wave resource. The suitability value for wave resource (S_{WR}) at each site is calculated via Eq. 5.2. The S_{WR} is calculated for gross, frequency filtered, and frequency-direction filtered wave resources independently, and the resulting S_{WR} maps are shown in Figure 5.2.

$$S_{WR} = \frac{J}{J_{max}} \times 100 \qquad 5.2$$

where J_{max} is the maximum annual average energy flux for each type of wave resources in the study area, and J_s is the energy flux at each site.

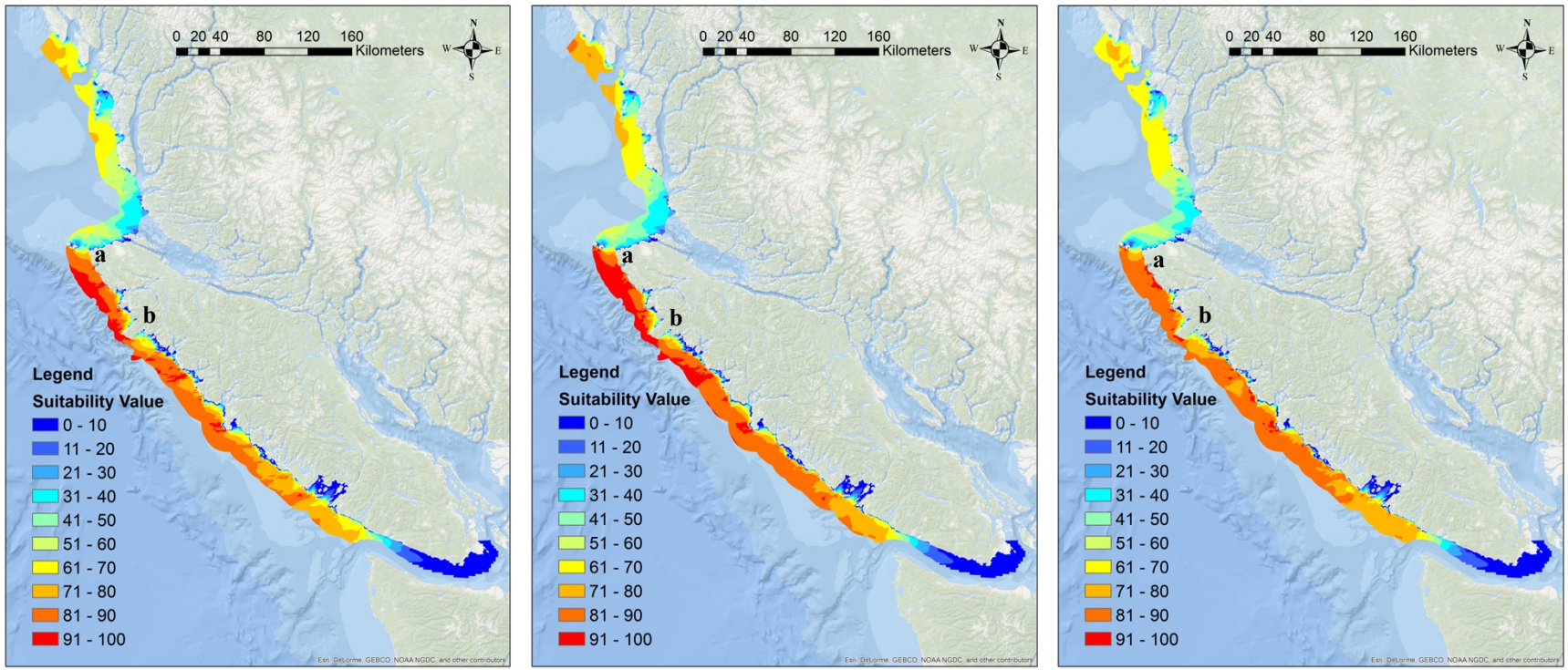

(a) *(b)* *(c)*

Figure 5.2 The spatial distribution of suitability value for (a) gross wave resource, (b) frequency filtered wave resource, and (c) frequency-direction filtered wave resource. (Classified Renderer is applied to display the data, and the dataset is classified to ten groups with equal intervals between value ranges.)

In general, the wave resources are abundant on the northern tip of Vancouver Island but sparse in the Strait of Juan de Fuca. The frequency filter significantly reduces the magnitude of the extractable resource but only slightly shifts the spatial distribution of energy flux. The areas with the highest resources remain concentrated between (a) San Josef Bay and (b) Brooks Peninsula. The subsequent application of the directional filter to the frequency filtered energy flux does shift the distribution of areas with highest wave energy flux closer to the coastline and makes the distribution more even.

The probability distribution of energy flux and the probability distribution of S_{WR} are plotted in Figure 5.3. In the context of wave energy flux, the probability of gross wave resources is distributed relatively evenly, whereas the probability of frequency filtered wave resources is distributed between 0 – 23 kW/m, which is around the half of the width of the gross wave resources probability distribution. The probability of frequency-direction filtered energy flux is further concentrated between 0 – 17 kW/m, and a peak of the probability occur around 13.5 kW/m.

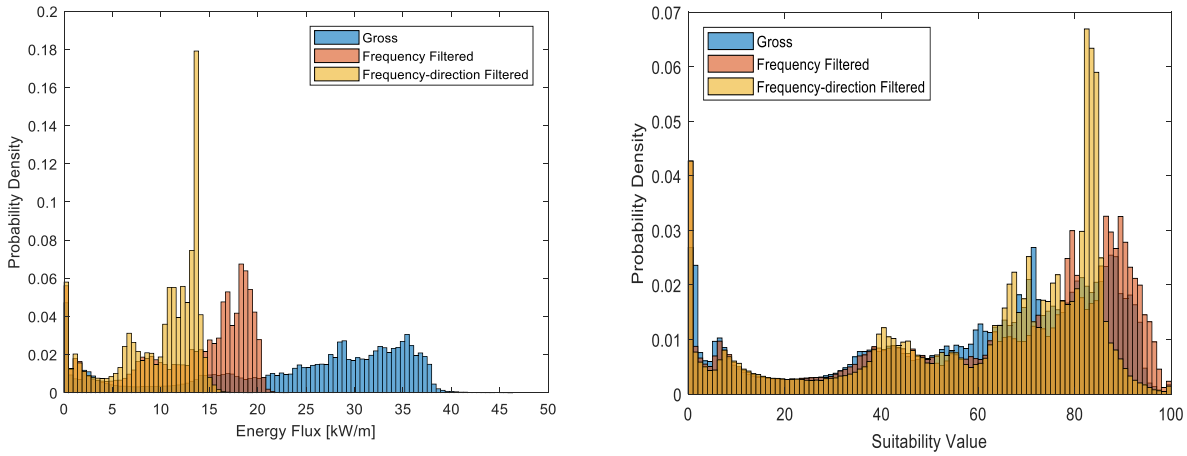

Figure 5.3 Probability distribution of (a) gross, frequency, and frequency-direction filtered energy flux and (b) their suitability value.

Figure 5.3 shows that converting energy flux to suitability values through a linear process maintains the probability distribution shape of the original energy flux. After converting to the suitability values, the range of the probability distribution of S_{WR} for the three different types of wave resources are at the same scale, from 0 to 100. The probability distributions

for the three S_{WR} have a similar shape, especially at lower S_{WR}. The probability of S_{WR} for frequency filtered wave resources are more concentrated between 80 and 100. This indicates that the frequency filter has more impact on the sites that have a higher energy flux than the sites that have a lower energy flux. The directional filter has a similar impact as the frequency filter leading to a greater concentration of probability between 80 and 90.

In this thesis, the frequency-direction filtered energy flux is selected as the WR criterion for the multi-criteria GIS analysis to follow. Although frequency-direction filtered energy flux is not directly proportional to gross energy flux, it is relatively well correlated: sites with relatively large frequency-direction filtered energy flux have relatively abundant gross wave resources as well. In addition, Figure 5.2 shows the areas with great frequency-direction filtered energy flux are further south and closer to the coastline, where there is more opportunity for conflict with existing human uses and marine ecosystem. As such, working with the frequency-direction filtered wave resource presents the greatest challenge to the multi-criteria GIS analysis.

5.1.2 Suitability Value for Net Revenue Index

For the NRI criterion, sites with the maximum economic opportunity are rated as 100, which is \$15,960/m at the utility market scale and \$77,040/m at the remote community market scale. Consistent with the WR criterion, values in excess of the 99.5 percentile of the NRI are removed to eliminate extreme values. The suitability value for the net revenue index (S_{NRI}) for each site is calculated through Eq. 5.3, and the resulting suitability value is shown in Figure 5.4.

$$S_{NRI} = \frac{NRI_s}{NRI_{max}} \times 100 \qquad 5.3$$

where NRI_{max} is the maximum NRI in the study area, and NRI_s is the NRI at each site.

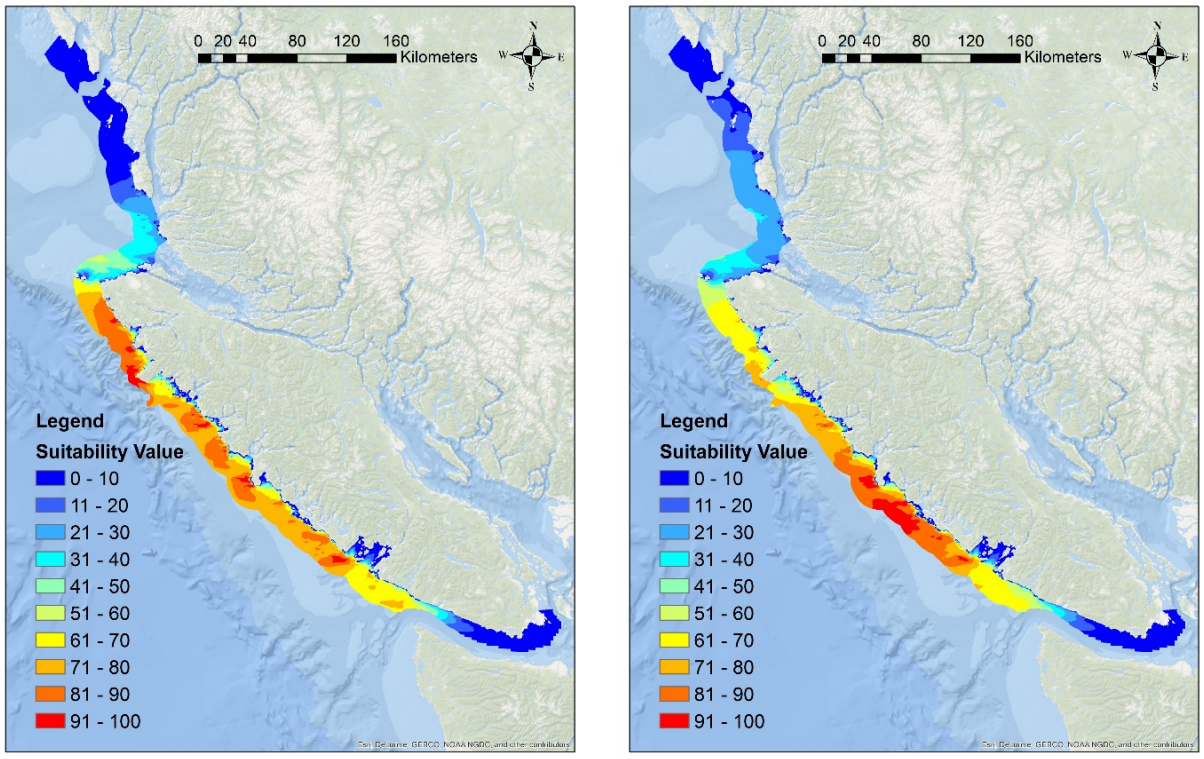

Figure 5.4 Suitability value for net revenue index at (a) utility market scale and (b) remote community market scale.

At utility market scale, the areas with highest S_{NRI} are relatively scattered and close to each of the sub-station. At remote community market scale, the areas with highest S_{NRI} only occur near Ahousaht.

5.2 Scenario Studies

In this section a series of multi-criteria GIS analyses, each referred to as a scenario, are conducted, and each scenario yield a SI map for the complete study area defined in Section 4.1. Four scenarios are designed to represent four different theoretical stakeholder perspectives by using a unique set of weighting applied to the criteria. Strategically important sites are the areas that have a high SI value in all scenarios; these are sites for WEC farm development that are 'good' from all stakeholder perspectives.

The process of identifying strategically important sites is illustrated in the flow chart shown in Figure 5.5. The first step of the process defines weighting schemes for each scenario,

from which a SI map is generated following the process introduced in Figure 5.1 (which is highlight by the red box in Figure 5.5). The next step defines hot-spots within each scenario. A hot-spot is defined as a location where the SI is within a selected threshold and thus is an ideal area for wave energy deployments from that specific stakeholder perspective; the 90th percentile of the SI is selected as the threshold in this study. The last step overlaps all hot spots from all scenarios to identify the intersections - strategically important sites that can satisfy all stakeholder perspectives.

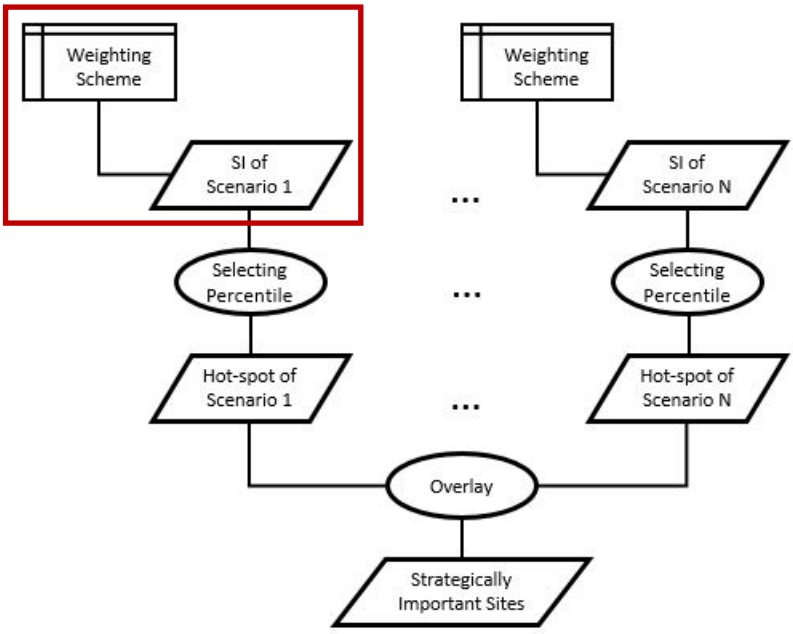

Figure 5.5 Summarized methodology of scenario study. (the process for generating a SI map according to a single stakeholder perspective is highlighted in the red box.)

Within each scenario, it is still a challenge to decide on the weighting for each criterion [59]. This is because the preferences of each stakeholder are usually vague and cannot be directly and exactly represented by numerical values. Usually, a stakeholder is more confident about the ranking of the criteria rather than specific weighting values. As such, it is more expedient to rank the criteria first and then convert the rank to precise weightings through a formulaic procedure [59]. In this study, a *Rank Ordering Weight* method [95], [96] is applied to approximate the stakeholder perspectives with numerical values. The *Rank Ordering Weight* method includes two steps [96]: 1) ranking the criteria based on their importance and 2) converting the ranks to weights via a rank order formula.

Four different scenarios are developed: *Egalitarian perspective, WEC development perspective, human uses perspective,* and *marine conservation perspective*. In the *Egalitarian perspective*, all criteria are assigned the same rank. In the *WEC development perspective*, the NRI and WR criteria are ranked higher than the other three criteria. In the *human uses perspective*, the existing human use criteria has higher priority while the wave resources has the lowest priority. In the *marine conservation perspective*, the marine conservation is given the highest rank. The lists of the ranks are shown in Table 5.1.

Table 5.1 The ranks of criteria for different scenarios.

Scenarios	WR	NRI	CF	MVT	MC
Egalitarian perspective	1	1	1	1	1
WEC development perspective	2	1	4	5	3
Human uses perspective	5	4	2	1	3
Marine conservation perspective	2	4	5	3	1

Here a simple weighting method called *Rank Sum* [59] is applied to convert the ranks to weightings. The list of ranks (r_i) can be converted into numerical weightings (w_i) through Eq. 5.4. The weighting scheme for each scenario is shown in Table 5.2.

$$w_i = \frac{n - r_i + 1}{\sum_{k=1}^{n}(n - r_k + 1)} \qquad 5.4$$

where n is the total number of criteria, and k is a counter for summing across all criteria.

Table 5.2 Weighting scheme for each scenario.

Scenarios	WR	NRI	CF	MVT	MC
Egalitarian perspective	20	20	20	20	20
WEC development perspective	27	33	13	7	20
Human uses perspective	7	13	27	33	20
Marine conservation perspective	27	13	7	20	33

Once the weighting schemes have been set, a SI map is generated following the weighting scheme from each scenario via Eq. 5.1. Hot-spots are then selected by determining the 90th percentile locations according to the SI distribution. This process is described by Eq. 5.5,

and if a site is selected as a hot-spot, H_j will be assigned to 1, otherwise H_j will be assigned to 0.

$$H_j = \begin{cases} 1, P(SI_j) > P_{th} \\ 0, P(SI_j) < P_{th} \end{cases} \quad 5.5$$

where H_j is the hot-spot selected in scenario j, SI_j is the suitability index, $P(SI_j)$ is the percentile of the sites sorted by SI_j value, and P_{th} is the threshold percentile decided by stakeholders, which is 90th percentile in this study.

The identification of strategically important sites is developed as two separated analyses – each is completed using a separate NRI suitability value layers. One is for the utility market scale of WEC farm development and the other is for the remote community market scale.

5.2.1 Egalitarian perspective scenario

The resulting SI at each site for *egalitarian perspective* scenario is shown in Figure 5.6. Compared to the hot-spots at the utility market scale, the hot-spots at the remote community market scale are further south, which are closer to the community of Ahousaht. Hot-spots mostly occur at (a) the north side of Brooks Peninsula, (b) Barrier Islands, (c) Nootka Island, and (d) Hesquiat Peninsula for both utility markets and remote community markets.

The probability distributions of the SI at both the utility market scale and the remote community market scale are shown in Figure 5.7. The probability distributions of the SI at the utility market scale and the remote community market scale follow a similar trend. Compared to the utility market scale, the SI at the remote community market scale shows a slightly lower probability between 90 to 100, and this is due to areas with high NRI at the remote community market scale being close to areas with busy marine traffic.

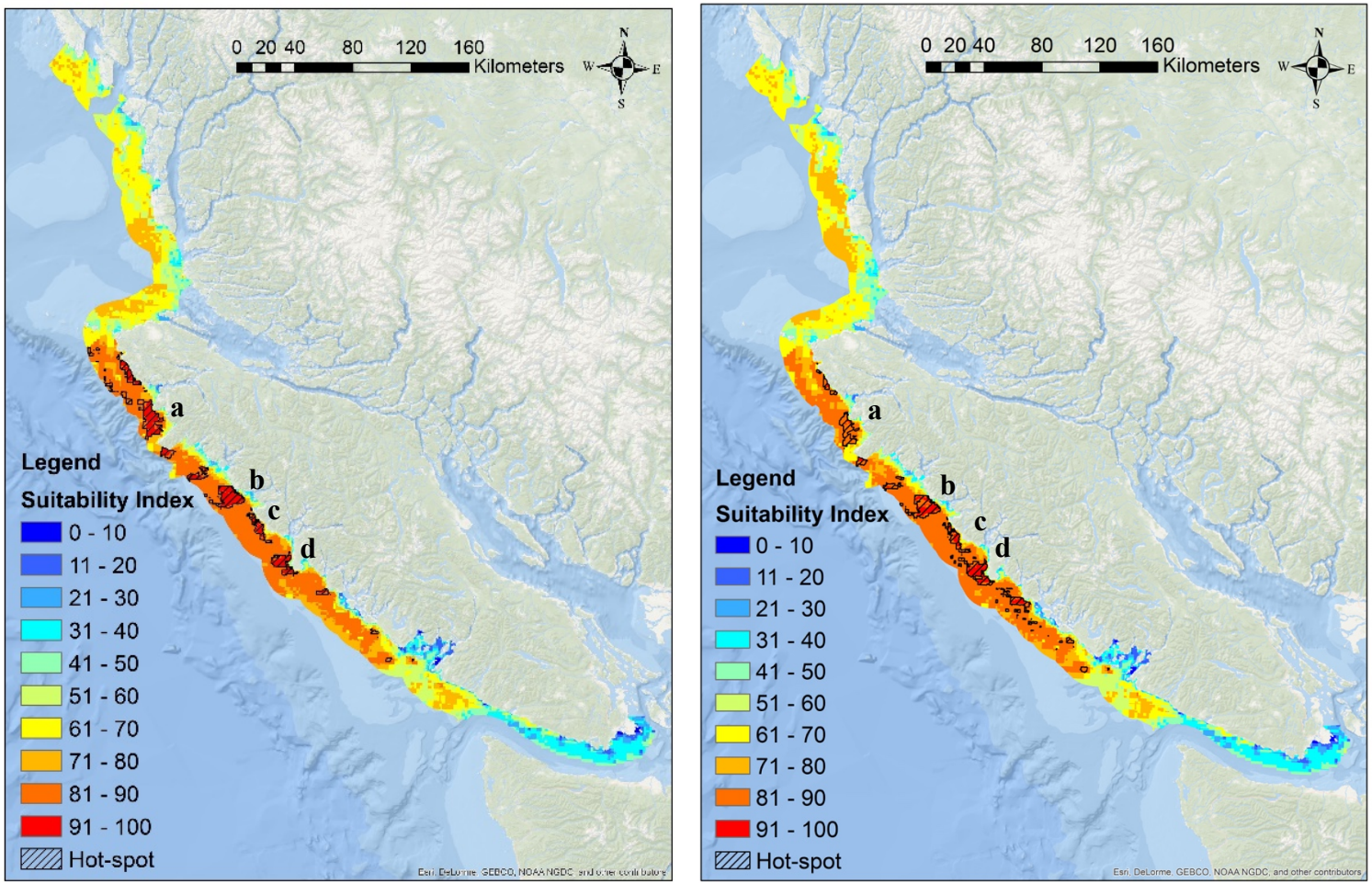

(a) Utility market scale *(b) Remote community market scale*

Figure 5.6 The SI at each site based on the egalitarian perspective.

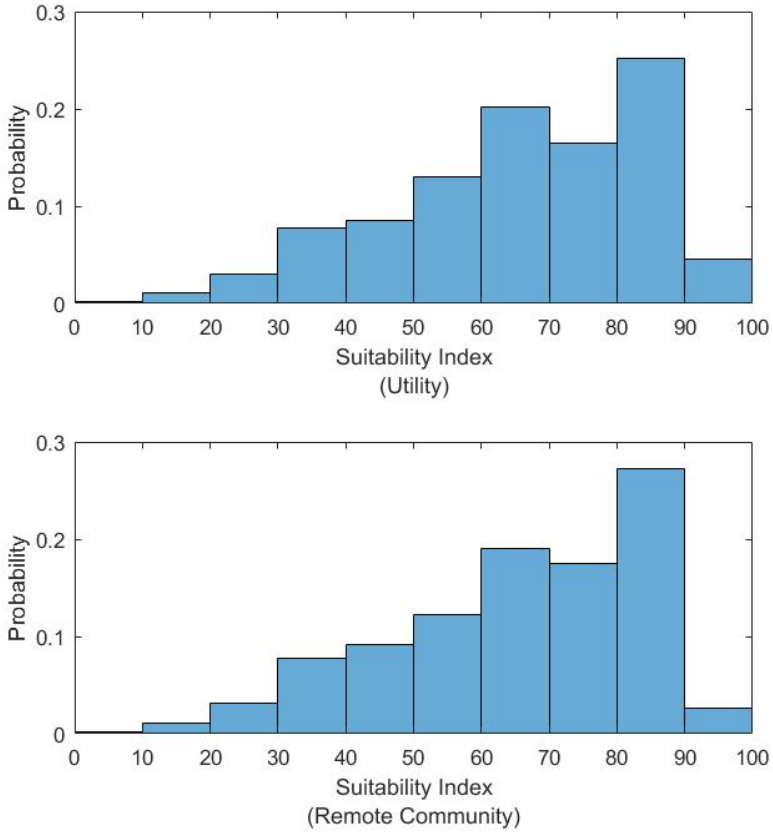

Figure 5.7 The probability distributions of the SI based on the egalitarian perspective.

5.2.2 WEC deployment perspective

The resulting SI at each site for *WEC development perspective* scenario is shown in Figure 5.8. The hot-spots for utility markets are mainly distributed between the northern tip of Vancouver Island and (a) Brooks Peninsula, whereas the hot-spots for remote community markets are mainly distributed between (c) Hesquiat Peninsula and (d) Ucluelet. The NRI criterion is given more weighting in this scenario, and this leads to very distinct SI distributions in hot-spots between the utility market and remote community market scales. The hot-spots between (b) Barrier Islands and (c) Hesquiat Peninsula that occurred in the egalitarian perspective scenario are still retained in this scenario.

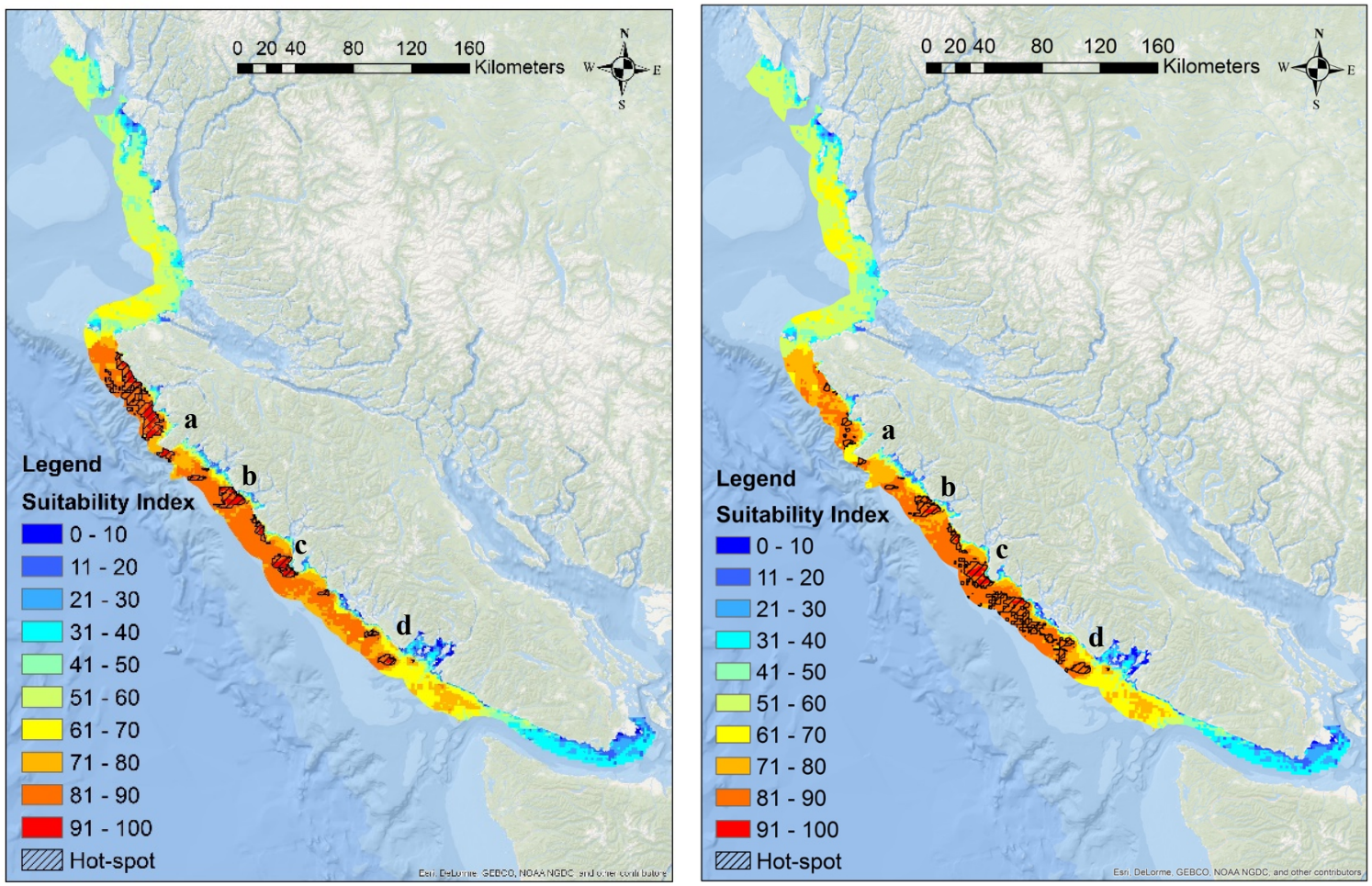

(a) Utility market scale *(b) Remote community market scale*

Figure 5.8 The SI at each site based on the WEC development perspective.

The probability distributions of the SI are shown in Figure 5.9. The probability distributions of SI at the utility market scale and the remote community market scale follow a similar trend. Compared to the utility market scale, the SI at the remote community market scale has a slightly lower probability between 90 to 100 and slightly higher probability between 60 and 70.

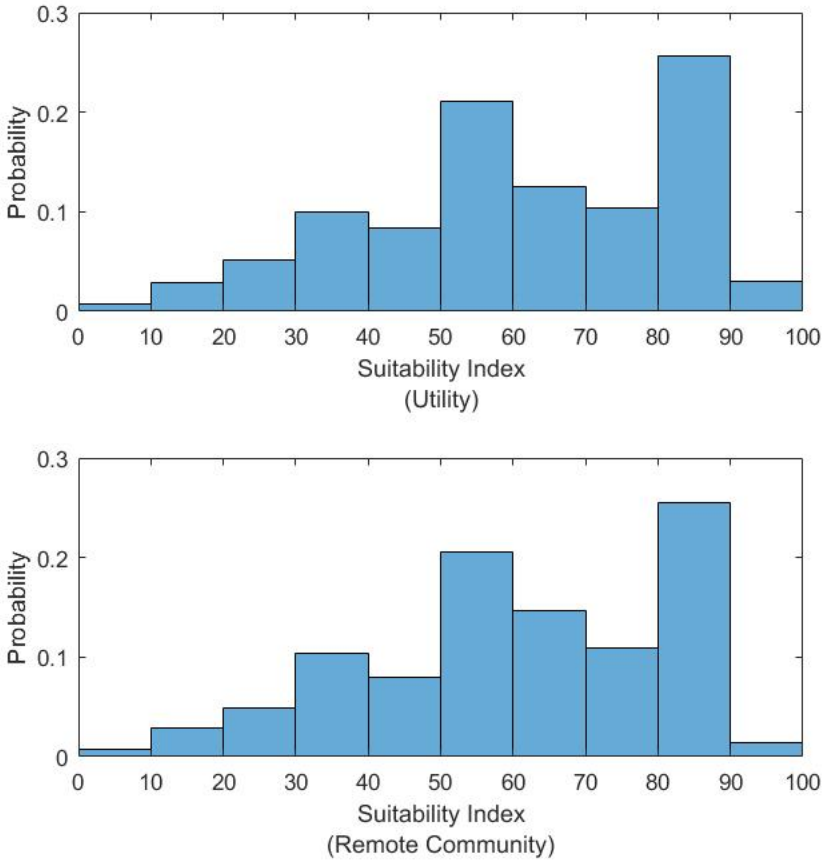

Figure 5.9 The probability distribution of the SI based on the WEC development perspective.

5.2.3 Human uses perspective

The resulting SI at each site for *human uses perspective* scenario is shown in *Figure 5.10*. In this scenario, the hot-spots at both market scales are distributed in a similar region, which is located between (a) the Lawn Point provincial park and (b) Hot Springs Cove. Compared to the utility market scale, more hot-spots at the remote community market scale occur at the south part of the region between (a) and (b).

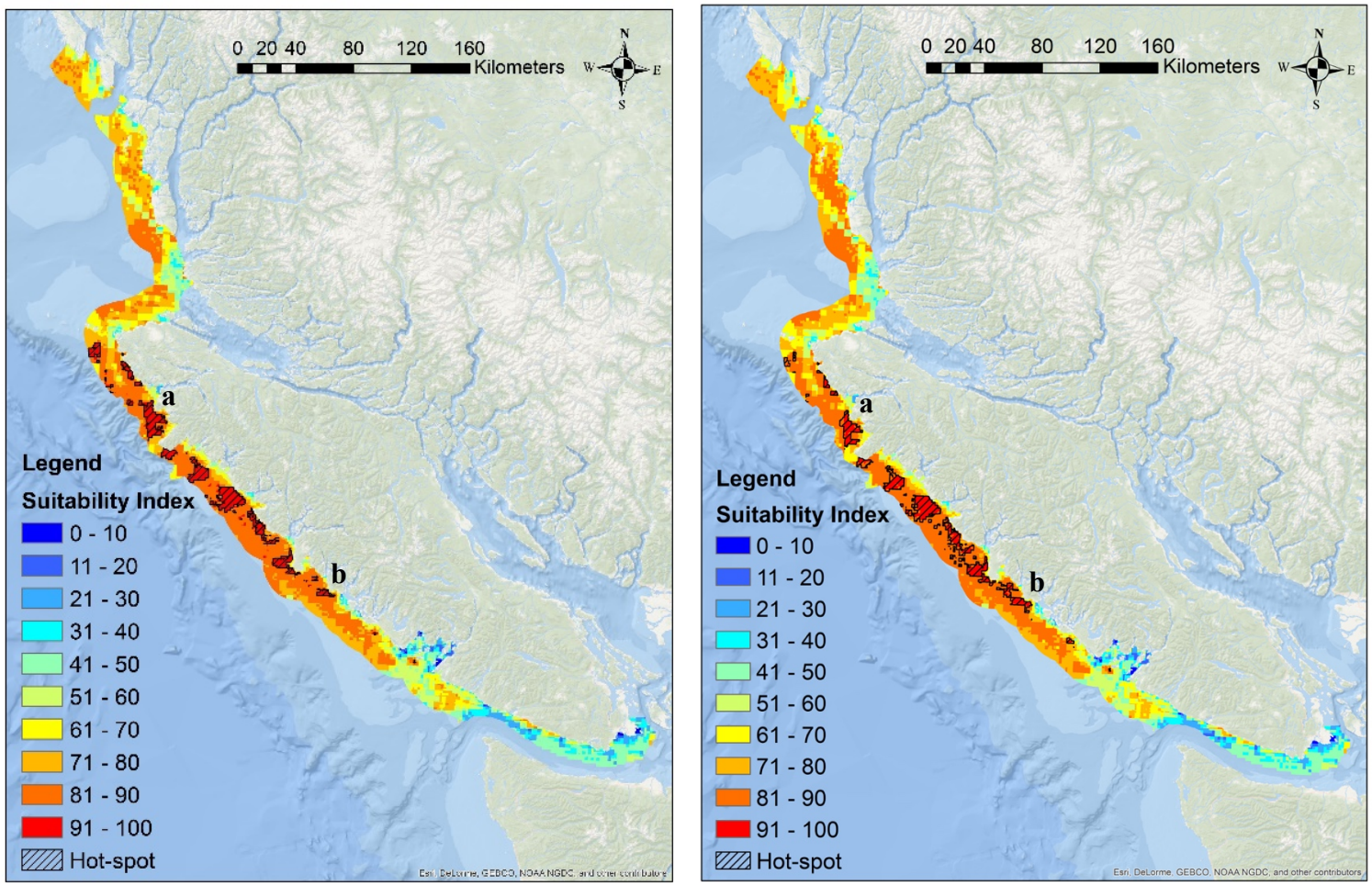

(a) Utility market scale *(b) Remote community market scale*

Figure 5.10 The SI at each site based on the human uses perspective.

The probability distributions of the SI are shown in Figure 5.11. In this scenario, the SI at both utility and remote community market scales have a higher probability between 90 to 100, compared to *egalitarian perspective* and *human uses perspective* scenario. Compared to the utility market scale in this scenario, the SI at the remote community market scale has a slightly lower probability between 90 to 100 and slightly higher probability between 80 and 90.

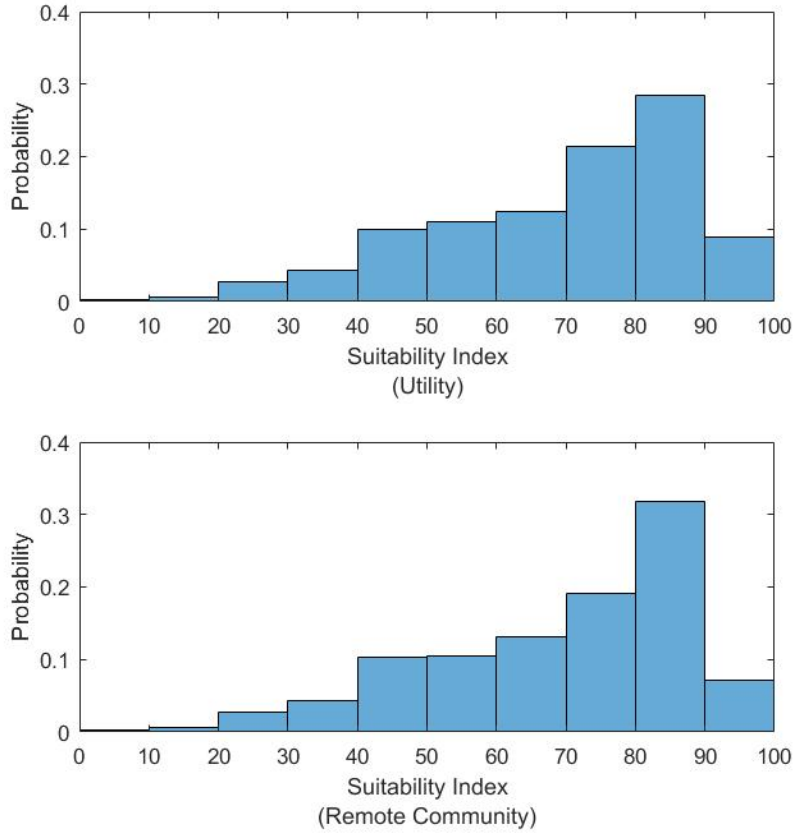

Figure 5.11 The probability distribution of the SI based on the human uses perspective.

5.2.4 Marine conservation perspective

The resulting SI at each site for *marine conservation perspective* scenario is shown in Figure 5.12. Large area of hot-spots show up between northern tip of Vancouver Island and (a) Brooks Peninsula. The hot-spots between (a) Brooks Peninsula and (b) Hesquiat Peninsula occurred in other scenarios are retained in this scenario.

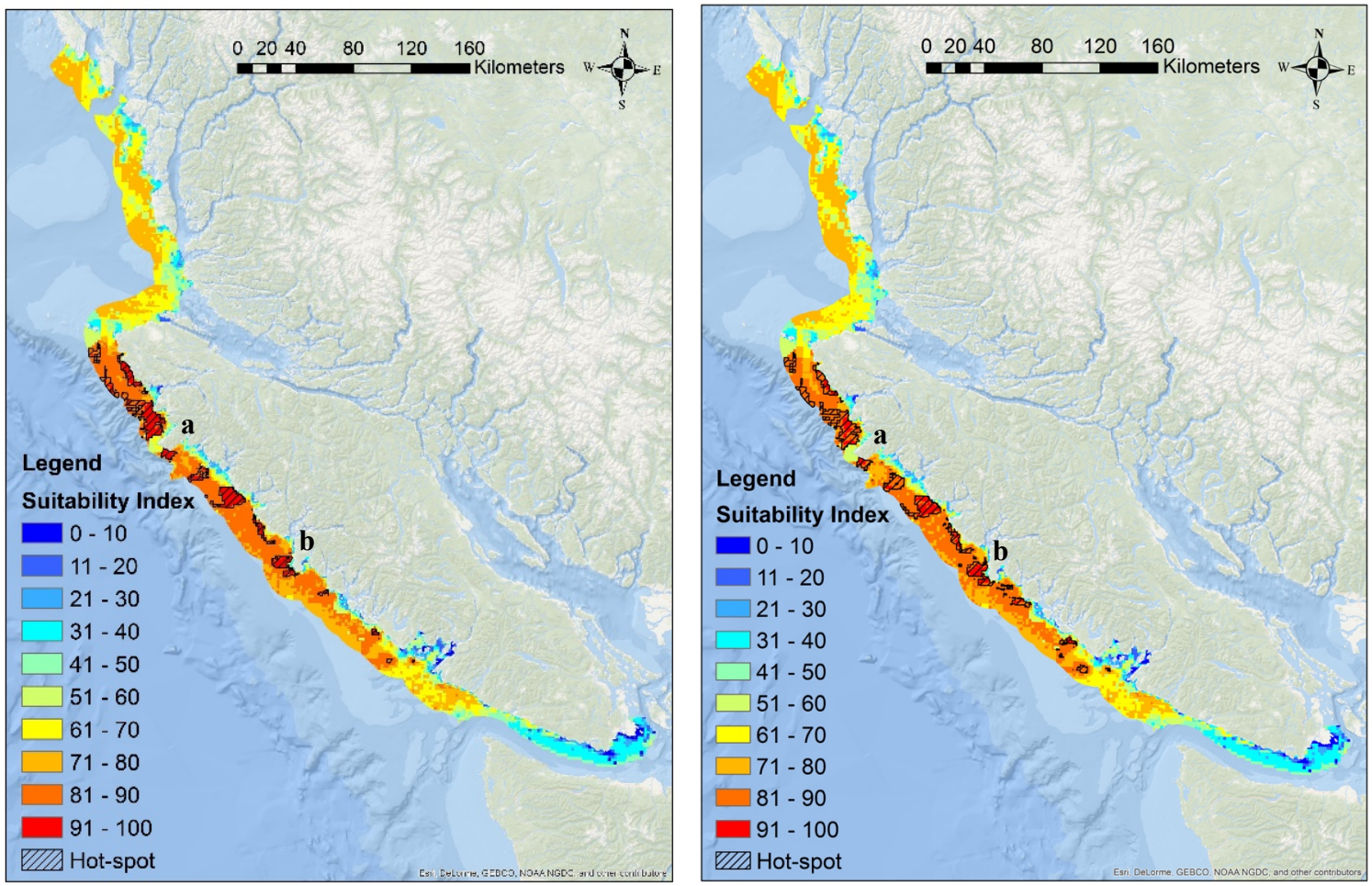

(a) Utility market scale *(b) Remote community market scale*

Figure 5.12 The SI at each site based on the conservation perspective.

The probability distributions of the SI are shown in Figure 5.13. The probability distributions of SI at the utility market scale and the remote community market scale follow a similar trend. The probability at both market scales distributed more evenly in this scenario than in other scenarios.

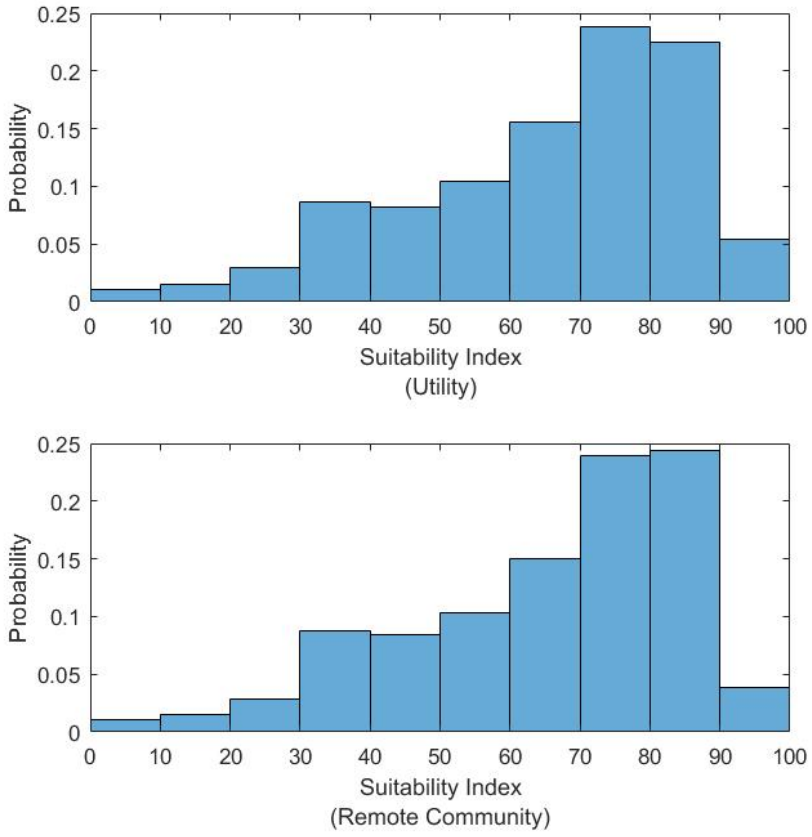

Figure 5.13 The probability distribution of the SI based on the marine conservation perspective.

In all four scenarios, the majority of hot-spots are located at the northern Vancouver Island. The hot-spots from each scenario significantly overlap with each other. This implies that areas with great wave resource and economic potential coincide to a certain extent in areas with less human uses and less conservation value. The areas with great wave resource are placed between the northern tip of Vancouver Island and Tofino. Luckily, the areas with busy marine traffic are concentrated at the Strait of Juan de Fuca, which do not possess

great wave resources. The areas with most commercial fisheries are located at the Barkley Sound, where is also an important region for marine conservation.

At the same time, the hot-spots from each scenario are distributed differently. In the *WEC development perspective* scenario, a region near Ucluelet is selected as a hot-spot but not selected in other scenarios. In the *WEC development perspective* scenario, the SI is influenced more by the WR and NRI criteria. This makes the region near Ucluelet, which has a higher NRI value, get a higher SI value and thus become a hot-spot. However, the other three scenarios assign weighting more on existing human uses and marine conservation criteria, which makes the region near Ucluelet not suitable for WEC farms anymore. In addition, the hot-spots located between northern tip of Vancouver Island and the Brooks Peninsula show as a continuous region in the *WEC development perspective* scenario, but they are broken into pieces by the commercial fishery and marine traffic in other three scenarios. In the *human uses perspective* scenario, the hot-spots between north tip of Vancouver Island and the Brooks Peninsula shrinks significantly, and the majority of hot-spots in this scenario move southward.

5.3 Strategically Important Wave Energy Sites

As a final step, the hot-spots from each scenario are overlaid to find strategically important sites; sites that can satisfy multiple stakeholder perspectives. A hot-spots count map is generated to record how many times for each site is selected as a hot-spot in different scenarios. This process is described by Eq. 5.6, and the resulting count (*HC)* is shown in Figure 5.14. The sites which are always selected as hot-spots in all scenarios are decided as the strategically important wave sites: these sites satisfy *HC* = 4.

$$HC = \sum H_j \qquad 5.6$$

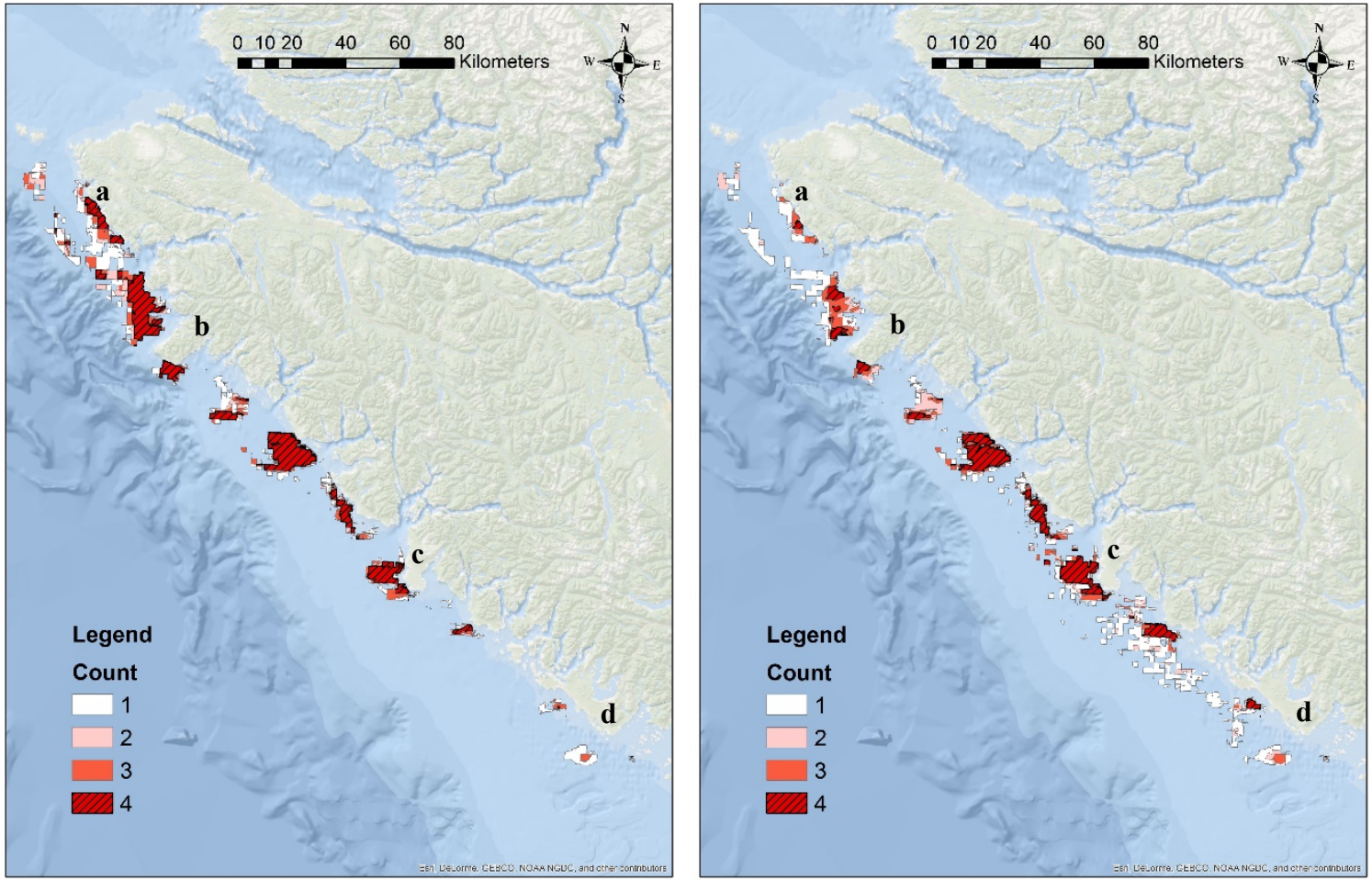

(a) *(b)*

Figure 5.14 The count of scenario hot-spots at (a) utility market scale and (b) remote community market scale.

At the utility market scale, the majority of hot-spots from different scenarios overlap with each other. The strategically important wave energy sites are the sites that have been selected as hot-spots for each of the four scenarios, shown as the red-dashed region. They cover a total of 638 km^2 area and account for 41% of the areas that have been identified as hot-spots in at least one scenario. This suggests the areas with great NRI at the utility market scale are highly coincident with the areas with fewer existing human uses or less marine conservation value.

At the remote community market scale, the hot-spots from different scenarios are less overlaid with each other. The strategically important sites cover a total of 490 km^2 area, only accounting for 25% of the areas that have been selected as hot-spot at least in one scenario. It should be noted that a large area located between (c) Hesquiat Peninsula and (d) Ucluelet, which either has high marine traffic or conservations zones, is selected as hot-spot in the *WEC development perspective* scenario but is not selected in the other scenarios. This causes fewer strategically important wave energy sites to be identified for the remote community market scale than at the utility market scale.

Both the strategical sites at utility market scale and the strategical sites at remote community market scale are located at the northern half of Vancouver Island, and the majority of them are next to the coastline. However, the total area of the strategical sites at remote community market scale is 23% less compared to the utility market scale. This decreased area is caused by the regions with high wave resources value having less intersection with the region with high NRI value at the remote community market scale. The strategically important sites identified between (a) Raft Cover and (b) Brooks Peninsula most notably show this decrease from utility to remote community market scales.

5.4 Site Characteristics

The site selection process accounts for multiple competing perspectives from stakeholders. As a result, the identified strategically important wave energy sites are

compromised when these competing perspectives are taken into accounted. This section examines how these compromises affect the potential wave energy production.

5.4.1 The Compromise on the Quality of the Wave Energy Resource

To revisit the quality of the wave resources at the identified strategically important sites (shown in Figure 5.15), Table 5.3 presents the averages and the standard deviations of the gross, frequency filtered, and frequency-direction filtered wave energy flux at these sites.

The regions with the frequency-direction filtered energy flux in excess of the 90th percentile are identified as sites with abundant extractable wave resources in Chapter 2. These regions are the hot-spots in the 'scenario' which only considers the wave resources and does not take into account any economic, other human uses, and marine conservation criteria; these regions are referred to as no compromise zones and are shown in Figure 5.15. The averages and the standard deviations of the gross, frequency filtered, and frequency-direction filtered wave resources within the no compromise zone are calculated as a comparison.

Table 5.3 The average and standard deviation of the gross, frequency filtered, frequency-direction filtered wave resources at strategically important wave sites and no compromise zones.

	Utility		Remote Community		No Compromise	
Wave resource [kW/m]	Average	Standard Deviation	Average	Standard Deviation	Average	Standard Deviation
Gross	35.68	2.15	35.57	2.46	35.76	2.13
Frequency filtered	19.09	1.06	19.07	1.13	19.24	0.98
Frequency-direction filtered	14.35	0.73	14.43	0.76	14.21	0.56
Area [km^2]	638		490		1821	

The averages of gross wave resources among the strategically important sites at utility market scale, remote community market scale, and no compromise zones are similar. This similarity is also found for the averages of frequency filtered and frequency-direction filtered wave resources. Figure 5.15 shows that the total area of the no compromise zone is around three times larger than the area of strategically important sites, and the majority of the statistically important sites are located within the no compromise zones. This

suggests that when accounting for other human uses and marine conservation areas, the strategical sites reduce in area but remain in the original no compromise zones. Therefore, the WEC deployment is not always in conflict with other human uses and marine ecosystems. It is possible to select a wave energy site that has less impact on human uses and marine ecosystem without losing too much wave energy potential.

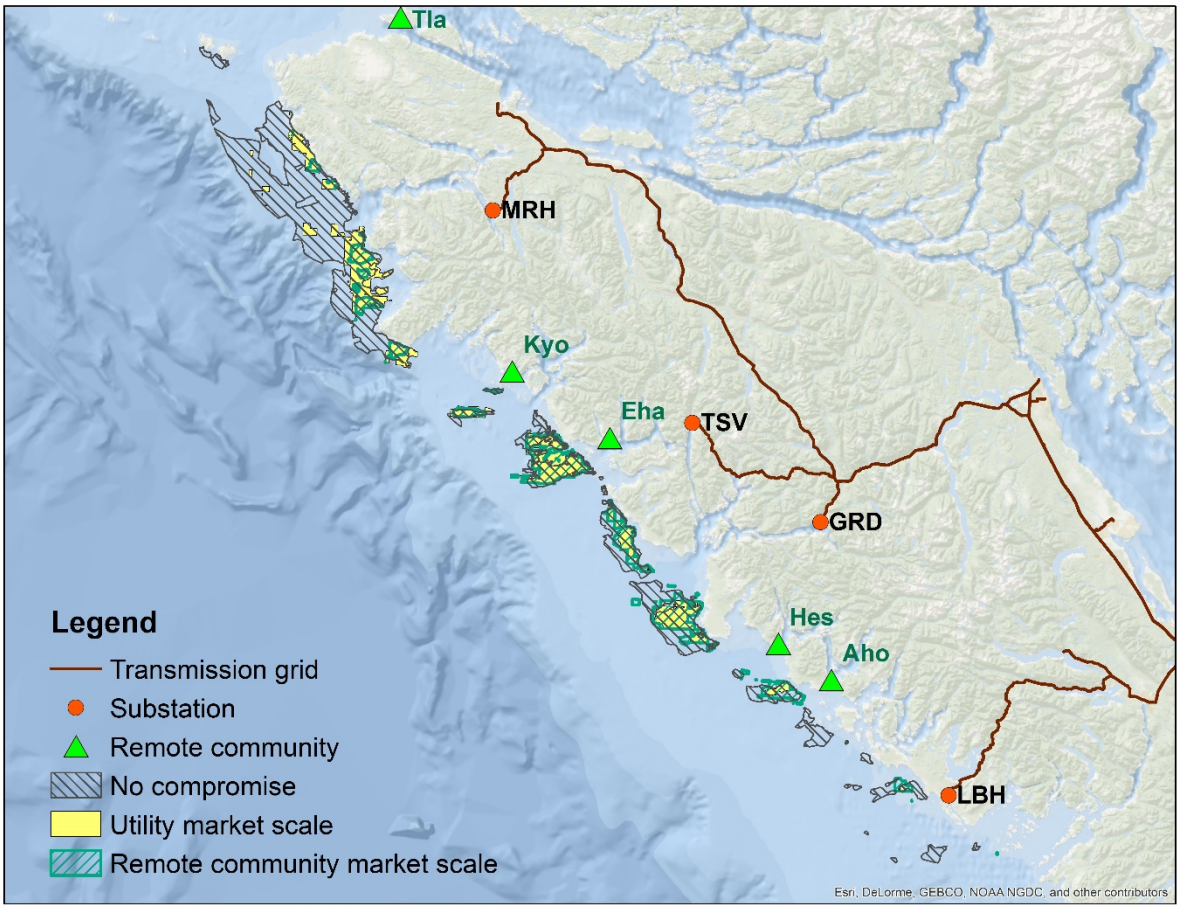

Figure 5.15 Strategically important wave energy sites and no compromise zones.

(Kyo stands for Kyoquot, Eha stands for Ehattesaht, Hes stands for Hesquaht, Aho stands for Ahousaht, MRH stands for Marble river substation, TSV stands for Tahsis village, GRD stands for Gold river pulp, LBH stands for Long beach.)

A further investigation on the compromise of the wave resource is developed by comparing the probability distributions of the energy flux at strategically important sites with the energy flux in the no compromise zones (see Figure 5.16). Since the total area

(sample size) of the strategically important sites and no compromise zone are different, it is difficult to compare them. The probability distributions are normalized so that the total area under the bar is equal to '1'.

The left boundary of the distribution for the no compromise zone indicates the 90th percentile for energy flux of the entire study area – the threshold for sites identified with abundant wave resources and selected for the compromise zone. Regarding the three different wave energy flux measures: the 90th percentiles for gross, frequency filtered, and frequency-direction filtered wave energy flux start at 35 kW/m, 19 kW/m and 13.5 kW/m.

A significantly lower probability of high energy flux is observed at strategically important sites, compared to energy flux within no compromise zone. The shifting areas of the probability distribution do not indicate lost sites, but they indicate lost probability. The decreasing probability of high energy flux is the cost of considering these human uses and marine conservation criteria. For instance, around 50% of the probability distribution of gross wave resource for strategically important sites are to the left of the probability distribution for the compromised zones. This implies that the strategically important sites are 50% more likely to produce less energy for a chosen wave farm site. However, the widths of the distributions for the strategically important sites are quite limited, and so the decreasing magnitude of the energy flux for compromised sites has a limited effect on energy production. As an example, the decrease in gross wave resource only reach the maximum of 7.5kW/m.

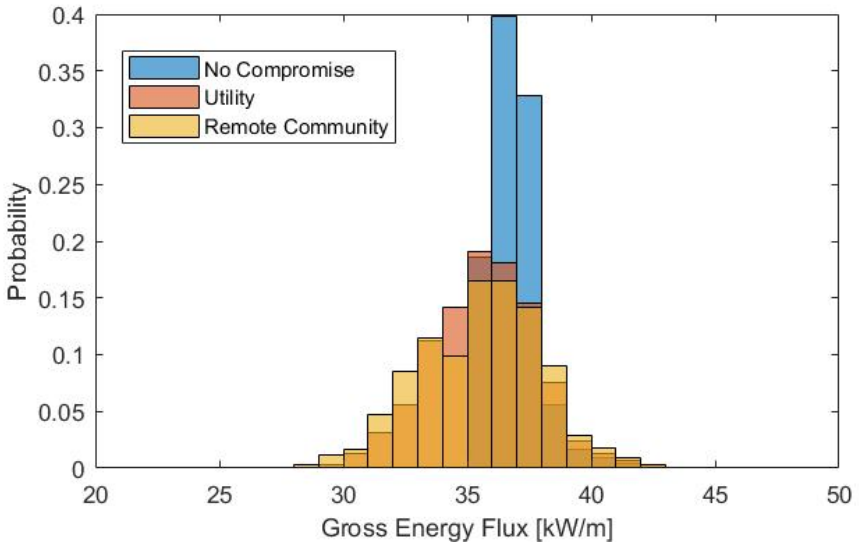
No Compromise
Utility
Remote Community
Probability
Gross Energy Flux [kW/m]
0.4
0.35
0.3
0.25
0.2
0.15
0.1
0.05
0
20
25
30
35
40
45
50

(a)

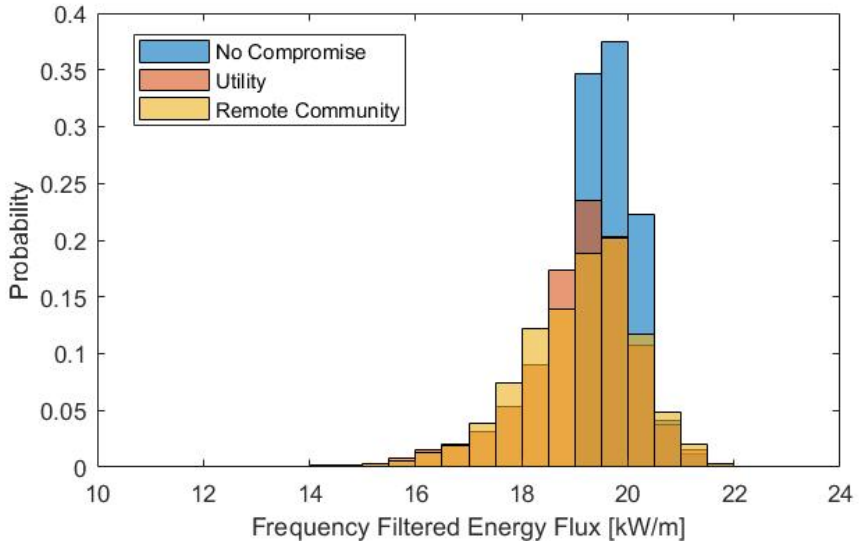
No Compromise
Utility
Remote Community
Probability
Frequency Filtered Energy Flux [kW/m]
0.4
0.35
0.3
0.25
0.2
0.15
0.1
0.05
0
10
12
14
16
18
20
22
24

(b)

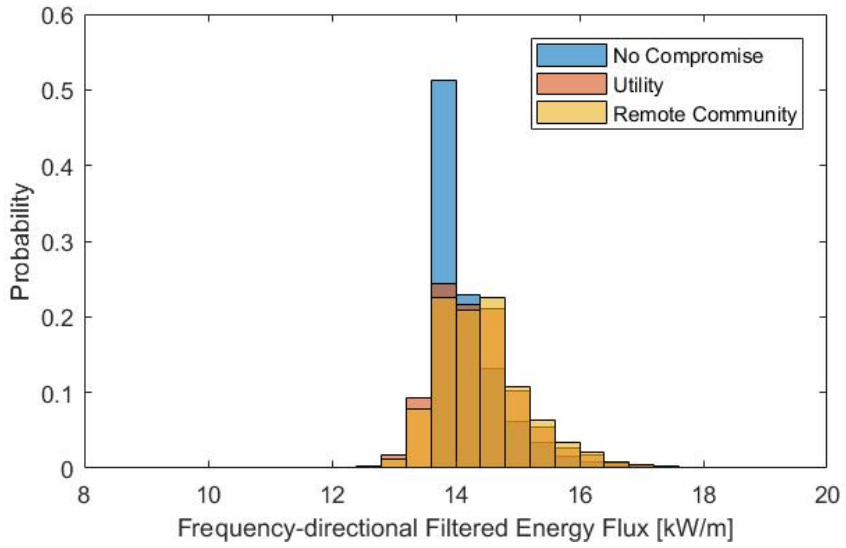

(c)

Figure 5.16 The probability distribution of the (a) gross, (b) frequency filtered, (c) frequency-direction filtered wave resources at strategically important wave sites and no compromise zones.

5.4.2 The Compromise on the Extent of the Wave Energy Resource

A significant number of sites are identified as the strategically important sites at both the utility market scale and the remote community market scale. As such, the strategical sites for utility market scale overlap with the sites for remote community market scale. The total area of the intersection between these sites is around 392 km^2. These intersecting areas are significant for both utility and remote community markets.

The frequency-direction filtered energy flux and the dominant wave direction (introduced in Section 2.5) within the intersection is plotted in Figure 5.17 and Figure 5.18. The energy flux varies between 12.37 kW/m and 18.6 kW/m with an average of 14.53 kW/m. The dominant wave directions range from -81˚ to - 145˚, and 28% of the dominant directions face toward -95˚ and 25% of the dominant directions face toward -105˚.

There is a total of 16 regions of intersection which have an area larger than 1 km^2. The mean, minimum, maximum, and the standard deviation of the frequency-direction energy

flux and dominant wave directions for each region are presented in Table 5.4. The regions are listed in the table by location - from north to south.

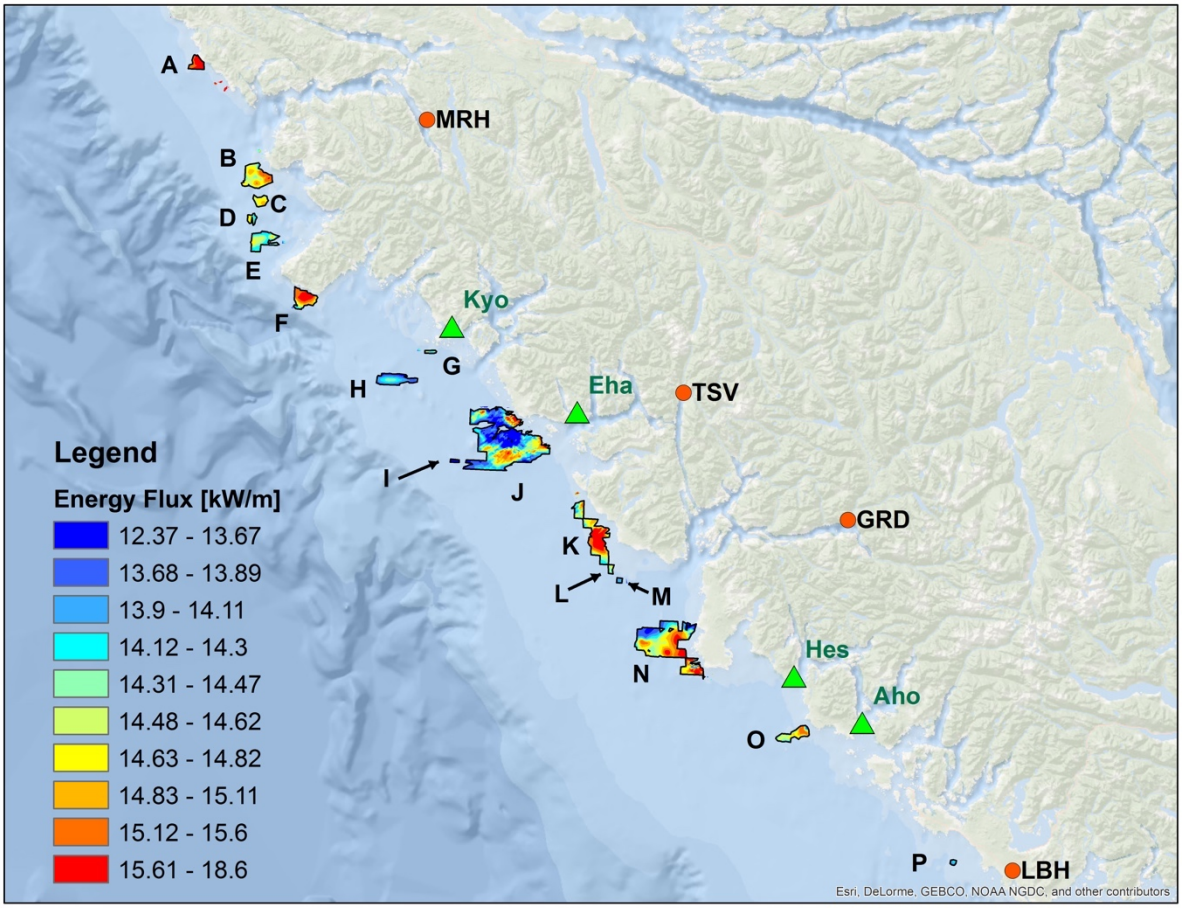

Figure 5.17 The frequency-direction filtered energy flux at sites which are significant for both utility and remote community markets.

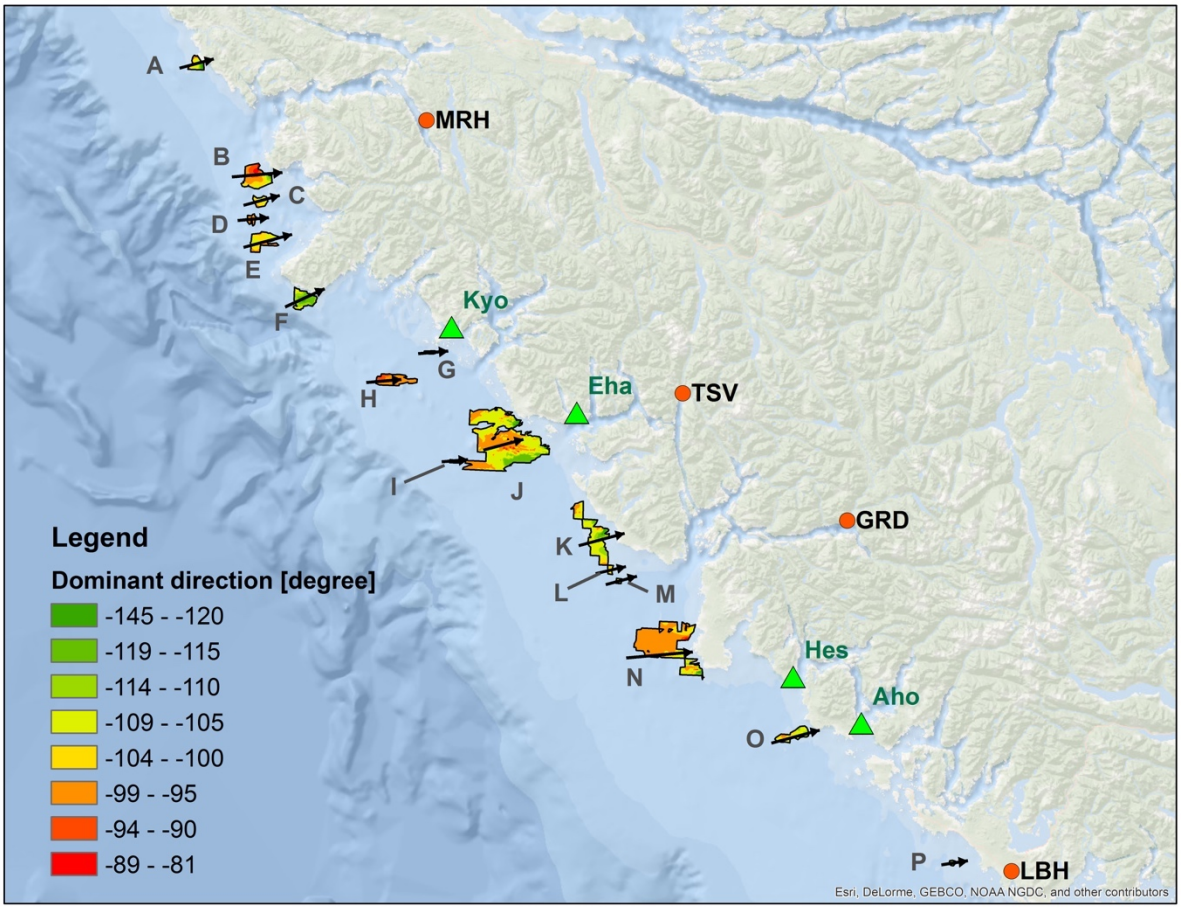

Figure 5.18 The dominant wave direction at sites are significant for both markets (the arrow is the mode direction in each region).

Table 5.4 The frequency-direction energy flux and dominant wave direction within each region which is significant for both utility and remote community markets.

No.	Area [km^2]	Frequency-direction filtered Energy Flux [kW/m]				Dominant Wave Direction [degree]			
		Min	Max	Mean	STD	Min	Max	Majority	STD
A	7.37	14.83	18.60	**16.27**	0.96	-133	-95	-105	9
B	24.55	13.62	15.69	14.76	0.32	-126	-81	-95	7
C	5.84	14.38	15.02	14.67	0.12	-105	-97	-105	2
D	3.26	14.08	14.86	14.45	0.20	-95	-95	-95	0
E	17.15	13.72	14.93	14.34	0.19	-105	-95	-105	3
F	15.94	13.99	16.28	**15.31**	0.57	-125	-105	-115	5
G	1.65	13.86	14.78	14.30	0.18	-122	-105	-105	4
H	16.87	13.45	14.53	13.96	0.22	-98	-87	-95	1
I	1.27	13.52	13.64	13.61	0.02	-95	-95	-95	0
J	147.99	12.37	18.08	14.15	0.60	-142	-85	-105	7
K	40.3	13.49	17.73	**15.11**	0.75	-144	-95	-105	6
L	2.04	14.22	14.84	14.43	0.13	-106	-99	-103	1
M	1.31	13.97	14.10	14.03	0.03	-105	-104	-105	0
N	88.09	12.68	18.40	14.71	0.74	-135	-85	-95	6
O	13.11	13.40	15.52	14.64	0.38	-117	-95	-105	4
P	1.31	13.84	14.26	14.01	0.11	-115	-108	-109	2

Within these strategically important sites, Region A, covering an area of 7.37 km^2, has the highest average energy flux, which is 16.27 kW/m. The most frequent dominant wave directions in this region face toward -105˚, with a range of 38˚. Region F has the second highest average flux of 15.31 kW/m, and it features an area of 15.94 km^2. The most frequent dominant wave directions in this region face toward -115˚, with a range of 20˚. Region K has the third highest average flux of 15.11 kW/m, and it is also the third largest area among all 16 regions. The most frequent dominant wave directions face toward -105˚, with a range of 49˚

When selecting a site for WEC farms with directional dependent devices, Region D, I, M should be considered first. The dominant wave directions at different sites within these regions almost face in the same direction, which simplifies the array design of the WEC

farm. However, all the three regions have small areas which may be not sufficient for large scale WEC farms. Region F is an adequate alternative that has a large area, high average flux, and similar dominant wave directions at each site.

In order to estimate the total extractable energy within each of the regions listed in Table 5.4, a characteristic width is assigned to each region. The characteristic width passes through the region centroid and is perpendicular to the dominant wave direction. These widths are listed for each region in Table 5.5. The total power (P_{tot}) along the characteristic width is calculated by multiplying the length of the region with the average energy flux within that region. The annual energy within each region is calculated via Eq. 5.7.

$$E_{ann} = P_{tot} \times 365 \frac{\text{day}}{\text{year}} \times 24 \frac{hour}{day} \qquad 5.7$$

The total power and annual energy within each region are calculated for gross, frequency filtered, and frequency-direction filtered wave resource respectively, and presented in Table 5.5.

Table 5.5 Total power and annual extractable energy within each statistically important region.

No	Length [m]	Gross		Frequency filtered		Frequency - direction filtered	
		Total power [MW]	Annual energy [GWh]	Total power [MW]	Annual energy flux [GWh]	Total power [MW]	Annual energy flux [GWh]
A	5307	206	1801	109	959	86	756
B	8499	308	2697	163	1428	125	1099
C	2827	102	891	55	478	41	363
D	2884	108	947	57	501	42	365
E	4520	170	1489	88	767	65	568
F	6638	245	2146	137	1197	102	890
G	996	36	314	19	170	14	125
H	3626	137	1198	72	633	51	443
I	945	35	302	19	163	13	113
J	18754	688	6029	368	3226	265	2325
K	13918	471	4124	258	2261	210	1842
L	3057	103	902	57	500	44	386
M	1741	57	502	32	280	24	214
N	13206	475	4159	252	2203	194	1702
O	2182	75	661	40	350	32	280
P	1828	62	541	34	295	26	224
Total	90928	3277	28704	1759	15412	1335	11696

Frequency-direction filtered energy flux represents a device-agnostic method to assess the extractable wave energy resource, and thus is a sufficient way to evaluate the quality of the wave resource. Except for regions I and G, the wave power within each of other regions exceeds 20MW indicating that these sites are adequate for the utility market scale. The wave power within Region B, J, K and N is larger than the capacity of the largest substation – 108 MW at Tahsis Village substation. Region J has the largest area of 148 km^2, and it can provide 2,325 GWh of energy each year. This is 25% of the electricity demand of Vancouver Island - 9069 GWh. The total energy of all 16 regions is 11,696 GWh, which is larger than the annual electricity demand of Vancouver Island.

Chapter 6 Conclusions

Given the unique nature of this research, the conclusion begins by summarizing the newly developed methodologies and resulting outcomes in each of the previous chapters in Section 6.1. Later, the limitations of this research are explained in Section 6.2. The recommended further work is introduced in Section 6.3.

6.1 Chapter Results and Conclusions

Generating electricity from the natural wave resource along the West Coast of Vancouver Island (WCVI) has the potential to meet a significant portion of the electricity demand of the utility grid, and coastal remote communities, on Vancouver Island. One of the most essential requirements for a developing wave energy industry is a comprehensive site selection process. Previous research developed in WCVI region, focused on detailed assessments on wave resources and site selections, were based exclusively on the gross and extractable wave resource and the proximity to utility transmission grid. However, coastal areas hold diverse marine activities, competing users, and possess sensitive marine ecosystems; no previous research in the WCVI region has taken these factors into consideration. This thesis performs a scenario based multi-criteria GIS analysis which accounts for wave resources, the economic potential, the pre-existing human uses, and the marine ecosystem.

In Chapter 2, a novel device-agnostic frequency filter and a directional filter are developed to quantify extractable wave resources, while accounting for the influence of the wave frequency and direction on the WEC-extractable energy flux. A full directional variance density spectrum is regenerated, using the IEC [39] specified wave parameters from SWAN model outputs, to quantify the variance distribution among different wave frequencies and directions. The frequency domain of this spectrum is generated using significant wave height (H_s) and energy period (T_e), and following a single peaked Pierson-Moskowitz shape [63]. The directional domain is generated using peak wave direction (θ_p) and directional spreading (δ_θ); following a $\cos^{2s}\theta$ model [63]. A device-agnostic frequency filter is then developed, based on power performance of four types of

WECs, to help estimate the portion of the total incident energy that can be captured by devices. The resulting frequency filter features a cosine bell shape with a peak at 0.095 Hz, and boundaries at 0.065 Hz and 0.154 Hz. A directional filter, following the IEC TC 114 TS 62600-101 [39], is developed to further describe the impact of wave direction on the WEC performance and associated power production. The resulting directional filter features a standard cosine window with a width of 180-degrees. Chapter 2 spatially identifies the gross, frequency filtered, and frequency-direction filtered wave resources in excess of 90^{th} percentile. The frequency filter reduces the gross resource by 45%, and the frequency-direction filter reduces it by an additional 25%. Interestingly, areas with gross wave resources and frequency filtered wave resource in excess of the 90^{th} percentile are highly correlated, whereas the direction filter shifts the areas with excellent resources southward. The observed shifts of areas with excellent wave resources prove the importance of the frequency filter and directional filter to improve the quantification of extractable wave resources.

In Chapter 3, a detailed economic evaluation estimates the influence of the distance from WEC array to the coastline and transmission grid, the electricity market size, and the wave farm physical layout on the selection of wave energy sites. In this evaluation, the economic potential is estimated on a unit WEC-farm basis. As such, the farm length is decided by the wave resources at each site. The Net Revenue Index (NRI), a novel metric developed by scaling the potential net revenue (revenue index subtract cost index) by the WEC farm length, characterizes the economic potential for WEC farms in $/m. The revenue index is calculated based on the net generation (the electricity output of a WEC farm that is utilized to meet the demand) and is defined by the present value of operating the WEC farm for an assumed 15 years. The cost index accounts for three major items; the exported cable cost (distance dependent), the inner-connection cable cost (farm length dependent), and the cost for electrical infrastructure (unit WEC-farm dependent). The NRI is evaluated at two market scales: the utility market scale (i.e. all energy generated from WEC farm will be utilized) and the remote community market scale (i.e. energy utilized is limited by community needs). At the utility market scale, the maximum NRI is $18,860/m, and the average is $8,940/m. At the remote community market scale, the NRI

is determined by the maximum value among the five communities. The majority of the WCVI region is dominated by Ahousaht, with a maximum of $94,260/m and an average of $30,080/m, which is around five and three time higher than at the utility market scale respectively.

In Chapter 4, three additional factors that strongly influence the site selection for WEC farms are introduced; commercial fisheries, marine vessel traffic, and marine conservation area. The annual commercial landing value, measured in $/km^2, quantifies economic value of the commercial fishery. This annual landing value is estimated based on the economic data published by the DFO and the spatial data published by the BCMCA. The hours of vessel traffic, a proxy for marine traffic, is derived by summing up the hours of all types and categories of vessels; recorded by the BCMCA. For marine conservation, the conservation value data, produced by the BCMCA based on a moderate conservation target defined by ecological experts, is used in this thesis. These three layers are independently used in the multi-criteria analysis to compete with the wave resources and economic layers described in Chapter 2 and 3 to select the strategically important wave energy sites.

In Chapter 5, a scenario-based, multi-criteria analysis is developed to identify strategically important sites for future wave energy development. A total of five competing criteria (wave resource – Chapter 2, net revenue index – Chapter 3, commercial fishery – Chapter 4, marine traffic – Chapter 4, and marine conservation – Chapter 4) are considered. Each criterion is represented by a single GIS layer, and is assigned a weight based on an assumed (but varied) importance. A Suitability Index (SI) map is generated by summing up all weighted criteria. To investigate the influence of altering the weights of criteria on the resulting potential location for WEC farm, a scenario study is undertaken. Four different ‘stakeholder-representative’ scenarios are developed to represent perspectives from distinct stakeholders; these include Egalitarian perspective scenario, WEC development perspective scenario, Human uses perspective scenario, and Marine conservation perspective scenario.

Strategically important sites are defined by the overlapping areas that are selected (areas with a SI of the 90th percentile) in all four scenarios. Utility market scale and remote community market scale opportunities are dealt with separately. Strategically important sites for utility market cover a total area of 638 km^2, with an average of 14.35 kW/m frequency-direction filtered wave resources. These sites are mainly located between the northern tip of Vancouver Island and Hesquiat Peninsula. The total areas of strategically important sites for remote communities is approximately 490 km^2, with an average of 14.43 kW/m frequency-direction filtered wave resources. These sites are located proximate to Ahousaht. Finally, the strategically important sites at both scales are plotted together, and an area of 392 km^2 is identified as important at both market scales – generally situated in northern Vancouver Island. A total of 28,704 GWh annual gross energy is presented at these sites, which is larger than the annual electricity demand of Vancouver Island.

6.2 Limitations

The identified strategically important sites for wave energy highly depend on the layers included, the criteria, and their associated weighting chosen within the study, and thus removing or adding criteria or replacing the input data used for the current criteria can significantly change the resulting sites. In this thesis, the wave resources criterion is represented by a novel device-agnostic assessment of the extractable wave energy resource. As the WEC technology starts to converge on a specific architecture, the site selection process should be applied with improved power matrices for the wave resources criterion. Additional criteria, such as the seafloor typology, military testing zones, existing undersea communication cables, and the distance to port facilities, are worth considering when selecting sites for WEC farms. There are two main obstacles that prevented these criteria to be adapted in this analysis. First, the source data for these criteria are not available through public databases and were not feasible to acquire given the project time constraints. Second, the effect of these criteria on the WEC deployment is vague; the criteria are difficult to be evaluated using the 0 – 100 suitability value scale. While the adaptation of additional criteria will modify the results of this analysis, the

novel process developed in this thesis will remain. Therefore, the outcomes of this study should only be assessed within the context of the criteria and datasets included within the analysis, but the process has wide and long-term application.

It should be noted that the accuracy and the precision of the results are decided by the quality of the source data. The spatial resolution of the source data used for wave resource and the net revenue index criteria is 100 by 100 m, whereas the resolution of the marine traffic and marine conservation data is 2000 by 2000 m. As a result, the overall accuracy of the results is constrained by the low resolution of social and environment data.

Last, the marine environment is highly dynamic, and thus the data need to be collected and updated frequently. The source data used for this analysis, although it was the latest data available when this analysis is conducted, may no longer represent the current situation. For example, the source data used for the commercial fishery was published by BCMCA in 2011, but the data used in their analysis could date back to the early 2000s. The commercial fishery activities today could be different from the activities in the early 2000s.

Overall, as more recent and increased spatial resolution data becomes available, updating the input source data for this framework, will improve the accuracy and robustness of the results. In addition, expanding the framework by incorporating additional criteria will improve the ability of the analysis to capture a broader range.

6.3 Further work

When stakeholders pre-select adequate areas for wave energy deployment, the identified strategically important sites would be worth consideration as appropriate locations for WEC deployments. In addition to building up the site selection framework with multiple wave resources, human uses, and marine conservation layers and incorporating different ‘stakeholder-representative’ scenarios in site selection process, several directions to further this study are suggested:

1) Develop a sensitivity study on the effect of the hot-spot definition on the results

In Chapter 5, the areas with 90th percentile of Suitability Index (SI) are defined as hot-spots. However, this definition of hot-spots is not fixed. The hot-spots can be modified by selecting lower or higher percentile of the SI. This modification will broaden and narrow the hot-spots within each scenario and thus reduce or increase the areas or shift the locations of the resulting strategical sites. An additional study that investigates the sensitivity of hot-spot definitions on the resulting strategically important sites is recommended.

2) Develop a detailed multi-criteria GIS analysis within the strategically important sites

The multi-criteria GIS analysis identifies areas that satisfy interests of stakeholders from diverse perspectives, and thus find the trade-off between wave energy development and the marine environment. This analysis greatly narrows the areas attractive for the WEC farms down to hundreds of square kilometers, by eliminating areas with less wave resources, areas utilized by other marine users, and marine conservation zones. However, the analyses conducted in this thesis are on a large scale, and the criteria in this analysis are limited by the resolutions of the data and types of the data that is available. A multi-criteria GIS analysis that uses data with finer resolution for smaller specific locations is recommended. For instance, a more detailed cable cost assessment can be conducted by incorporating the local seafloor topology, given that the composition and the slope of seafloor have influence on setting up the cables. In addition, a more detailed wave resources assessment, the marine ecosystem, and other human uses data, as well as the seafloor geomorphology data for anchoring WECs will be easier to obtain at a small scale.

3) Develop a web-based analytical application based on this multi-scenario framework

The scenario based multi-criteria GIS analysis establishes an applicable framework which can assist multiple stakeholders to identify the strategical wave sites that strike

a reasonable compromise between their competing priorities. A web-based analytical application based on this framework will be valuable for two reasons. First, manually reprocessing all steps in the framework can be a tedious and error prone procedure. The analytical web application will allow any change in the site selection process to be directly made and the whole procedure of the analysis to run automatically. Second, the theoretical scenarios were set up by varying the ranks of the criteria to simulate preferences of different stakeholders in this thesis. The web-based analytical application will support stakeholders to participate and be involved in the site selecting processes. Stakeholders will set up the scenarios following their real interests, and this application will be able to produce the resulting strategical sites immediately and present them in a map format. This analytic tool will enable this site selection process interactively and geo-visibly. With regard to technique aspect, the emergence of web-GIS developer software, such as ArcGIS Pro, makes it easier to develop a personal GIS application by writing scripts. Therefore, developing an analytical web application is highly recommended as further work.

Bibliography

[1] B. Robertson, C. Hiles, E. Luczko, and B. Buckham, "Quantifying wave power and wave energy converter array production potential," *Int. J. Mar. Energy*, vol. 14, pp. 143–160, 2016.

[2] World Energy Council, "World Energy Resources 2016," *World Energy Resour. 2016*, pp. 1–33, 2016.

[3] World Energy Council, "World Energy Issue Monitor 2017," p. 156, 2017.

[4] F. Flocard, D. Ierodiaconou, and I. R. Coghlan, "Multi-criteria evaluation of wave energy projects on the south-east Australian coast," *Renew. Energy*, vol. 99, pp. 80–94, 2016.

[5] T. Flannery, *The Weather Makers*. Melbourne, Australia: Text Publishing, 2005.

[6] J. Goldemberg, "The promise of clean energy," *Energy Policy*, vol. 34, no. 15, pp. 2185–2190, 2006.

[7] T. V. Ramachandra and B. V. Shruthi, "Spatial mapping of renewable energy potential," *Renew. Sustain. Energy Rev.*, vol. 11, no. 7, pp. 1460–1480, 2007.

[8] A. Clément, P. McCullen, A. Falcão, A. Fiorentino, F. Gardner, K. Hammarlund, G. Lemonis, T. Lewis, K. Nielsen, S. Petroncini, M. T. Pontes, P. Schild, B. O. Sjöström, H. C. Sørensen, and T. Thorpe, "Wave energy in Europe: Current status and perspectives," *Renew. Sustain. Energy Rev.*, vol. 6, no. 5, pp. 405–431, 2002.

[9] UNFCCC, "Paris Agreement," *Conf. Parties its twenty-first Sess.*, no. December, p. 32, 2015.

[10] H. Bernhoff, E. Sjöstedt, and M. Leijon, "Wave energy resources in sheltered sea areas: A case study of the Baltic Sea," *Renew. Energy*, vol. 31, no. 13, pp. 2164–2170, 2006.

[11] Z. Defne, K. A. Haas, and H. M. Fritz, "Wave power potential along the Atlantic coast of the southeastern USA," *Renew. Energy*, vol. 34, no. 10, pp. 2197–2205, 2009.

[12] Leo H.Holthuijsen, *Waves in oceanic and coastal waters*. New York: Cambridge University Press, 2007.

[13] D. Mollison, "Wave climate and the wave power resource Actuarial Mathematics and Statistics," pp. 133–156, 1986.

[14] G. Reikard, B. Robertson, B. Buckham, J. R. Bidlot, and C. Hiles, "Simulating and forecasting ocean wave energy in western Canada," *Ocean Eng.*, vol. 103, pp. 223–236, 2015.

[15] D. J. Arent, A. Wise, and R. Gelman, "The status and prospects of renewable energy for combating global warming," *Energy Econ.*, vol. 33, no. 4, pp. 584–593, 2011.

[16] A. Cornett, "Inventory of Canada's Offshore Wave Energy Resources," *Ocean Eng. Polar Arct. Sci. Technol.*, vol. 2, no. January 2006, pp. 353–362, 2006.

[17] G. Reikard, B. Robertson, and J. R. Bidlot, "Combining wave energy with wind and solar: Short-term forecasting," *Renew. Energy*, vol. 81, pp. 442–456, 2015.

[18] S. Behboodi, D. P. Chassin, C. Crawford, and N. Djilali, "Renewable resources portfolio optimization in the presence of demand response," *Appl. Energy*, vol.

162, pp. 139–148, 2016.
[19] L. Kilcher and R. Thresher, “Marine Hydrokinetic Energy Site Identification and Ranking Methodology Part I : Wave Energy Marine Hydrokinetic Energy Site Identification and Ranking Methodology Part I : Wave Energy,” no. October, 2016.
[20] S. De Chowdhury and J. Nader, “A review of hydrodynamic investigations into arrays of ocean wave energy converters,” *arXiv Prepr. arXiv …*, 2015.
[21] P. S. Liss and P. G. Slater, “© 1974 Nature Publishing Group,” 1974.
[22] J. Hodes, Gary; Cahen, David; Manassen, “© 1976 Nature Publishing Group,” *Nature*, vol. 260, no. März 25, pp. 312–313, 1976.
[23] E. Mansard, “Different Methods of Evaluating Wave Power in a Random Sea State: A Comparative Study.,” 1978.
[24] W. Baird and G. Mogridge, “Estimates of the Power of Wind-Generated Water Waves at Some Canadian Coastal Locations.,” 1976.
[25] J. A. Crabb., “assessment of wave power available at key UK sites.pdf.” 1984.
[26] M. T. Pontes, G. A. Athanassoulis, S. Barstow, L. Cavaleri, B. Holmes, D. Mollison, and H. Oliveira-Pires, “An Atlas of the Wave-Energy Resource in Europe,” *J. Offshore Mech. Arct. Eng.*, vol. 118, no. 4, p. 307, 1996.
[27] V. R. Swail, E. A. Ceccacci, A. T. Cox, and C. Cob, “the Aes40 North Atlantic Wave Reanalysis : Validation and Climate Assessment,” *Situ*, no. 1994, 2000.
[28] D. Mollison, “The UK wave power resource,” *Wave Energy, I Mech Eng*. pp. 1–6, 1991.
[29] G. Iglesias and R. Carballo, “Wave energy resource in the Estaca de Bares area (Spain),” *Renew. Energy*, vol. 35, no. 7, pp. 1574–1584, 2010.
[30] E. Luczko, B. Robertson, H. Bailey, C. Hiles, and B. Buckham, “Representing non-linear wave energy converters in coastal wave models,” *Renew. Energy*, vol. 118, pp. 376–385, 2018.
[31] D. Adytia, M. Ramdhani, and E. Van Groesen, “Phase resolved and averaged Wave Simulations in Jakarta Harbour,” *Proc. 6th Asia- …*, vol. 1, no. March 2018, pp. 218–223, 2012.
[32] T. J. Thomas and G. S. Dwarakish, “Numerical Wave Modelling – A Review,” *Aquat. Procedia*, vol. 4, no. Icwrcoe, pp. 443–448, 2015.
[33] A. Allievi and G. Bhuyan, “Assessment of Wave Energy Resources for the West Coast of Canada,” Vancouver, 1994.
[34] A. Cornett and J. Zhang, “Nearshore Wave Energy Resources, Western Vancouver Island, B.C.,” *Energy*, no. April, p. 78, 2008.
[35] C. E. Hiles, M. R. Tarbotton, and B. J. Buckham, “A model for wave energy assessment on the West Coast of Vancouver Island,” 2011.
[36] B. Robertson, C. E. Hiles, and B. J. Buckham, “Characterizing the near shore wave energy resource on the west coast of Vancouver Island, Canada,” *Renew. Energy*, vol. 71, pp. 665–678, 2014.
[37] B. Robertson, C. Hiles, E. Luzko, and B. Buckham, “Quantifying the Wave Energy Resource and Farm Siting Opportunities for Western Canada,” *Int. Conf. Ocean energy*, vol. 1, no. 250, 2014.
[38] A. J. van der Westhuysen, M. Zijlema, and J. A. Battjes, “Nonlinear saturation-based whitecapping dissipation in SWAN for deep and shallow water,” *Coast.*

Eng., vol. 54, no. 2, pp. 151–170, 2007.
[39] IEC, "IEC 62600-101:Wave energy resource assessment and characterization," 2014.
[40] W. M. Instrument, "– 2 – 62600-100/cdv © iec(e)."
[41] H. Bailey, J. P. Ortiz, B. Robertson, B. J. Buckhamn, and R. S. Nicoll, "A Methodology for Wave-to-Wire WEC Simulations," *2nd Mar. Energy Technol. Symp.*, pp. 1–15, 2014.
[42] H. Bailey, B. R. D. Robertson, and B. J. Buckham, "Wave-to-wire simulation of a floating oscillating water column wave energy converter," *Ocean Eng.*, vol. 125, pp. 248–260, 2016.
[43] B. Robertson, H. Bailey, D. Clancy, J. Ortiz, and B. Buckham, "Influence of wave resource assessment methods of wave power production estimates," *Int. Conf. Ocean Energy*, vol. 1, no. 250, pp. 1–19, 2014.
[44] D. Dunnett and J. S. Wallace, "Electricity generation from wave power in Canada," *Renew. Energy*, vol. 34, no. 1, pp. 179–195, 2009.
[45] L. Li, Z. Gao, and T. Moan, "Joint Environmental Data At Five European Offshore Sites for," *32nd Int. Conf. Ocean. Offshore Artic Eng.*, pp. 1–12, 2013.
[46] S. Astariz and G. Iglesias, "The collocation feasibility index – A method for selecting sites for co-located wave and wind farms," *Renew. Energy*, vol. 103, pp. 1–14, 2017.
[47] G. Iglesias, M. López, R. Carballo, A. Castro, J. A. Fraguela, and P. Frigaard, "Wave energy potential in Galicia (NW Spain)," *Renew. Energy*, vol. 34, no. 11, pp. 2323–2333, 2009.
[48] C.-K. Kim, J. E. Toft, M. Papenfus, G. Verutes, A. D. Guerry, M. H. Ruckelshaus, K. K. Arkema, G. Guannel, S. A. Wood, J. R. Bernhardt, H. Tallis, M. L. Plummer, B. S. Halpern, M. L. Pinsky, M. W. Beck, F. Chan, K. M. A. Chan, P. S. Levin, and S. Polasky, "Catching the Right Wave: Evaluating Wave Energy Resources and Potential Compatibility with Existing Marine and Coastal Uses," *PLoS One*, vol. 7, no. 11, p. e47598, 2012.
[49] A. Ceballos-Silva and J. López-Blanco, "Delineation of suitable areas for crops using a Multi-Criteria Evaluation approach and land use/cover mapping: A case study in Central Mexico," *Agric. Syst.*, vol. 77, no. 2, pp. 117–136, 2003.
[50] J. R. San Cristóbal, "Multi-criteria decision-making in the selection of a renewable energy project in spain: The Vikor method," *Renew. Energy*, vol. 36, no. 2, pp. 498–502, 2011.
[51] S. Ghosh, T. Chakraborty, S. Saha, M. Majumder, and M. Pal, "Development of the location suitability index for wave energy production by ANN and MCDM techniques," *Renew. Sustain. Energy Rev.*, vol. 59, pp. 1017–1028, 2016.
[52] A. Azzellino, V. Ferrante, J. P. Kofoed, C. Lanfredi, and D. Vicinanza, "Optimal siting of offshore wind-power combined with wave energy through a marine spatial planning approach," *Int. J. Mar. Energy*, vol. 3–4, pp. e11–e25, 2013.
[53] M. Vasileiou, E. Loukogeorgaki, and D. G. Vagiona, "GIS-based multi-criteria decision analysis for site selection of hybrid offshore wind and wave energy systems in Greece," *Renew. Sustain. Energy Rev.*, vol. 73, no. February, pp. 745–757, 2017.
[54] I. Galparsoro, P. Liria, I. Legorburu, J. Bald, G. Chust, P. Ruiz-Minguela, G.

Pérez, J. Marqués, Y. Torre-Enciso, M. González, and Á. Borja, “A Marine Spatial Planning Approach to Select Suitable Areas for Installing Wave Energy Converters (WECs), on the Basque Continental Shelf (Bay of Biscay),” *Coast. Manag.*, vol. 40, no. 1, pp. 1–19, 2012.

[55] L. Zubiate, J. L. Villate, Y. Torre-Enciso, H. C. Soerensen, B. Holmes, M. Panagiotopoulos, F. Neumann, N. Rousseau, and D. Langston, “Methodology for site selection for wave energy projects,” *Proceeding 8th Eur. Wave Tidal Energy Conf. (EWTEC08).*, pp. 1089–1095, 2005.

[56] A. Nobre, M. Pacheco, R. Jorge, M. F. P. Lopes, and L. M. C. Gato, “Geo-spatial multi-criteria analysis for wave energy conversion system deployment,” *Renew. Energy*, vol. 34, no. 1, pp. 97–111, 2009.

[57] F. Van Cleve, C. Judd, A. Radil, J. Ahmann, and S. Geerlofs, “Geospatial Analysis of Technical and Economic Suitability for Renewable Ocean Energy Development on Washington ’ s Outer Coast,” 2013.

[58] J. J. Wang, Y. Y. Jing, C. F. Zhang, and J. H. Zhao, “Review on multi-criteria decision analysis aid in sustainable energy decision-making,” *Renew. Sustain. Energy Rev.*, vol. 13, no. 9, pp. 2263–2278, 2009.

[59] E. Roszkowska, “Rank Ordering Criteria Weighting Methods – a Comparative Overview,” *Optimum. Stud. Ekon.*, vol. 5, no. 5(65), pp. 14–33, 2013.

[60] N. Booij, R. C. Ris, and L. H. Holthuijsen, “A third-generation wave model for coastal regions: 1. Model description and validation,” *J. Geophys. Res.*, vol. 104, no. C4, pp. 7649–7666, 1999.

[61] G. J. Komen, K. Hasselmann, and K. Hasselmann, “On the Existence of a Fully Developed Wind-Sea Spectrum,” *Journal of Physical Oceanography*, vol. 14, no. 8. pp. 1271–1285, 1984.

[62] P. A. E. M. Janssen, “Quasi-linear Theory of Wind-Wave Generation Applied to Wave Forecasting,” *Journal of Physical Oceanography*, vol. 21, no. 11. pp. 1631–1642, 1991.

[63] L. H. Holthuijsen, N. Booji, J. G. Haagsma, a. T. M. M. Kieftenburg, R. C. Ris, a. J. van derWesthuysen, and M. Zijlema, “USER MANUAL SWAN Cycle III version 40.51,” *Cycle*, p. 137, 2006.

[64] Det Norske Veritas, “Environmental conditions and environmental loads,” *Dnv*, no. October, pp. 9–123, 2010.

[65] S. J. Beatty, B. J. Buckham, and P. Wild, “Frequency Response Tuning for a Two-Body Heaving Wave Energy Converter,” *Proc. Eighteenth Int. Offshore Polar Eng. Conf.*, vol. i, no. January, pp. 342–349, 2008.

[66] RME, “Resolute Marine Energy Website,” 2018. [Online]. Available: http://www.resolutemarine.com/. [Accessed: 20-Aug-2006].

[67] Seawood Designs Inc., “SeaWood Design’s website,” 2018. .

[68] D. Bull, C. Smith, D. S. Jenne, P. Jacob, A. Copping, S. Willits, A. Fontaine, D. Brefort, G. Copeland, M. Gordon, and R. Jepsen, “Reference Model 6 (RM6): Oscillating Wave Energy Converter,” *Sandia Natl. Lab.*, vol. 6, no. September, 2014.

[69] BC Hydro, “Integrated Resource Plan, Chapter 2: Load-resource Balance,” 2013.

[70] BC Hydro, “Historical Transmission Data,” 2015. .

[71] BC Hydro, “Resource Options Report Update,” 2013.

[72] British Columbia Utilities Commission, “Vancouver Island Transmission Reinforcement (VITR) Project Status Report,” 2004.
[73] BC Hydro, “Strathcona Dam,” 2015.
[74] I. Moazzen, B. Robertson, P. Wild, A. Rowe, and B. Buckham, “Impacts of large-scale wave integration into a transmission-constrained grid,” *Renew. Energy*, vol. 88, pp. 408–417, 2016.
[75] Government of Canada, *Status of remote/off-grid communities in Canada*. 2011.
[76] D. Cook, M. A. Candidate, E. Fitzgerald, M. A. Candidate, and J. Sayers, “First Nations and Renewable Energy Development in British Columbia,” 2017.
[77] MacArtney Underwater Technology, “WEC Infrastructure Review,” 2016.
[78] Bank of Canada, “Annual Exchange Rates,” 2017. .
[79] BC Hydro, “Rating for All Transmission Circuits 60 KV or Higher,” 2014.
[80] Worldwide Inflation Data, “Historic inflation Canada - CPI inflation,” 2018.
[81] The World Bank, “Real Interest Rate,” 2018. .
[82] BC Hydro, “Electricity Rates,” 2018. [Online]. Available: https://www.bchydro.com/accounts-billing/rates-energy-use/electricity-rates.html.
[83] BC Hydro, “BC Hydro files interim rate application for year three of 10-Year Rates Plan,” 2016.
[84] BC Hydro, “2015 Rate Design Application (RDA) Residential Rate Workshop - May 21 , 2015 RDA Workshop 9 (b),” 2015.
[85] Government of Canada, “Welcome to the First Nation Profiles Interactive Map,” 2016. [Online]. Available: http://fnpim-cippn.aandc-aadnc.gc.ca/index-eng.html.
[86] British Columbia Marine Conservation Analysis Project Team, “Marine Atlas of Pacific Canada: A Product of the British Columbia Marine Conservation Analysis,” 2011. [Online]. Available: www.bcmca.ca.
[87] Fisheries and Oceans Canada, “Economic Impact of Marine Related Activities in Canada,” no. 1, 2009.
[88] S. Dogfish, “PACIFIC REGION AMENDED INTEGRATED FISHERIES MANAGEMENT PLAN,” 2009.
[89] Fisheries and Oceans Canada, “Commercial Fisheries,” 2017. [Online]. Available: http://www.dfo-mpo.gc.ca/stats/commercial-eng.htm.
[90] Fisheries and Oceans Canada, “Canada’s Oceans Strategy,” Ottawa, Ontario, 2002.
[91] Minister of Transport Canada, “TP 15357 E - Transportation in Canada 2016 - Comprehensive Report,” 2017.
[92] Minister of Public Works and Government Services Canada, “Transportation in Canada 2011,” 2012.
[93] Government of Canada and Government of British Columbia, *Canada - British Columbia Marine Protected Area Network Strategy*. 2014.
[94] J. Atalah, “Threats to Marine Biodiversity,” 2013. [Online]. Available: http://www.coastalwiki.org/wiki/Threats_to_Marine_Biodiversity.
[95] W. G. Stillwell, D. A. Seaver, and W. Edwards, “A comparison of weight approximation techniques in multiattribute utility decision making,” *Organ. Behav. Hum. Perform.*, vol. 28, no. 1, pp. 62–77, 1981.
[96] C.-L. Hwang and K. Yoon, *Multiple Attribute Decision Making: Methods and*

Applications. Berlin: Springer, 1981.

[97] Pacific Region, "SHRIMP TRAWL FISHERY OFF THE WEST COAST OF," vol. 8, no. August, pp. 6–9, 1999.

[98] R. Yonis, *The Economics of British Columbia's Crab Fishery: Socio-Economic Profile, Viability, and Market Trends*, no. 1. 2010.

[99] L. Bijsterveld, S. Di Novo, A. Fedorenko, and L. Hop Wo, "Comparison of Catch Reporting Systems for Commercial Salmon Fisheries in British Columbia," *Can. Man. Rep. Fish. Aquat. Sci. 2626*, p. vii+ 44, 2002.

Appendix A Detail Cost of WEC Farm with Different Power Producing Units (PPUs)

A.1 The Configurations of a Wave Farm with Different PPUs

The configurations of wave farms with different PPUs, as well as the cable types and cable lengths which used to connect PPUs within each farm are presented below.

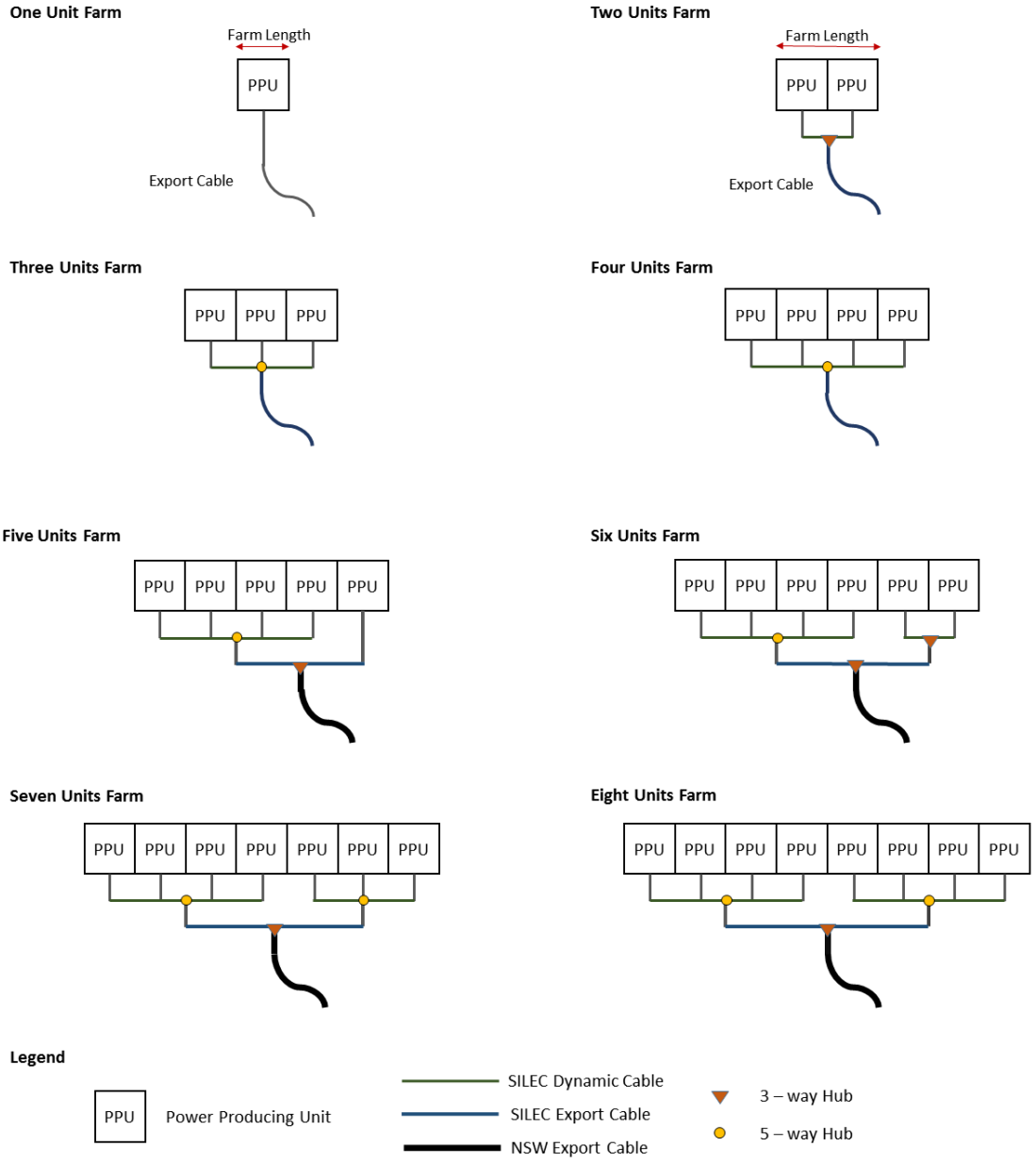

Figure A.1 The configurations of wave farms with different PPUs.

A.2 Summary of Cost for a Wave Farm with Different PPUs

The quantities and the prices for the connection components used for wave farms with different PPUs are summarized in the table below. The total cost of transmission infrastructure for each farm is calculated. In addition, the cable types, the cable lengths, and the prices of the inter-connection cables used for each farm are also presented in this table (where l_F is the farm length).

Table A.1 The summary of cost for wave farms with different PPUs.

Items	**Price**	**Number of Requirement**							
		One PPU	**Two PPU**	**Three PPU**	**Four PPU**	**Five PPUs**	**Six PPUs**	**Seven PPUS**	**Eight PPUs**
Non-recurring engineering costs	41,150	1	1	1	1	1	1	1	1
Components at PPU									
Cable hang-off	8,500	1	2	3	4	5	6	7	8
Reusable tip-clamp	12,370	1	1	1	1	1	1	1	1
Dynamic bend stiffer with tip-clamp at structure entrance point	21,200	1	2	3	4	5	6	7	8
Half in-line termination with bend stiffer for SILEC dynamic cable	33,100	2	2	3	4	5	6	7	8
Cable protection equipment									
Distributed module (10 per unit)	5,653	10	20	30	40	50	60	70	80
Uraduct cable protection (30m per unit)	5,300	1	2	3	4	5	6	7	8
Components at intermediate hub									
Half in-line termination with bend stiffener for SILEC export cable	38,600	0	1	1	1	1	2	2	2
3-way hub	49,600	0	1	0	0	0	1	0	0
5-way hub	99,200	0	0	1	1	1	1	2	2
Components at export hub									
Half in-line termination with bend stiffener for SILEC export cable	38,600	0	0	0	0	2	2	2	2
3-way hub	99,200	0	0	0	0	1	1	1	1
Half in-line termination with bend stiffener for SILEC export cable	44,100	0	0	0	0	1	1	1	1
Total cost for electrical infrastructures		211,250	390,980	565,210	689,840	1,034,970	1,247,800	1,422,030	1,546,660
Inter-connection cables									
SILEC dynamic cable	133.5 /m	0	1/2 l_F	2/3 l_F	3/4 l_F	3/5 l_F	2/3 l_F	5/7 l_F	3/4 l_F
SILEC export cable	233.5 /m	0	0	0	0	1/2 l_F	1/2 l_F	1/2 l_F	1/2 l_F

Appendix B The Net Revenue Index for Each Community

For each remote community, the optimal number of Power Producing Units (PPUs) that provides the maximum Net Revenue Index (NRI) and the corresponding NRI is presented in each individual map in this appendix. The NRI map for Tlatlasikuala are obtained by comparing a wave farm that has one PPU with a wave farm that has two PPUs. The NRI maps for Kyoquot, Ehattesaht and Hesquiaht are obtained by comparing four wave farms with different capacities (from one PPUs to four PPUs). The NRI map for Ahousaht is obtained by comparing five wave farms with different capacities (from one PPUs to five PPUs) at each site.

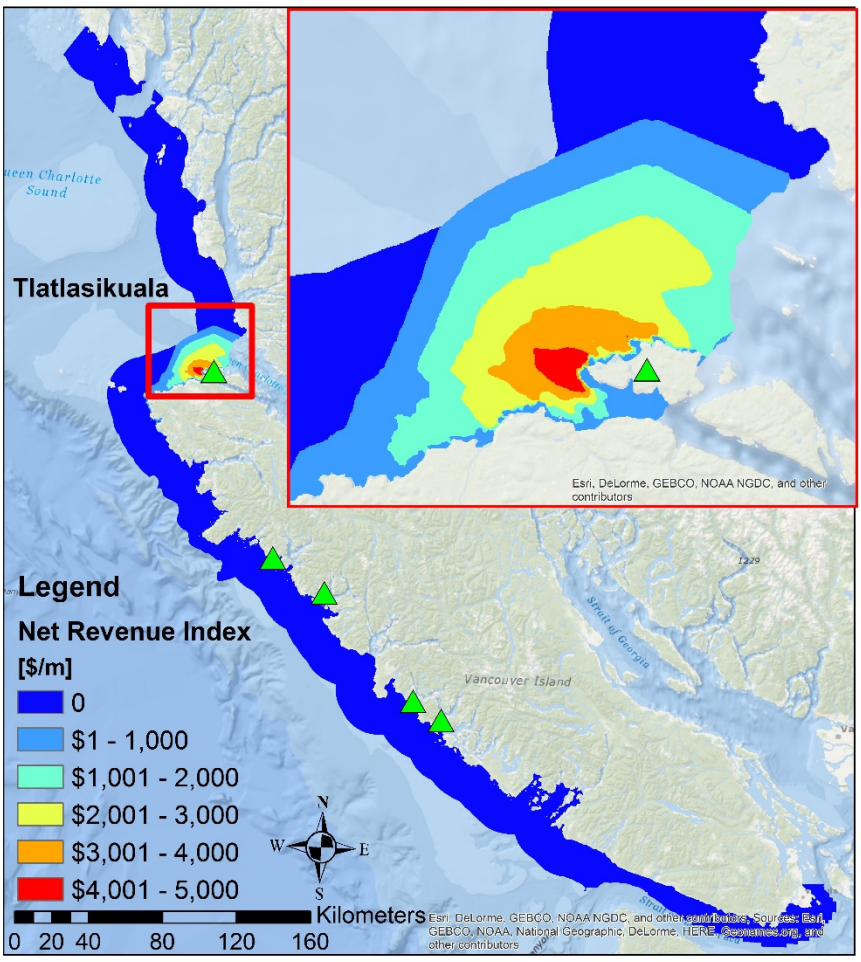

Figure B.1 the net revenue index map for Tlatlasikuala.
(the wave farm with one PPU always provides greater NRI than the wave farm with two PPUs.)

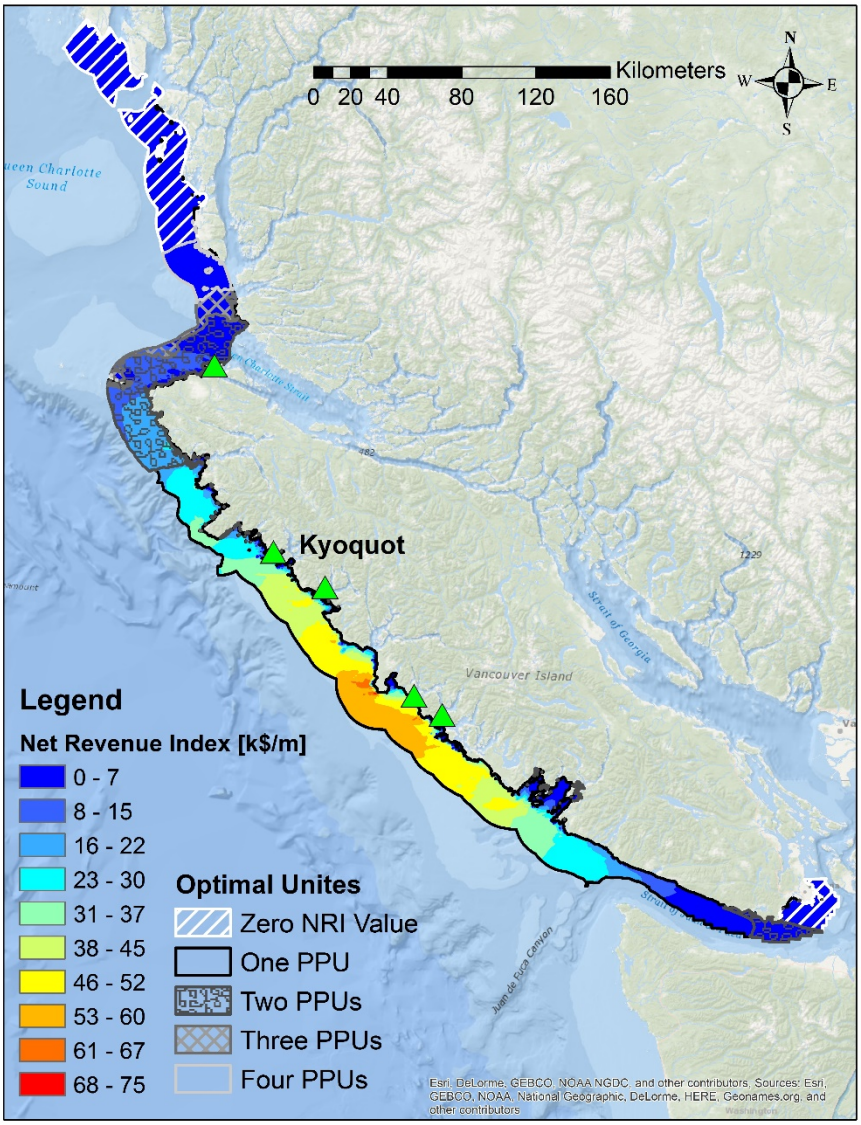

Figure B.2. the net revenue index map for Kyoquot.

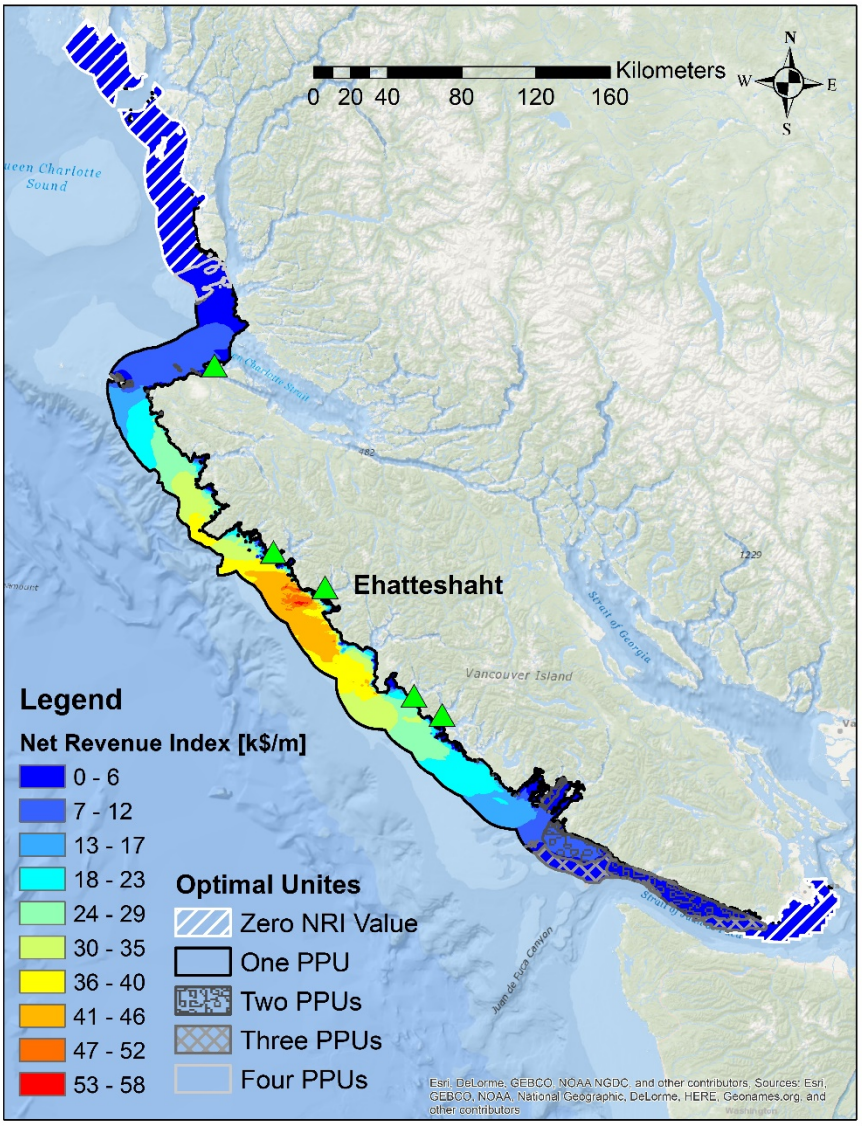

Figure B.3. the net revenue index map for Ehatteshaht.

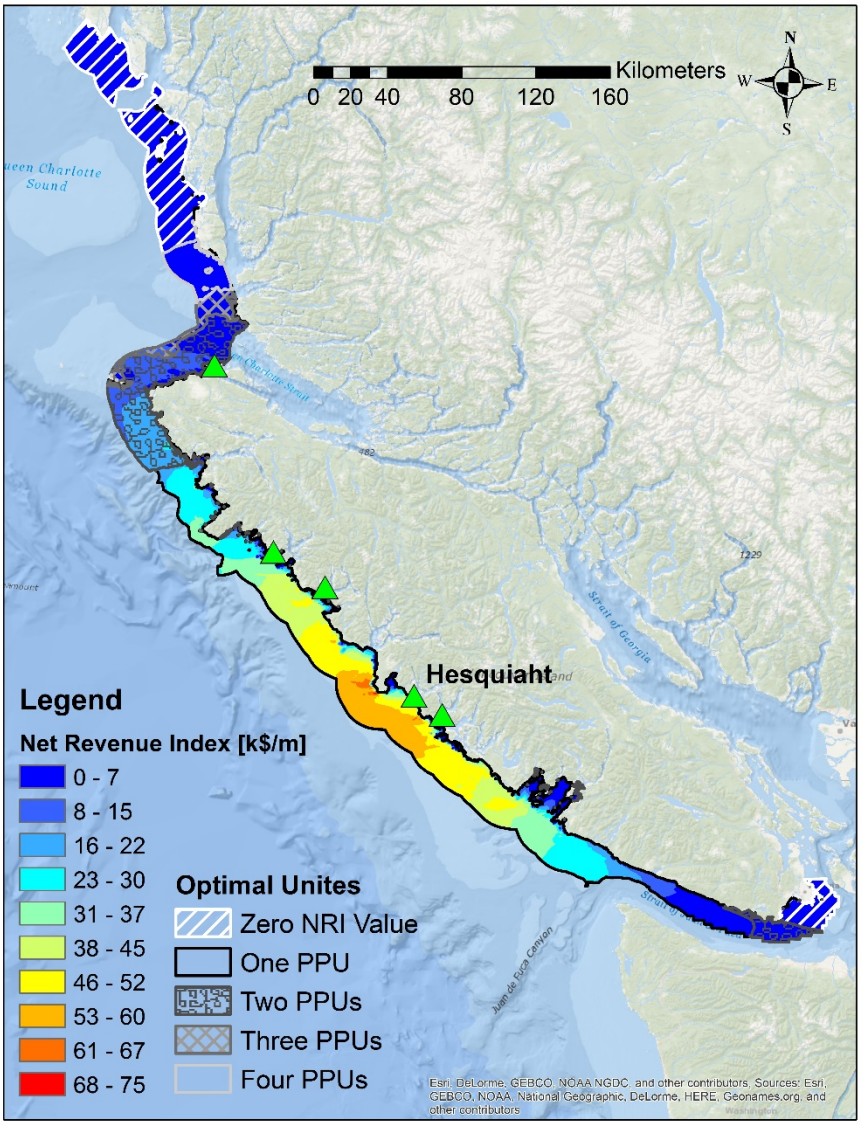

Figure B.4. the net revenue index map for Hesquiaht.

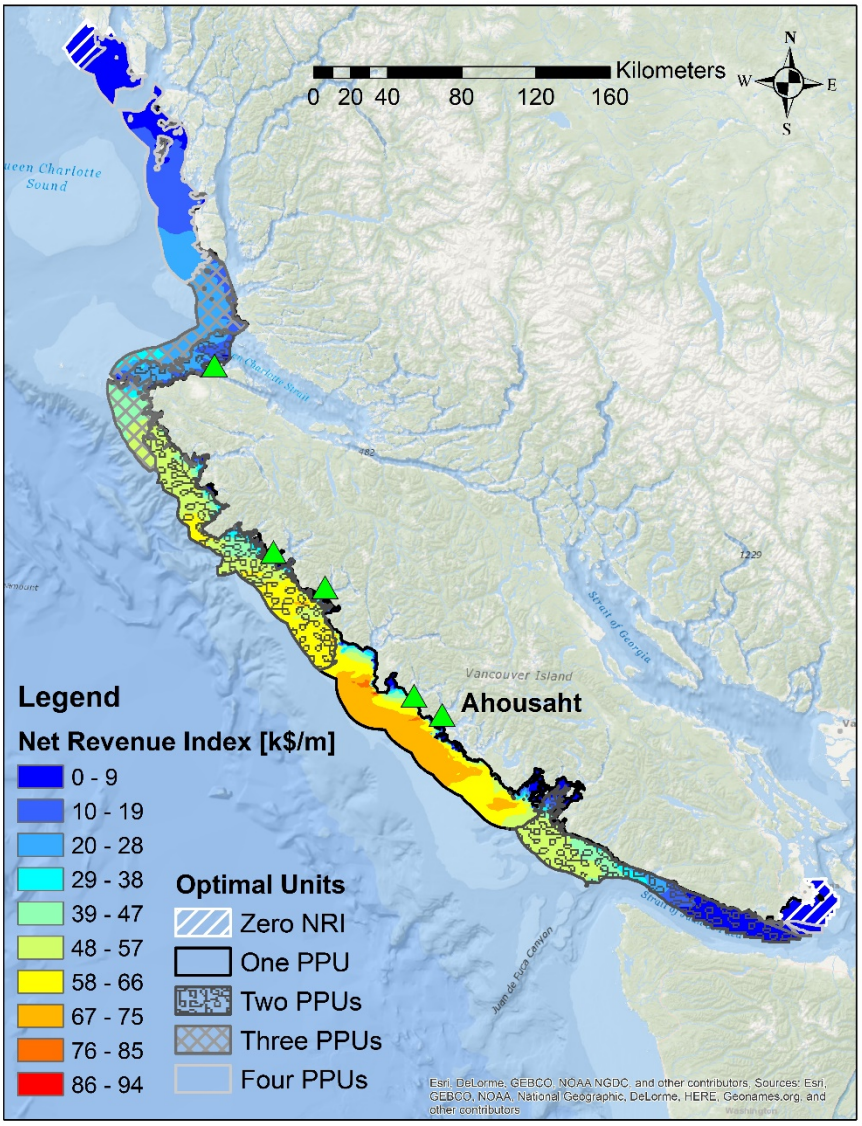

Figure B.5. the net revenue index map for Ahousaht.

Appendix C Additional information for commercial fisheries species and their prices

After screening and sorting, the original BCMCA data is reduced and combined to 17 species that belong to four species-groups: groundfish, shellfish, herring, and salmon. Addition to Table 4.3, the information about how BCMCA collected and sorted their original data and how to match the DFO data with BCMCA data is explained in detail.

Groundfish

Groundfish is a broad term that refers to the fish dwelling and inhabiting at or near the ocean floor. Groundfish includes over 452 unique species of demersal, benthic and pelagic fish. In commercial fisheries, groundfish show a high degree of diversity as well; 35 species composed the majority (95%) of the landing. The groundfish fishery in BC has a long history that dates back to the 1900s, and it is the most valuable commercial fishery sector in BC. In 2005, groundfish, with a $145 million landed value, composed 37% of the total landing value for all species [86], [88].

The groundfish data is collected by the Groundfish Stock Assessment and modified by DFO. The groundfish is sorted into six datasets according to the method of fishing and the license required for fishing: *Groundfish Trawl, Rock Fish, Schedule II, Sablefish (also known as blackcod) longline, sablefish trap, and halibut*. Because *groundfish trawl* and *rock fish* data contain multiple species, the price for the general groundfish group is selected as their price. The species caught in *schedule II* are primarily lingcod and dogfish, the average price between the lingcod and dogfish is used for schedule II. Finally, the prices of sablefish and halibut can be found from DFO data directly.

Shellfish

The shellfish fishery is another important commercial fishery activity in BC. The data collected by BCMCA includes seven species: shrimp trawl, prawn tap, crab, geoduck, sea cucumber, green sea urchin and red sea urchin.

The west coast of Vancouver Island is one of the historically predominant shrimp fishery grounds. More than 90 species of shrimp were found in BC waters, and the shrimp is mainly harvested by trawl and traps. The BCMCA's shrimp data is published in two datasets, *Shrimp Trawl* and *Prawn Tap*, according to their method of harvested. The *Shrimp Trawl* dataset includes seven species which are commercially harvested by the shrimp trawl fishery. The majority of the catch is pink shrimp (includes smooth pink shrimp, spiny pink shrimp, and spiny pink shrimp), followed up by the sidestripe shrimp; the rest are the coonstripe shrimp and humpback shrimp, along with some incidental catch of prawn. The target catching specie of *Prawn Trap* dataset is spawn, which is the largest of the seven shrimp-species that is commercially harvested by any gear type in BC waters. The catching in this dataset also includes humpback shrimp and coonstripe shrimp caught incidentally [86], [97]. The price for shrimp derived from DFO data will be used for both the *Shrimp Trawl* and *Prawn Trap* data.

Other than shrimp fishery, crab is another important species in shellfish fisheries. Crab fishery in BC has a long history that can date back to as early as 1885. Nowadays, the crab fishery accounts for around 34% of the total wild shellfish landing and 12% of the total landing of all wild fish species in BC. The major methods for commercial crab fishing are traps and ring nets. The major target includes four species, which are the Dungeness crab, the red rock crab, the golden king crab, and the red king crab. Among these four species, the Dungeness crab is the most important species for both commercial, First Nation, and recreational crab fishers in BC [86], [98]. In the DFO dataset, the price of crab category can be found.

Beyond the shrimp and crab, another four species of shellfish (geoduck, sea-cucumber, green sea-urchin and red sea-urchin) are important portions of commercial shellfish fisheries in BC. The geoduck landing includes the caught weight of geoduck (the largest burrowing clam) and the horse clam (the second largest bivalve in BC). Sea-cucumber landing only accounts the Giant Pacific sea-cucumber, which is the only commercial harvested sea-cucumber [86]. Each of the four species of shellfish was recorded in an individual layer in BCMCA datasets, and the value information of the corresponding species can be found in DFO data.

Herring

The herring has long been harvested off the west coast of BC, with a recorded landing that dates back to 1877 [86]. Herring is valuable in many ways, such as food, sport bait, commercial bait, zoo and aquarium food. Two types of herring fishery activities were recorded by BCMCA, which are roe herring and sardine. The roe herring landing was separated into two datasets by their method of catching: seine and gillnet. The Pacific sardine, which is a small pelagic fish, is another important target in the herring fishery. Due to the lack of roe herring and sardine price, the price of herring in general is used for both of them.

Salmon

Salmon is an important part of people's daily diet. The tradition of taking salmon as one of the First Nation main food dates back to thousands of years ago. Salmon has been the target of the commercial fishery after the arrival of Europeans in BC, in the late 1800s. The salmon landing was recorded in 15 datasets separately according to their types and harvested methods. The data covers five different types of salmon (chinook salmon, chum salmon, coho salmon, pink salmon and sockeye salmon) which caught by three different methods (gillnet, seine and troll). However, the salmon landing was originally accounted by pieces rather than weight [86]. An average of 5.48 lbs. per piece were used to convert the salmon landing to weight [99]. Regardless of the difference between each sub-species, the landing weight is calculated by summing up the 15 types of salmon, and the uniform price for salmon from DFO data were used.

Appendix D The BCMCA Analysis on Marine Conservation

BCMCA started an analysis in 2006 to identify marine areas with high conservation value [86]. This analysis covers a total of 169 ecological features. Each ecological feature is recorded in a GIS layer which is sampled in a 2 km by 2 km plan-unit grid and projected in *NAD 1983 BC Environment Albers*. The recorded information of each layer includes the occurrence of the species, specific species' habitats, general habitat types, seascape features, etc. The BCMCA uses Marxan, a decision support tool developed by the University of Queensland, to process the huge volume of data and computations in their analysis.

The Marxan analysis includes three major steps. The first step is setting up targets, which is defining how much of each feature must be contained in an effective solution. Second, Marxan searches millions of potential solutions to find the combination of plan-units that can meet all targets with the total area of these plan-units. When Marxan is searching the potential solutions or testing different combinations of plan-units, it makes some randomized choices about which plan-units to be included in each new combination for comparison. Therefore, the solution from each run of Marxan analysis is slightly different from each other. All of the selected plan-units in any of the solutions have equal conservation value. The final step is to run Marxan analysis 100 times with the identical features and targets. How often each planning unit is selected as part of 100 solutions is counted and named Selection Frequency. The Selection Frequency can be interpreted as a measure of irreplaceability for marine ecosystem or conservation value.

The BCMCA designed six different settings of targets to study the areas of high conservation value. Three of these settings are proposed by ecological experts during the workshop; the other three are set up by the BCMCA project team after consulting best practices, peer reviewed scientific literature and the advice of the ecological experts. When setting up the target for each feature, experts or project team recommend target range which spans from a minimum to a preferred amount to be included in the solution. The values at the low, middle, and high end of the range were used for the settings. The middle end of the expert setting was selected to represent the marine conservation in this thesis. In this setting, the target for each feature varied from 17.5% to 100%, and the average target of all features is around 30%. In addition, within

each setting, *Boundary Length Modifier* can be adjusted to control the clumps' size of selected plan-units. Because the focus of this thesis is to study how the conservation value change from one area to the other, the results with highest resolution (no clumps) is selected. In the middle end of the expert without clumps setting, an average of around 30% percent of the study area (around 139,000 km^2) has been selected in the solution from each run.